

LEWIS GRANT

IN-32

97607

139P.

ADAPTIVE ARRAYS FOR WEAK INTERFERING SIGNALS

-- AN EXPERIMENTAL SYSTEM

A Thesis

Presented in Partial Fulfillment of the Requirements for  
the degree Master of Science in the  
Graduate School of The Ohio State University

by

James Ward, B.E.E.

\* \* \* \* \*

The Ohio State University

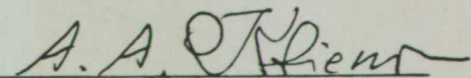
1987

Master's Examination Committee:

Prof. Aharon A. Ksienski

Prof. R.T. Compton, Jr.

Approved by:



Advisor  
Department of Electrical  
Engineering

(NASA-CR-181181) ADAPTIVE ARRAYS FOR WEAK  
INTERFERING SIGNALS: AN EXPERIMENTAL SYSTEM

M.S. Thesis (Ohio State Univ.) 139 p

Avail: NTIS HC A07/MF A01

CSCL 20N

N87-28814

Unclass

63/32 0097607

**THESIS ABSTRACT**

**THE OHIO STATE UNIVERSITY  
GRADUATE SCHOOL**

**NAME:** Ward, James

**QUARTER/YEAR:** Summer 1987

**DEPARTMENT:** Electrical Engineering

**DEGREE:** M.Sc.

**ADVISOR'S NAME:** Ksienski, Aharon A.

**TITLE OF THESIS:** Adaptive Arrays for Weak Interfering Signals -- An  
Experimental System

An experimental adaptive antenna system was implemented to study the performance of adaptive arrays in the presence of weak interfering signals. It is a sidelobe canceler with two auxiliary elements. Modified feedback loops, which decorrelate the noise components of the two inputs to the loop correlators, control the array weights. Digital processing is used for algorithm implementation and performance evaluation. The results show that the system can suppress interfering signals which are 0 dB to 10 dB below the thermal noise level in the main channel by 20 dB to 30 dB. When the desired signal is strong in the auxiliary elements the amount of interference suppression decreases. The amount of degradation depends upon the number of interfering signals incident on the communication system. A modified steering vector which overcomes this problem is proposed.

  
Advisor's Signature

## ACKNOWLEDGEMENTS

I wish to express sincere appreciation to Professor A.A. Ksienski, Dr. Inder J. Gupta and Dr. Eric K. Walton for their guidance and support throughout this project. Sincere thanks also go to Mr. Robert W. Evans and Mr. Donald E. Henry for their assistance during the experimental phases of this work.

I would also like to thank Dr. E.F. Miller of NASA - Lewis Research Center, Cleveland, Ohio, for his constant interest in the work reported in this thesis. This work was supported by NASA - Lewis Research Center under Grant NAG3-536 to The Ohio State University.

## VITA

..... Born .....

1985 ..... B.E.E., University of Dayton,  
Dayton, Ohio.

1985 to present ..... Graduate Research Associate,  
The Ohio State University  
ElectroScience Laboratory,  
Columbus, Ohio.

## FIELDS OF STUDY

**Major Field: Electrical Engineering**

## TABLE OF CONTENTS

Acknowledgement .....	ii
Vita .....	iii
List of Tables .....	vi
List of Figures .....	vii
I INTRODUCTION .....	1
II ADAPTIVE ARRAYS FOR SATELLITE COMMUNICATIONS .....	5
2.1 Introduction .....	5
2.2 Array and Algorithm Selection .....	5
2.3 Array Feedback Control .....	10
2.4 Modifications for the Suppression of Weak Interfering Signals .....	14
III THE EXPERIMENTAL SYSTEM AND ITS IMPLEMENTATION .....	22
3.1 Introduction .....	22
3.2 Signal Scenario and Antenna Configuration .....	22
3.3 The Experimental System .....	25
3.4 Signal Simulator .....	28
3.5 Array Simulator .....	32
3.6 Array Processor .....	40
3.7 System Calibration .....	52
3.8 System Computer .....	54
3.9 Data Acquisition .....	55
IV EXPERIMENTAL PROCEDURES .....	58
4.1 Introduction .....	58
4.2 Algorithm Implementation .....	58
4.2.1 Weight Control .....	58
4.2.2 Steering Vector Generation .....	63
4.2.3 Phase Compensation .....	64
4.2.4 Loop Gain and Integration Time .....	68
4.3 Performance Evaluation .....	70
V EXPERIMENTS AND RESULTS .....	77

5.1	Introduction .....	77
5.2	Experimental Procedure .....	77
5.3	Tests and Results .....	77
5.4	Results Using the Steering Vector .....	95
5.5	Summary .....	102
VI	SUMMARY AND CONCLUSIONS .....	104
	REFERENCES .....	107
	APPENDICES .....	108
A	CIRCUIT SCHEMATICS .....	108
B	SYSTEM SOFTWARE .....	114

## LIST OF TABLES

Table 1	Experimental Procedure .....	78
---------	------------------------------	----

## LIST OF FIGURES

Figure 1. Earth station receiving a desired signal and interfering signals. ....	2
Figure 2. An adaptive antenna array. ....	6
Figure 3. A sidelobe canceler. ....	8
Figure 4. Steered beam adaptive array feedback loop. ....	11
Figure 5. Modified feedback loop - two amplifiers. ....	18
Figure 6. Modified feedback loop - two antennas. ....	19
Figure 7. Signal scenario and antenna configuration. ....	24
Figure 8. The experimental system. ....	26
Figure 9. Block diagram of the experimental system. ....	27
Figure 10. Signal simulator block diagram and staggered pulse modulation. ....	30
Figure 11. Simplified block diagram of the array simulator. .	33
Figure 12. Array simulator detailed block diagram. ....	35
Figure 13. Phase shifter control characteristic. ....	38
Figure 14. Schematic of a noise source. ....	40
Figure 15. Noise source control characteristic. ....	41
Figure 16. Simplified block diagram of the array processor. .	42
Figure 17. System implementation of a modified feedback loop. ....	43
Figure 18. Detailed block diagram of the array processor. ...	45
Figure 19. Schematic of vector demodulator. ....	47
Figure 20. Schematic of vector modulator. ....	47



Figure 21. Vector modulator control characteristics. ....	48
Figure 22. Vector modulator weighting capabilities. ....	50
Figure 23. Phase measurement set-up. ....	53
Figure 24. Diagram of sampling procedure. ....	55
Figure 25. Signal processing in VDM. ....	60
Figure 26. Time delays in feedback loops. ....	66
Figure 27. I and Q VDM outputs. ....	71
Figure 28. Performance vs. $INR_{(main)}$ . ....	79
Figure 29. Performance vs. $INR_{(main)}$ . ....	80
Figure 30. Performance vs. $INR_1(aux-1)$ . ....	84
Figure 31. Performance vs. $INR_1(aux-1)$ . ....	85
Figure 32. Performance vs. $INR_1(aux-1)$ . ....	86
Figure 33. Performance vs. interfering signal I1 angle of arrival. ....	89
Figure 34. Performance vs. I2 angle of arrival. ....	90
Figure 35. Performance vs. I2 angle of arrival -- no injected system noise. ....	92
Figure 36. Performance vs. I2 angle of arrival -- desired signal attenuated, 20 dB. ....	93
Figure 37. Performance vs. $SIR_1(aux-1)$ -- using steering vector. ....	97
Figure 38. Performance vs. $SIR_1(aux-1)$ -- using steering vector. ....	98
Figure 39. Performance vs. $SIR_1(aux-1)$ -- using modified steering vector. ....	101
Figure 40. Pulse generator circuit of signal simulator. ....	109
Figure 41. 69 MHz oscillator circuit. ....	110

Figure 42. Level shifting circuit for programmable attenuator control. ....	111
Figure 43. Array output VDM output circuitry. ....	112
Figure 44. Auxiliary channel VDM output circuitry. ....	113

## CHAPTER I

### INTRODUCTION

A major problem in satellite communications is interference caused by transmissions from satellites adjacent to the desired signal satellite located in geostationary orbit. These transmissions enter the receive system through the sidelobes of the earth station receive antenna and interfere with the communication link (Figure 1). This problem has recently become more serious due to the crowding of the geostationary orbit and the move towards reduced angular separations between satellites. Indeed, it is this type of interference which limits the capacity of the geostationary orbit.

One method to overcome this problem is to suppress the interference at the earth station receive site. This could be done with a uniform reduction in the receive antenna sidelobes. However, a uniform reduction in sidelobe level also results in a loss of gain and consequent degradation in the desired signal. Alternatively, interference could be suppressed by lowering the receive antenna sidelobes only in the directions of the interfering signals. This is one function of an adaptive array. An adaptive array is an antenna array, which through feedback control, changes its pattern in response to the signal and interference environment in order to optimize the desired signal-to-interference plus noise ratio. It does so by steering pattern nulls in the directions of interfering signals and a pattern

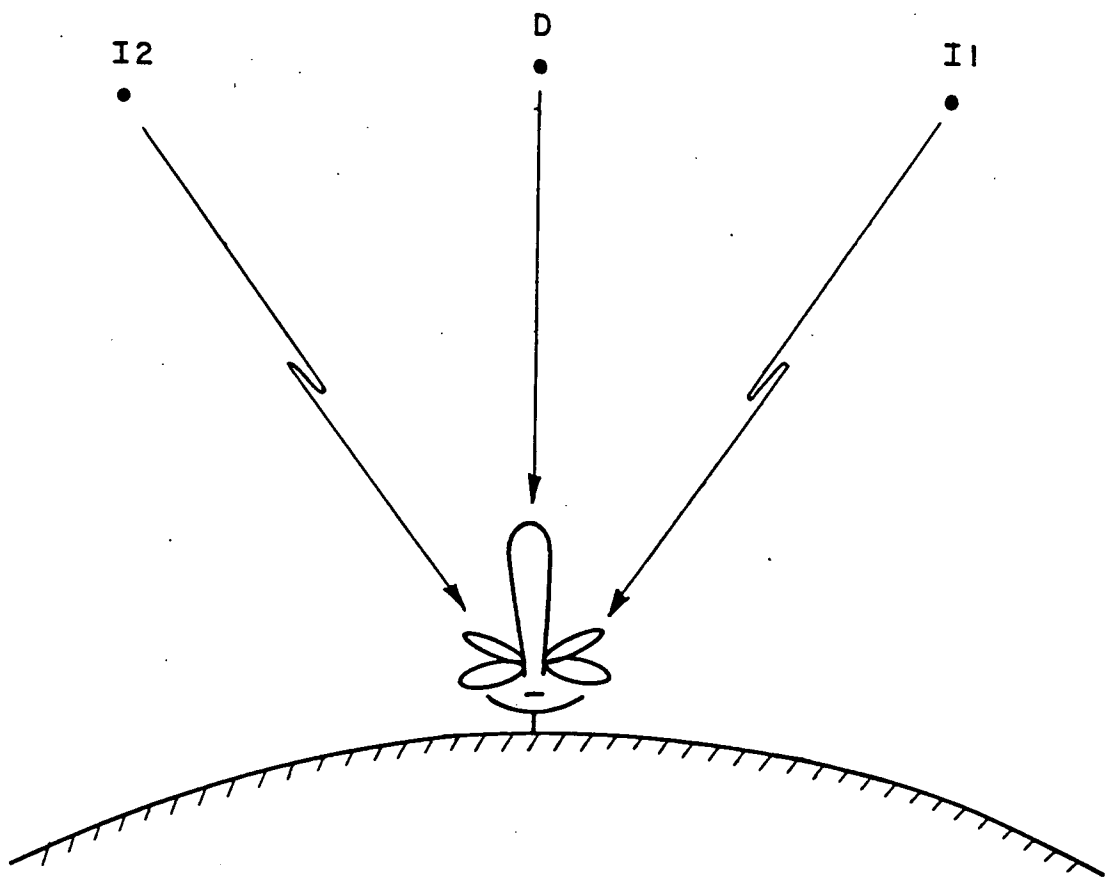


Figure 1. Earth station receiving a desired signal and interfering signals.

maximum in the direction of the desired signal. Furthermore, an adaptive array operates in real time, making it useful in a changing interference environment. Therefore, it appears that adaptive arrays could be useful for suppressing interference in a satellite communications environment.

Traditionally, adaptive arrays have been used for interference suppression in radar and communications systems where the interference to desired signal ratio is large and the interference to noise ratio is even larger. Intentional uplink jamming of a satellite communications system fits into this category. However, in the satellite communications scenario under consideration here, the interference typically originates from satellites different from the desired signal satellite, but which serve the same geographical region as the desired signal satellite. Thus the desired signal source and the interfering signal sources have approximately the same effective isotropic radiated power. Because the interferer enters through the receive antenna sidelobes, the interference is significantly weaker than the desired signal and in fact may be several dB below noise level. Although weak, these undesired signals, because their spectral characteristics and modulations are similar to those of the desired signal, still cause objectionable interference. This type of interference manifests itself in the form of faint wavy lines in the background of a television picture, or 'ghost' images of pictures other than the desired picture, and must be suppressed by 20-30 dB.

Conventional adaptive arrays are unable to suppress such weak interfering signals. This is because in the presence of weak

interfering signals, it is the thermal noise, rather than the interference, which controls the array weights and the adapted array pattern. The array adapts to minimize thermal noise and the interference remains unsuppressed. A theoretical study was done which shows that modifications can be made to the conventional array feedback loops which would yield the desired interference protection [1]. An experimental system was designed with the goals of first, verifying the theoretical work and determining the performance achievable in the laboratory; and second, to use the system with an actual antenna array in an existing interference environment. The first of these goals is the focus of this thesis: the construction and implementation of the experimental system, and the study of adaptive array performance achievable in a practical situation, for the general case of weak interfering signals and a specific application where these conditions exist -- that of an earth station receiving satellite communications.

Chapter II discusses adaptive arrays in general, their application to the present problem, and the modifications necessary to suppress weak interfering signals. Chapter III details the experimental system, including system calibration. Chapter IV describes the implementation of the adaptive algorithm with the system, and the method of performance evaluation. Chapter V presents the experiments conducted and the results obtained. Finally, Chapter VI contains a summary of the work, conclusions reached, plus comments on system limitations and potential for future investigations.

## CHAPTER II

### ADAPTIVE ARRAYS FOR SATELLITE COMMUNICATIONS

#### 2.1 Introduction

The purpose of this chapter is to provide the necessary adaptive array background from which the experimental system, and the tests and results obtained, can be explained. Much of the material in this chapter is due to the theoretical work of Gupta [1], and Gupta and Ksienski [2], which essentially provided the impetus for the implementation of the experimental system which is the focus of this thesis. First we will discuss adaptive arrays in general, and their application as a receive antenna for satellite communications. Then it will be shown that conventional adaptive arrays are unable to suppress weak interfering signals which arise in the present satellite communications environment. The modifications to the conventional adaptive array that enable the suppression of such weak interfering signals will then be discussed.

#### 2.2 Array and Algorithm Selection

Figure 2 shows an adaptive antenna array. The array output pattern adapts by means of the feedback control network which changes the amplitude and phase of the weights on each of the outputs of the array elements. In order for the array to selectively cancel the interference while maintaining a pattern maximum on the desired signal,

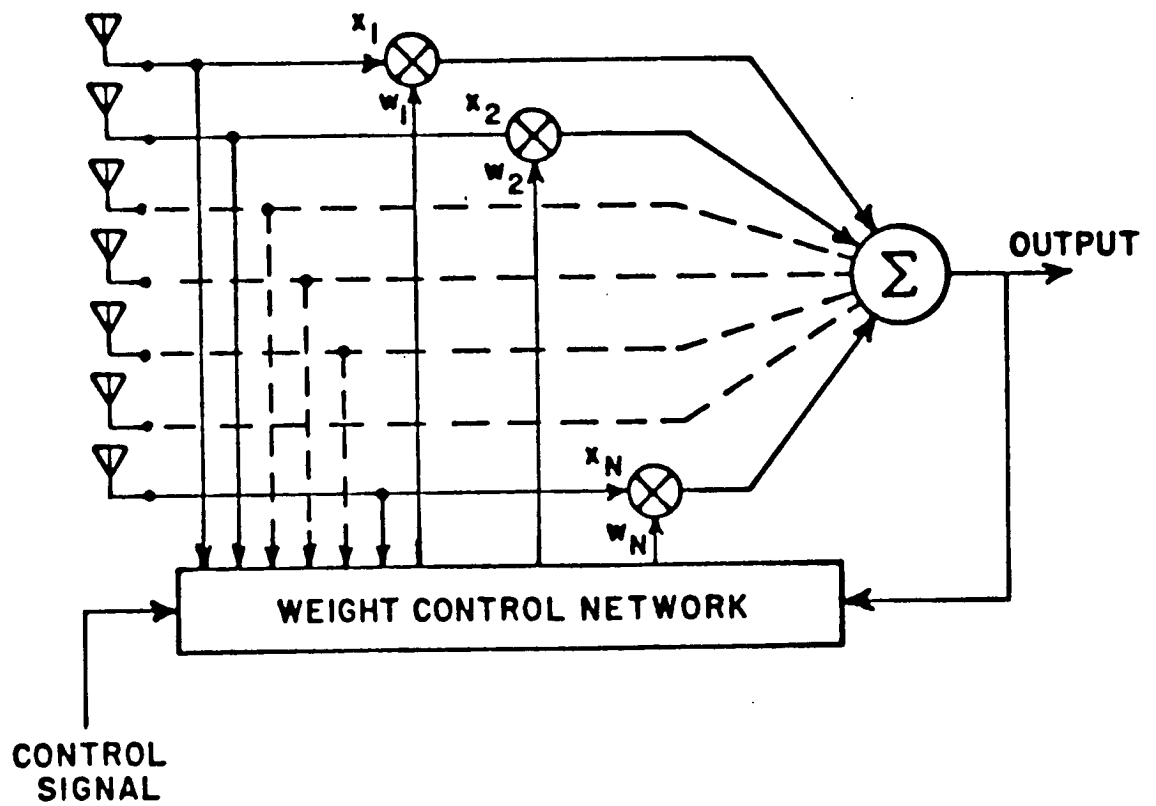


Figure 2. An adaptive antenna array.



the adaptive array must be provided with some information about the desired signal, which makes it different from the interfering signals. This information is the control signal in Figure 2, and its nature determines the proper adaptive algorithm for a particular application. If a reference signal which is correlated with the desired signal and uncorrelated with the interfering signals can be derived, then the LMS Algorithm of Widrow, et al. [3] is appropriate. If the angle of arrival of the desired signal is known, one can use the Applebaum [4], or steered beam algorithm. In the satellite communication systems under investigation, the desired signal direction of arrival is assumed to be known, while the spectral characteristics and modulations of the desired signal and the interfering signal are assumed to be very similar. Such is the case for groups of geostationary satellites providing broadcast television services for the same geographical area. Therefore, an Applebaum, or steered beam type adaptive array will be used to provide interference suppression.

A specific type of steered beam adaptive array is shown in Figure 3. It consists of a main antenna directed toward the desired signal and  $N$  auxiliary elements. Note that this configuration differs slightly from the general adaptive array shown in Figure 2, in that the signal from the main antenna is not adaptively weighted. It is a special case of an  $N+1$  element fully adaptive array, with the main antenna having a fixed weight, and is called a sidelobe canceler. This name originates from the visualization of using the auxiliary elements to create independent, equal amplitude and opposite phase replicas of the sidelobes of the main antenna, such that when the weighted auxiliary

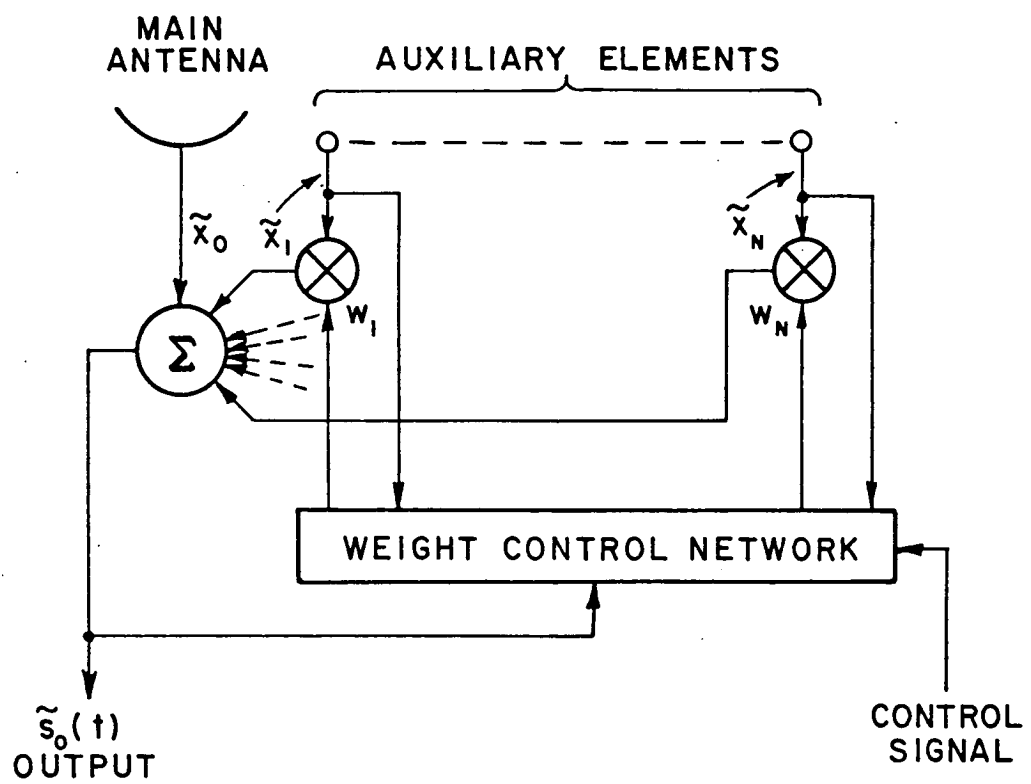


Figure 3. A sidelobe canceler.

element signals are summed with the main element signal to form the array output, the interfering signals are perfectly canceled. The control signal in Figure 3 is called the steering vector, and it prevents the cancellation of the desired signal, which may also be received by the auxiliary elements. The steering vector is generated from the knowledge of the desired signal direction of arrival and its amplitude in the auxiliary elements. It can be shown that the feedback loops controlling the weights in both a sidelobe canceler and a fully adaptive array are the same [4]. Also the performance achievable by the two are the same, as long as an appropriate steering vector is used with the sidelobe canceler. The number of auxiliary elements in the array is dictated by the expected number of incident interfering signals. Since an  $N+1$  element array has  $N$  degrees of freedom, at most  $N$  interfering signals can be nulled by a sidelobe canceler with a main antenna and  $N$  auxiliary elements. There are several reasons for using a sidelobe canceler as a receive antenna for satellite communications. First, since the direction of arrival of the desired signal is assumed to be known exactly, an accurate steering vector can be derived. Secondly, in the ensuing experimental system implementation, one less feedback loop is needed than in a fully adaptive array, which translates into a hardware savings. Also, since the main beam is not adaptively weighted, the pattern maximum on the desired signal is not likely to be compromised should the number of incident interfering signals exceed the number of degrees of freedom of the array.

### 2.3 Array Feedback Control

The array amplitude and phase weights are determined by feedback loops, such as the loop shown in Figure 4. There are  $N$  such loops, one for each auxiliary element of the array. From Figure 4, the differential equation governing one of the auxiliary element weights is

$$\frac{dw_i}{dt} = k \left( u_{si} - \tilde{x}_i^*(t) \tilde{s}_0(t) \right) \quad ; i=1,2,\dots,N \quad (1)$$

where  $w_i$  is the complex weight applied to auxiliary element  $i$ ,  $k$  is the loop gain,  $u_{si}$  is the steering vector component or control signal for the  $i^{\text{th}}$  element,  $\tilde{x}_i(t)$  is the signal received at the  $i^{\text{th}}$  element, and  $\tilde{s}_0(t)$  is the array output signal. An asterisk (\*) denotes complex conjugate. In this development, analytic signal representation is used and denoted by  $\sim$ . Also from Figure 4:

$$\tilde{s}_0(t) = \tilde{x}_0(t) + X^t W \quad (2)$$

where  $x_0(t)$  is the signal received at the main antenna,  $X$  is an  $N$ -element column vector of the received signals in the auxiliary elements, and  $W$  is an  $N$ -element column vector of the auxiliary element weights. Using (2), the differential equations governing all the weights may be put into vector form:

$$\frac{dW}{dt} = k \left( U_s - X^* \tilde{x}_0(t) - X^* X^t W \right) \quad (3)$$

where  $U_s$  is the steering vector. Assuming that received signals are ergodic random processes, and that the weights follow relatively slow changes in the signal scenario, (3) can be approximated as

$$\frac{dW}{dt} = k (U_s - R - \Phi W) \quad (4)$$

where  $R$  is an  $N$ -element column vector equal to the correlation between the auxiliary element signals and the main antenna signal,

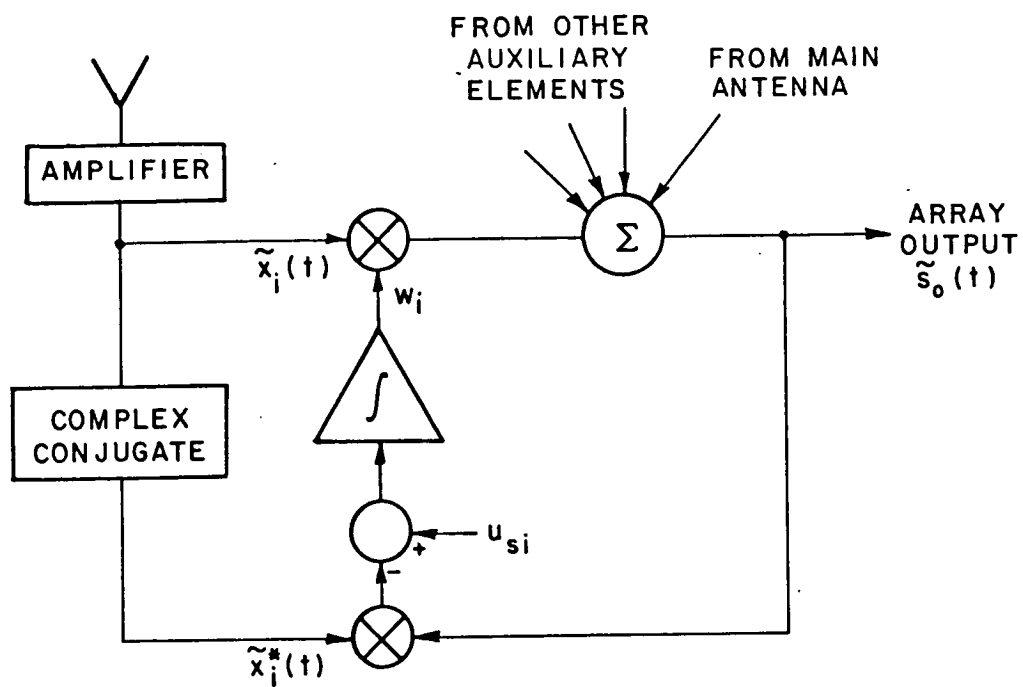


Figure 4. Steered beam adaptive array feedback loop.

$$R = E\{X^* \tilde{X}_0(t)\} \quad (5)$$

and  $\Phi$  is the  $N \times N$  covariance matrix of the auxiliary element signals.

$$\Phi = E\{X^* X^t\} \quad (6)$$

In Equations (5) and (6),  $E\{\}$  denotes ensemble average. To get the expression for the steady state weight vector, set

$$\frac{dW}{dt} = 0 \quad (7)$$

This yields, from (4)

$$W_{ss} = \Phi^{-1} (U_s - R) \quad (8)$$

Furthermore assuming that the desired signal and interfering signals incident on the array are all uncorrelated with each other and with the thermal noise at each element, and that the thermal noise components of different element signals are uncorrelated,

$$R = U_d + \sum_{i=1}^M U_{Ii} \quad (9)$$

where  $U_d$  is an  $N$ -element column vector of the correlations between the desired signal components of the auxiliary element signals and the desired signal component of the main element signal, and  $U_{Ii}$  is an  $N$ -element column vector of the correlations between the  $i^{\text{th}}$  interfering signal component of the auxiliary element signals and the  $i^{\text{th}}$  interfering signal component of the main antenna signal, and  $M$  is the total number of interfering signals. Substituting (9) into (8), the steady state weight vector expression becomes

$$W_{ss} = \Phi^{-1} \left( U_s - U_d - \sum_{i=1}^M U_{Ii} \right) \quad (10)$$

In order to prevent the array weights from moving to cancel the desired signal, the steering vector should be exactly equal to the desired signal correlation vector:

$$U_s = U_d . \quad (11)$$

Then, (10) becomes

$$W_{ss} = - \Phi^{-1} V \quad (12)$$

where we have defined  $V$  as

$$V = \sum_{i=1}^M U_{Ii} . \quad (13)$$

The operation of the array feedback loop can be understood by viewing it as a correlation loop. This description can be seen from Figure 4 and by rewriting (1) as

$$w_i = -k \int_{-\infty}^t \left( \tilde{x}_i^*(t) \tilde{s}_o(t) - u_{si} \right) dt . \quad (14)$$

The product of the auxiliary element signal and array output is formed. Subtracting  $u_{si}$  removes the component of this product due to the desired signal. This prevents the array weights from moving to suppress the desired signal. This quantity is integrated, forming an estimate of the correlation between the interfering signal and thermal noise components of  $\tilde{x}_i(t)$  and the interfering signal and thermal noise components of  $\tilde{s}_o(t)$ . The array weights move to minimize this correlation. Since the array cannot change the interference in  $\tilde{x}_i(t)$ , the correlation is minimized by the suppression of the interfering signals in the array output  $\tilde{s}_o(t)$ . Because the array uses a correlation estimate to determine the weights, it is essential that an interfering signal component of  $\tilde{x}_i(t)$  be highly correlated with the corresponding

interfering signal component of  $\tilde{s}_0(t)$ , at the inputs to the correlator multiplier (see Figure 4). If they are uncorrelated, it will appear to the array as if there were no interference at the array output and the interference present will remain unsuppressed. In fact, anything that tends to decorrelate the interfering signals in the two branches of the feedback loop will degrade adaptive array performance. Examples of such factors include differential time delays in the feedback loops, frequency response mismatches, and multiplier offset voltages [5-7]. Many of these factors will be encountered in the experimental system implementation.

#### 2.4 Modifications for the Suppression of Weak Interfering Signals

Conventional adaptive array feedback loops, such as those of Figure 4, are incapable of suppressing weak interfering signals. This is because it is the thermal noise, rather than the weaker interference, which dominates and thus dictates the array weights. Since the thermal noise in the main antenna signal is uncorrelated with the thermal noise in the auxiliary elements, any non-zero weight values add noise to the array output. The only way for the array to minimize noise at the array output and consequently maximize output SINR is to shut off the auxiliary elements, by driving their weights to zero. With a zero weight vector the auxiliary elements do not contribute to the array output and the interfering signals remain unsuppressed. To enable the suppression of weak interfering signals, either the interfering signal magnitude in the feedback loops must be increased or the effect of thermal noise must be reduced.



Increasing the magnitude of the interfering signals in the feedback loops, while relative to the noise level, can be accomplished by using directive antennas as auxiliary elements and pointing them in the directions of the interfering signals. The higher the directivity of the auxiliary elements, the greater the interference suppression which can be obtained. The use of directive auxiliary antennas also improves the output SNR by reducing the amount of thermal noise added to the array output by the weighted auxiliaries. The amount of noise that a particular auxiliary element contributes to the array output is proportional to that element's weight magnitude. Assuming that interference is being cancelled, the weight magnitude for a particular element depends on the relative amplitude of the interfering signal in the auxiliary element as compared to its amplitude in the main antenna. When the interfering signal amplitude in the auxiliary element is small compared to that in the main element, the weight magnitude will be large and consequently that auxiliary element will contribute a significant amount of noise to the array output. Conversely, when the interfering signal amplitudes in the auxiliary elements are large compared with their amplitudes in the main antenna, the array weights will be small. Then the weighted auxiliary elements will contribute less noise to the array output, and the output SNR will be improved (assuming desired signal is not suppressed). This is the case when directive antennas pointed towards the interfering signals are used as auxiliary elements. However, the directivity of the antennas one can use as auxiliary elements depends on the accuracy to which the locations of the interfering signal sources are known. In the satellite communications

scenario of interest, it is not unreasonable to assume that the directions of the interference would be approximately known. In many cases the interfering signals will originate from satellites in the vicinity of the desired signal satellite, which are transmitting on the same transponder (frequency) and/or with the same polarization as the desired signal. For broadcast television satellites, the interfering signal directions will be known, and directive auxiliary elements could be used to provide interference protection.

To understand the modifications necessary to reduce the effect of thermal noise on the array weights, it is necessary to discuss how thermal noise affects the array weights. It has been assumed that the thermal noise components of the element signals are uncorrelated. Therefore, the noise power at the array output consists of the noise power in the main antenna, plus noise components from each of the weighted auxiliary elements, with the amount of the noise power in the output due to a particular auxiliary element dependent on that element's weight magnitude. The weight itself depends on the correlation between the auxiliary element signal and the array output. This quantity depends on thermal noise because the noise power in the auxiliary element signal and a portion of the array output noise power essentially originate from the same noise source, that of the particular auxiliary antenna itself along with any amplifiers, mixers, etc. between the physical antenna and the entry of the element signal into the array feedback loop. Because the noise components of the two correlator inputs are from the same noise source, they are highly correlated and thus affect the array weight. When the interference is weak, the

correlation is dominated by thermal noise. To reduce the dependence of this correlation on thermal noise, the noise components of the two inputs to the loop correlator must be decorrelated.

For clarity, the branch of a feedback loop connecting the antenna element signal to the correlator will be referred to as the 'correlator branch,' and the branch which proceeds through the weight multiplier and sum junction will be referred to as the 'signal branch' of the particular feedback loop. The problem becomes that of decorrelating the noise in the signal branch from the noise in the correlator branch, in each feedback loop. When the primary source of thermal noise is internal, noise decorrelation between the feedback loop branches could be achieved by placing a different amplifier in each branch as in Figure 5. The assumption is that the correlation between the outputs of two different noise sources is negligible. Alternatively, when the dominant noise source is external or sky noise, or when both externally and internally generated thermal noises are troublesome, two spatially separate antennas, each followed by its own amplifier (Figure 6) could be used with each feedback loop. Since two spatially separate antennas will be looking at different portions of the sky, the sky noise entering the two antennas will be only partially correlated. (For uniformly distributed sky noise, noise entering two antennas separated by a multiple of  $1/2$  wavelength will be uncorrelated.) This modification to the conventional adaptive array requires twice the number of auxiliary elements, and a careful distribution of these additional antennas, but provides more noise decorrelation than the modification using one antenna and two amplifiers for each feedback loop. The distribution of

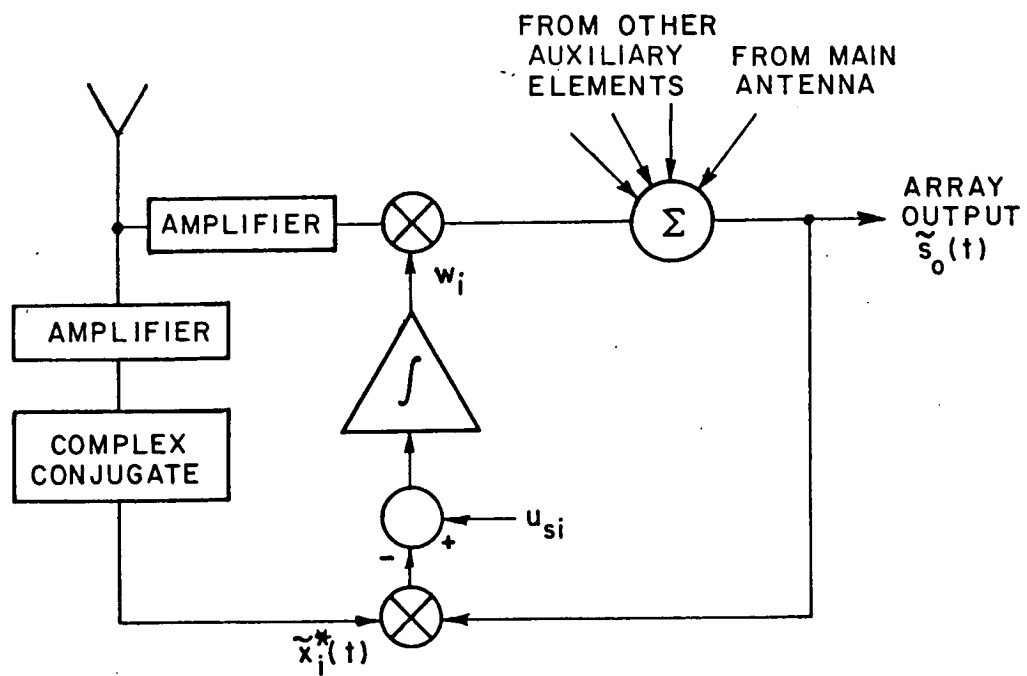


Figure 5. Modified feedback loop - two amplifiers.

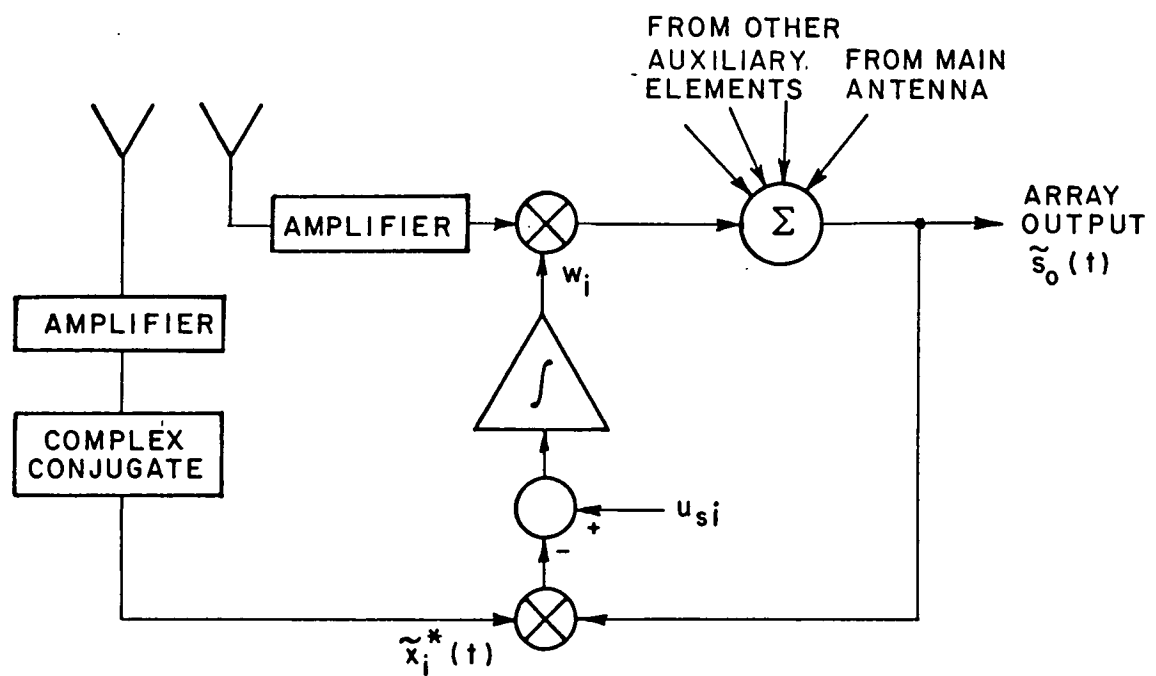


Figure 6. Modified feedback loop - two antennas.

the additional auxiliary elements must be chosen not only so that the sky noise entering the different feedback loop branches is uncorrelated, but also such that a directional signal will be received with the same phase at each of the two antennas now forming each feedback loop. This is necessary so that noise decorrelation is not achieved at the expense of interference decorrelation, which would also degrade adaptive array performance.

The theoretical work [1] shows that when using noise decorrelation alone, to achieve the desired interference suppression may require that the decorrelation be reduced to impractically low levels. Similarly, if directive antennas are used without noise decorrelation, the required auxiliary element gain necessary to get the desired interference suppression may become impractically large. However, by implementing a combination of the two techniques, one can trade off the amount of noise decorrelation necessary with the required auxiliary antenna gain to achieve a given interference suppression, such that both are within practical limits. Therefore, to suppress weak interfering signals, modified feedback loops using two spatially separate antennas for each loop, where the antennas are directive and pointed in the general directions of the interference, should be used.

In this chapter, adaptive arrays, and their application in a satellite communications scenario have been discussed. More detail on steered beam adaptive arrays can be found in [4] and [7]. The modifications to conventional adaptive array feedback control which allow the suppression of weak interfering signals were then discussed.

To test these concepts in a practical situation, an experimental system has been designed [8] and built, and is the subject of the next chapter.

## CHAPTER III

### THE EXPERIMENTAL SYSTEM AND ITS IMPLEMENTATION

#### 3.1 Introduction

The purpose of this chapter is to describe in detail the experimental system used to determine the capabilities of adaptive arrays to suppress weak interfering signals. First, the particular signal scenario and array configuration for which the system was designed is described. Then the experimental system is presented. A general description of the system is given and is followed by discussions of each of the system components, with emphasis on the hardware details of their implementation.

#### 3.2 Signal Scenario and Antenna Configuration

The particular signal scenario of interest is that of an earth station receiving television signals from a satellite in geostationary orbit. The location of this desired signal satellite is known exactly. Interfering signals originate from other satellites in geostationary orbit, which are located at arbitrary angular separations from the desired signal satellite. If these interfering satellites serve the same geographical region as the desired signal satellite, the effective isotropic radiated power (EIRP) of the desired signal satellite and the EIRPs of the interfering signal satellites will be approximately equal. Then, because the interfering signals enter the



receive system through the receive antenna sidelobes, the signal-to-interference ratio (SIR) in the receiver is 20-30 dB. The signal-to-noise (SNR) in the receiver is assumed to be 13-16 dB, which means the interference may be well below thermal noise level. Still, since the spectral characteristics of the desired and interfering signals are very similar, these weak interfering signals do cause objectionable interference and must be further suppressed by 20-30 dB. The experimental system is designed for the case where up to three signals are incident on the earth station, one desired signal and up to two interfering signals.

The antenna used to receive these signals is a five element array consisting of a high gain main antenna and two auxiliary antenna element pairs. Thus, the experimental adaptive array is a sidelobe canceler with two auxiliary elements. Modified feedback loops, with two spatially separate antennas for each loop, control the auxiliary element weights. These antennas could be separate reflectors, or separate feeds of a common reflector antenna. The signal scenario and element distribution is shown in Figure 7. D is the desired signal and I1 and I2 represent two interfering signals. All the signals are assumed to be coplanar. The high gain main antenna M is pointed in the direction of the desired signal, and receives the interfering signals through its sidelobes. At an earth station without adaptive array interference protection, only the main antenna is present. Auxiliary antennas 1a, 1b, 2a, and 2b are elements of moderate directivity, with elements 1a and 1b pointed in the general direction of I1, and elements 2a and 2b pointed in the general direction of I2. Thus the INR in the auxiliary elements will be larger

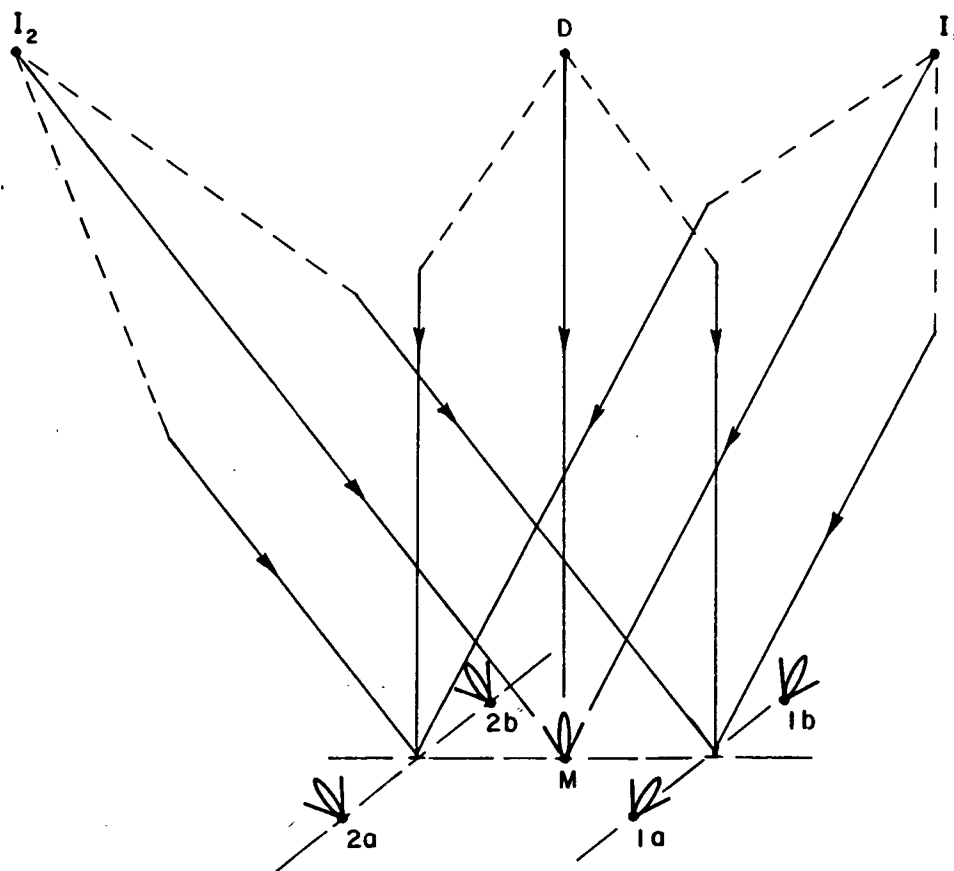


Figure 7. Signal scenario and antenna configuration.

than the INR in the main antenna. Antennas 1a and 1b will also receive signals D and I2 and elements 2a and 2b will also receive signals D and I1 through their sidelobes. Furthermore, antennas 1a and 1b are symmetrically located along a line perpendicular to the plane of the signal sources. This ensures that the phases of the three incident signals received by antenna 1a are exactly equal to the phases of the three signals received at antenna 1b. Because of the separation between antennas 1a and 1b, the sky noise received at element 1a is only partially correlated with the sky noise received at element 1b. Thus antennas 1a and 1b form appropriate inputs to a modified feedback loop and comprise one auxiliary element of the sidelobe canceler. Similarly, antennas 2a and 2b form the inputs to the other modified feedback loop of the adaptive array. For this investigation, actual antennas are not used. For the purposes of operator control and quantitative performance evaluation, the incident signals and the received array element signals are synthesized in the experimental system, which is discussed next.

### 3.3 The Experimental System

Figure 8 shows the experimental system, and Figure 9 is a block diagram of the system. The whole system, with the exception of the system computer, is contained in four rack mounted chassis. It is a sidelobe canceler with two auxiliary elements. Modified feedback loops with two antennas for each loop are used for noise decorrelation. The signal simulator synthesizes the desired signal and the interfering signals incident on the array. The array simulator creates the signals received at the five antennas of the adaptive array described in 3.2.

ORIGINAL PAGE IS  
OF POOR QUALITY

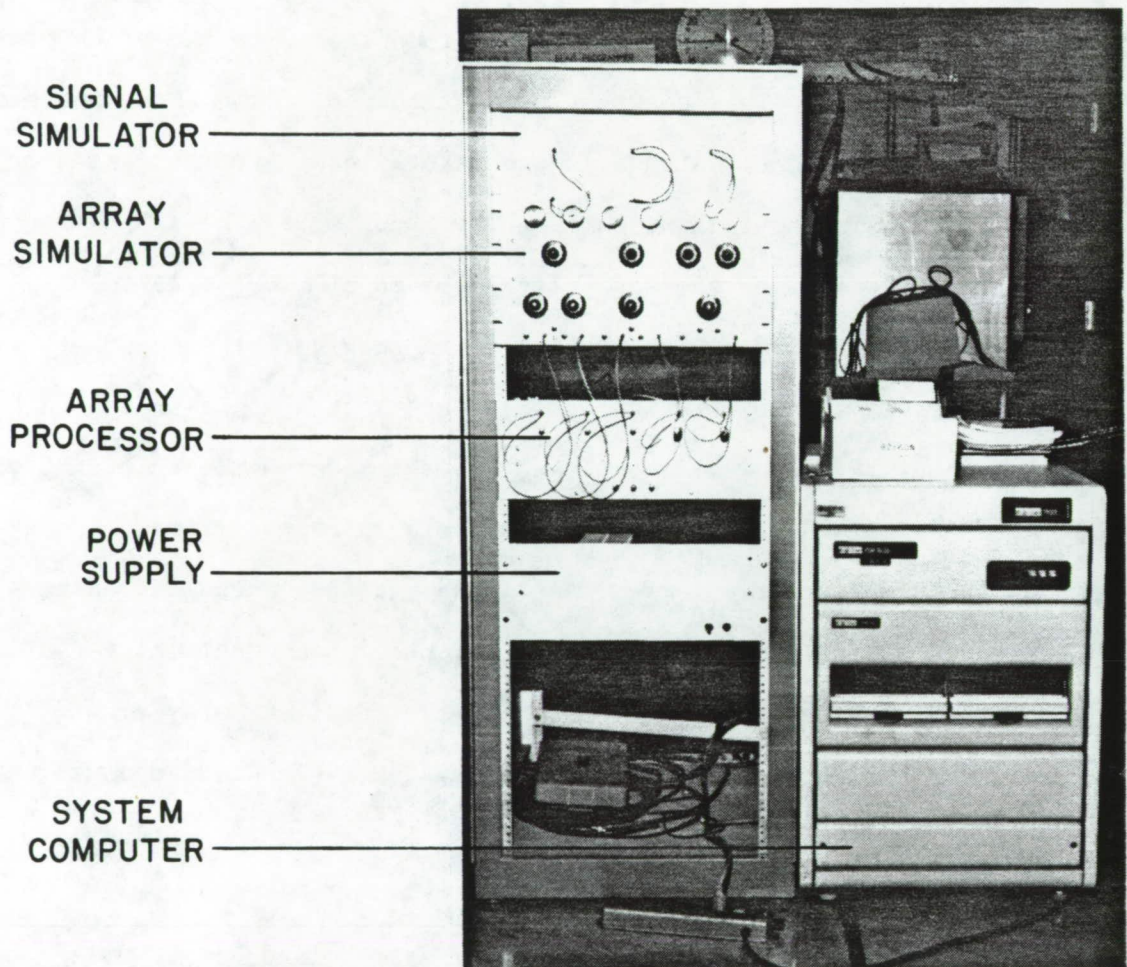


Figure 8. The experimental system.

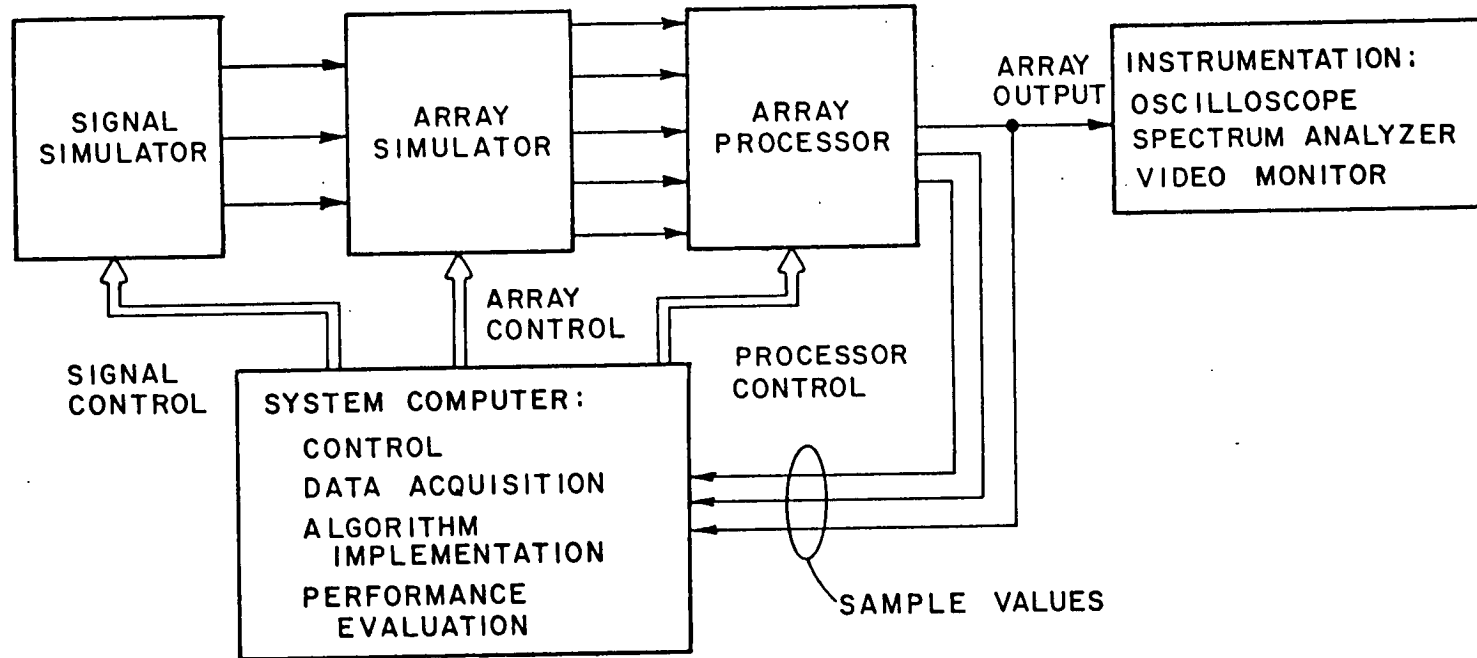


Figure 9. Block diagram of the experimental system.

The array simulator also provides the necessary control over the pertinent signal and array parameters which allows quantitative performance evaluation. The array processor and the system computer form the adaptive array feedback loops. The system computer calculates the array weights from sampled data, and the array processor applies these weights to the auxiliary element signals to form the adapted array output. In addition, the system computer also provides control for the signal simulator and the array simulator. The system operates at 69 MHz and has a channel bandwidth of 6 MHz, to represent a typical television channel. Many of the devices used in the system implementation are 70 MHz IF components. This choice of center frequency also permits qualitative testing of adaptive array performance through the observation of the improvement in a channel 4 television signal corrupted by interference. In a future implementation of the system, the signal simulator and the array simulator will be replaced by an actual antenna array, whose outputs will be down converted to the system IF of 69 MHz and fed to the array processor. The hardware details of the individual system blocks are discussed next.

### 3.4 Signal Simulator

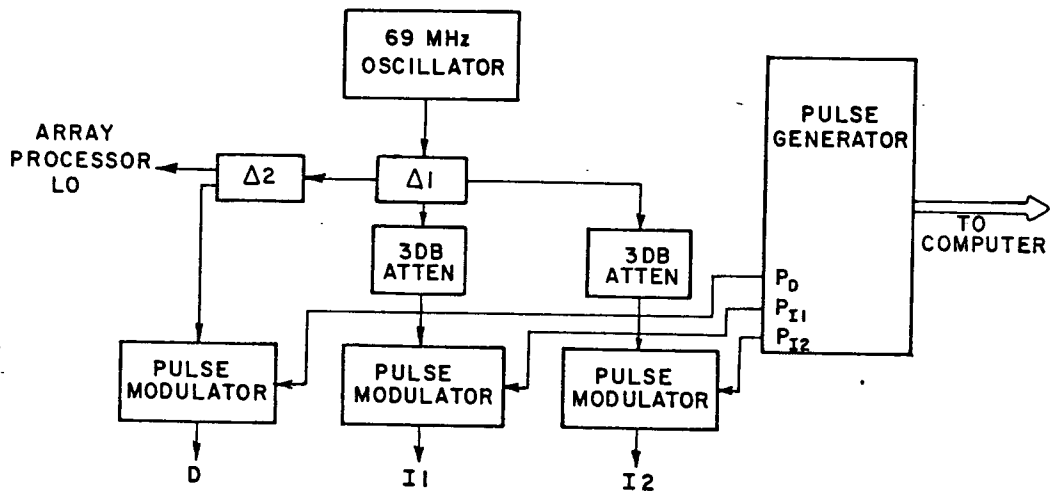
The signal simulator synthesizes the desired and the two interfering signals incident on the array, which are then combined in the array simulator to form the received signals at each array element. In order to measure adaptive array performance characteristics such as interference suppression, output signal-to-noise ratio, and output signal-to-interference plus noise ratio, it is necessary to measure

separately the desired signal power, the interference power, and the noise power present in each of the array element signals and in the array output. An appropriate modulation scheme is used in the signal simulator to accomplish this objective.

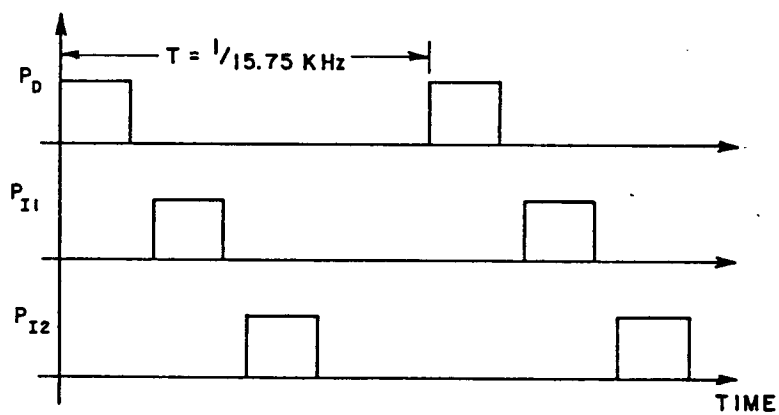
A block diagram of the signal simulator is shown in Figure 10(a). The desired signal is a carrier whose envelope is modulated by a pulse train as in Figure 10(b). The carrier frequency is 69 MHz, that of a channel 4 television signal, and the pulse repetition frequency is 15.75 kHz, which is the horizontal scan rate of a black and white television picture. The interfering signals are also pulse modulated sinusoids, except that the modulation on one interfering signal,  $P_{I1}$ , is delayed by one-quarter of the pulse repetition period from that of the other interfering signal,  $P_{I2}$ , and from that of the desired signal modulation,  $P_D$ . Thus, each signal occupies a different portion of the pulse repetition period. In other words, the cross-correlation between any two signal simulator outputs  $x(t)$  and  $y(t)$ ,

$$R_{xy}(\tau) = \frac{1}{T} \int_0^T x(t)y(t+\tau)dt \quad (15)$$

is zero for  $\tau=0$ . In fact  $R_{xy}(\tau)=0$  for  $\tau < 3.97 \mu\text{sec}$ , which is much greater than any interelement time delay possible for a spacing between antennas less than  $7940\lambda$  (595m at 4 GHz). For all conditions to be simulated, the desired signal and the interfering signals are all uncorrelated with each other. This satisfies an assumption made in the development of the weight control equation (Section 2.3) and is essential to proper adaptive array performance.



(a) block diagram



(b) desired and interfering signal pulse modulation

Figure 10. Signal simulator block diagram and staggered pulse modulation.



This staggered pulse modulation scheme allows the separate calculation of desired signal and interfering signal amplitudes in the array output, where components due to each are present. This is done either by observation of the different pulse levels on a calibrated oscilloscope display, or by sampling only across portions of the pulse repetition period corresponding to the particular component signal under measurement. By exploiting this modulation, a quantitative study of adaptive array performance can be conducted. However, this particular modulation is not exploited during adaptation. The correlation between auxiliary element signals and array output is performed over several periods of the pulse modulation. Thus as far as the adaptive array is concerned, all the desired and interfering signals appear to be simultaneously present. This modulation scheme will also be useful for a qualitative test where the desired signal is a television signal. The pulse modulated interfering signals will appear on a television picture as vertical bands (ghosts) which should disappear from the picture as the array adapts and interference is suppressed.

This modulation is implemented by using a single oscillator and dividing it into three channels, which are separately pulse modulated to form the desired and interfering signals. In Figure 10, the  $\Delta$ 's are commercial in-phase power dividers. The pulse modulators are PIN diode switches which gate their respective inputs according to the TTL level control inputs  $P_D, P_{I1}, P_{I2}$ . These TTL pulse trains are generated in a digital circuit denoted "pulse generator" in the figure, and enabled by the system computer. An output of  $\Delta 2$  is sent to the array processor to provide the local oscillator signal for demodulation. The 3 dB

attenuators compensate for the loss through  $\Delta 2$  such that all three signal simulator outputs are of equal power. This condition represents the case where the desired signal and the interfering signals originate from satellites serving the same geographical area, and thus have approximately equal EIRPs. Additional control of the received signal levels is provided in the array simulator. Detailed circuit diagrams of both the 69 MHz oscillator circuit and the pulse generator circuit are given in Appendix A.

### 3.5 Array Simulator

The array simulator accepts the signals incident from the signal simulator and combines them to form the signals received at each array element, such that each element signal contains a component due to the desired signal, components due to both interfering signals, and additive thermal noise. Thus the array simulator has three inputs for the three incident signals, and five outputs corresponding to the five elements of the array. These five outputs are designated MAIN, AUX-1 SIGNAL, AUX-1 CORRELATOR, AUX-2 SIGNAL, and AUX-2 CORRELATOR. The MAIN output is the signal received at the main antenna. The other outputs are the signals received in the auxiliary antennas of the modified feedback loops of our two auxiliary element sidelobe canceler. Using the notation of Chapter II, AUX-1 SIGNAL and AUX-2 SIGNAL outputs form (in the array processor) the feedback loop branches which are multiplied by the array weights, and AUX-1 CORRELATOR and AUX-2 CORRELATOR outputs form the feedback loop branches which are direct inputs to the loop correlators (Figure 6). A simplified block diagram of the array simulator is shown in Figure 11.

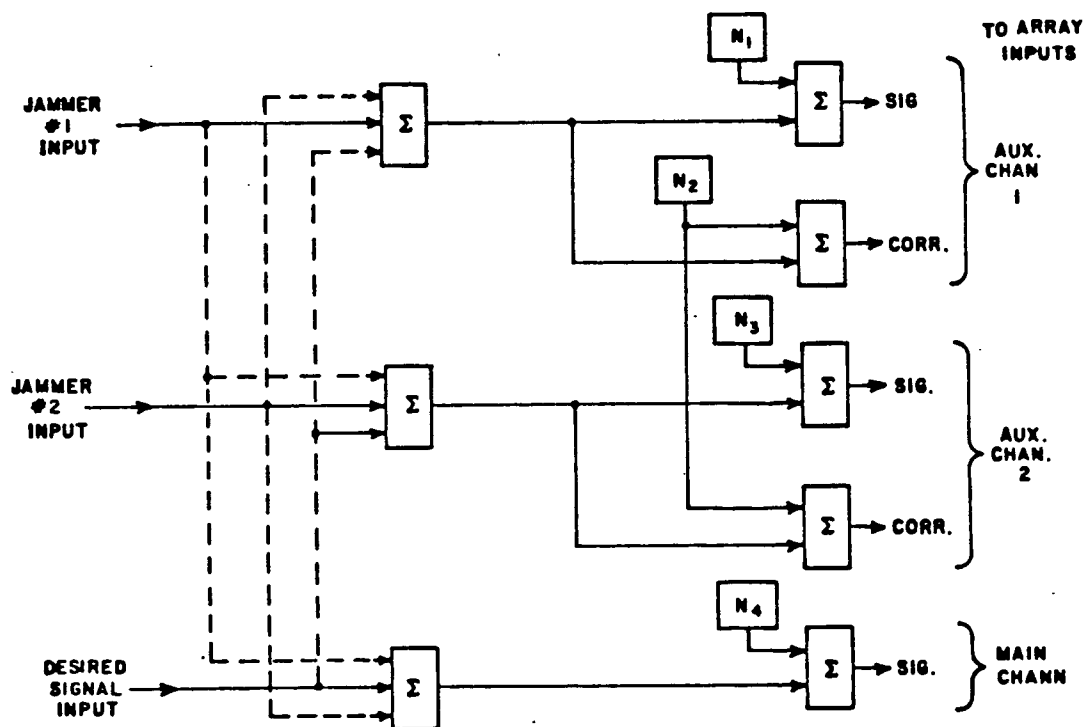


Figure 11. Simplified block diagram of the array simulator.

The front panel of the array simulator as well as the system computer, provide operator control over pertinent signal and array parameters such as simulated sidelobe levels, desired and interfering signal directions of arrival, signal-to-noise ratios, and interference-to-noise ratios in the different array elements (array simulator outputs).

A detailed block diagram of the array simulator is shown in Figure 12. The  $\Delta$ 's are SMA connectorized in-phase power dividers. The  $\Sigma$ 's are summing junctions, which are in-phase power dividers connected as summers. The  $\alpha$ 's are variable attenuators and the  $\phi$ 's denote variable phase shifters. N1 through N4 are variable output noise sources. All of the components of the array simulator are 50 ohm devices, and connections between components of the array simulator, and the other system blocks, are made with 0.141" diameter, 50 ohm semi-rigid coaxial cable.

Referring to Figure 12, the level attenuators,  $\alpha_1$ ,  $\alpha_2$ , and  $\alpha_3$  are 70 dB, 10 dB step attenuators used to control the incident signal levels at each array simulator input. They can be viewed as varying the gain of an antenna in a particular direction: either the gain of an auxiliary element in an interfering signal direction or the gain of the main antenna in the direction of the desired signal. Increments smaller than 10 dB are obtained by placing 1, 2, or 3 dB fixed coaxial attenuators in the lines from the signal simulator to the array simulator.

Each antenna of the array is pointed in the general direction of a particular incident signal. The leakage attenuators  $\alpha_4$ ,  $\alpha_5$ ,  $\alpha_6$  control the amount of the other incident signals received in each antenna. For

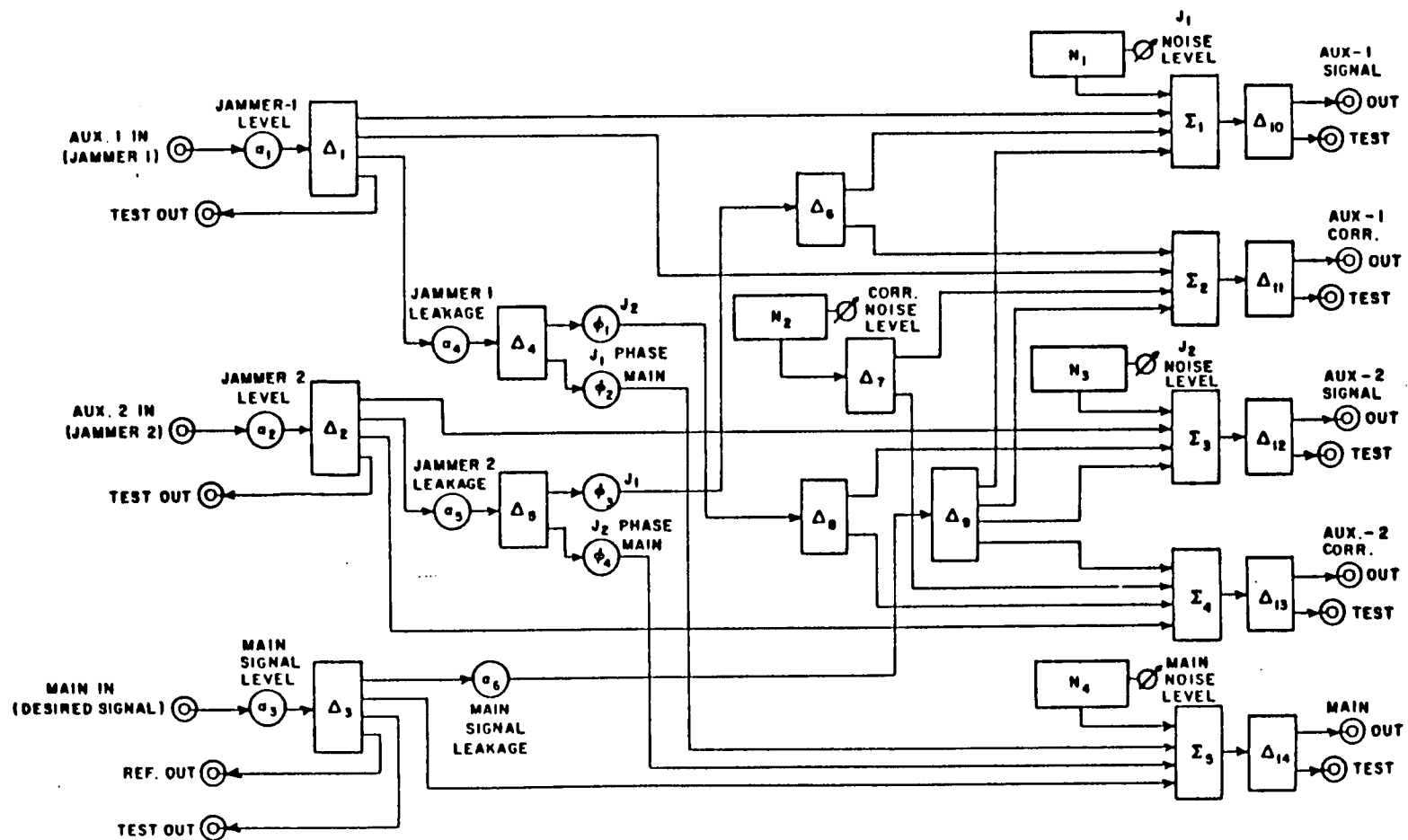


Figure 12. Array simulator detailed block diagram.

example,  $\alpha_6$  controls the level of the desired signal in the auxiliary element channels, while  $\alpha_4$  fixes the level of interfering signal I1 in both the main antenna and in the AUX-2 antennas. In terms of antenna parameters, these signal levels depend on the antenna directivity, sidelobe level, as well as the angular separation between sources and the incoming signal power. Thus by fixing  $\alpha_3$  and  $\alpha_4$  such that the interfering signal component in the main channel is 20 dB below the desired signal level, a sidelobe level of -20 dB in the main antenna is simulated. (It is assumed that the incident signals are of equal power.) Auxiliary element sidelobe levels can be similarly simulated. Each leakage attenuator actually consists of a cascade of two attenuators. The first is a step attenuator identical to those used for level attenuators, and the second is a 63 dB, 1 dB step programmable attenuator which can be controlled either manually or by the system computer. Appropriate settings of the level and leakage attenuators can be used to eliminate an incident signal for a particular test. This is useful in testing, for example, with only one interfering signal, or if it is desired to only allow desired signal in the main antenna and not in the auxiliaries.

Four variable phase shifters simulate interfering signal directions of arrival by varying the interelement phase shift between interfering signal components of the array elements.  $\phi_1$  sets the phase shifts between the I1 component of the AUX-1 signals and the I1 components of the MAIN signal, and  $\phi_2$  sets the phase shift between the I1 component of the AUX-1 signals and the I1 component of the AUX-2 signals.  $\phi_3$  and  $\phi_4$  do the same for the I2 components of the element

signals. There are no phase shifters associated with the desired signal, because it is assumed to be arriving from broadside, and thus arrives at all of the array elements with the same phase. The devices used are 360 degree voltage variable phase shifters, where a control voltage varies a capacitance to induce changes in phase shift. Since in our application, the directions of arrival of the interfering signals are assumed to be known approximately, and assumed to be stationary or very slowly varying, potentiometers are used for manual control of the variable phase shifters. A typical device control characteristic is shown in Figure 13. The use of a dial calibrated in hundredths of turns in conjunction with a potentiometer yields a resolution in controllable phase shift of less than 1 degree.

An important consideration in constructing the simulator was to ensure that the phase shifts of the three components of each auxiliary element signal branch are nearly equal to the phases of the corresponding signal components in the corresponding auxiliary element correlator channel. This is to maintain the signal and interference correlation between the two branches of each feedback loop. Any non-zero phase shift between signal and correlator branches partially decorrelates the signal components in the two feedback loop branches, and results in degraded adaptive array performance. In practice, small differential phase shifts will exist between the two outputs of an in-phase power divider, or between the insertion phases of similar devices in each channel. To minimize the cumulative effect of all sources of differential phase shift, cable lengths are made equal wherever applicable. Furthermore, it will be shown in Chapter IV how the use of

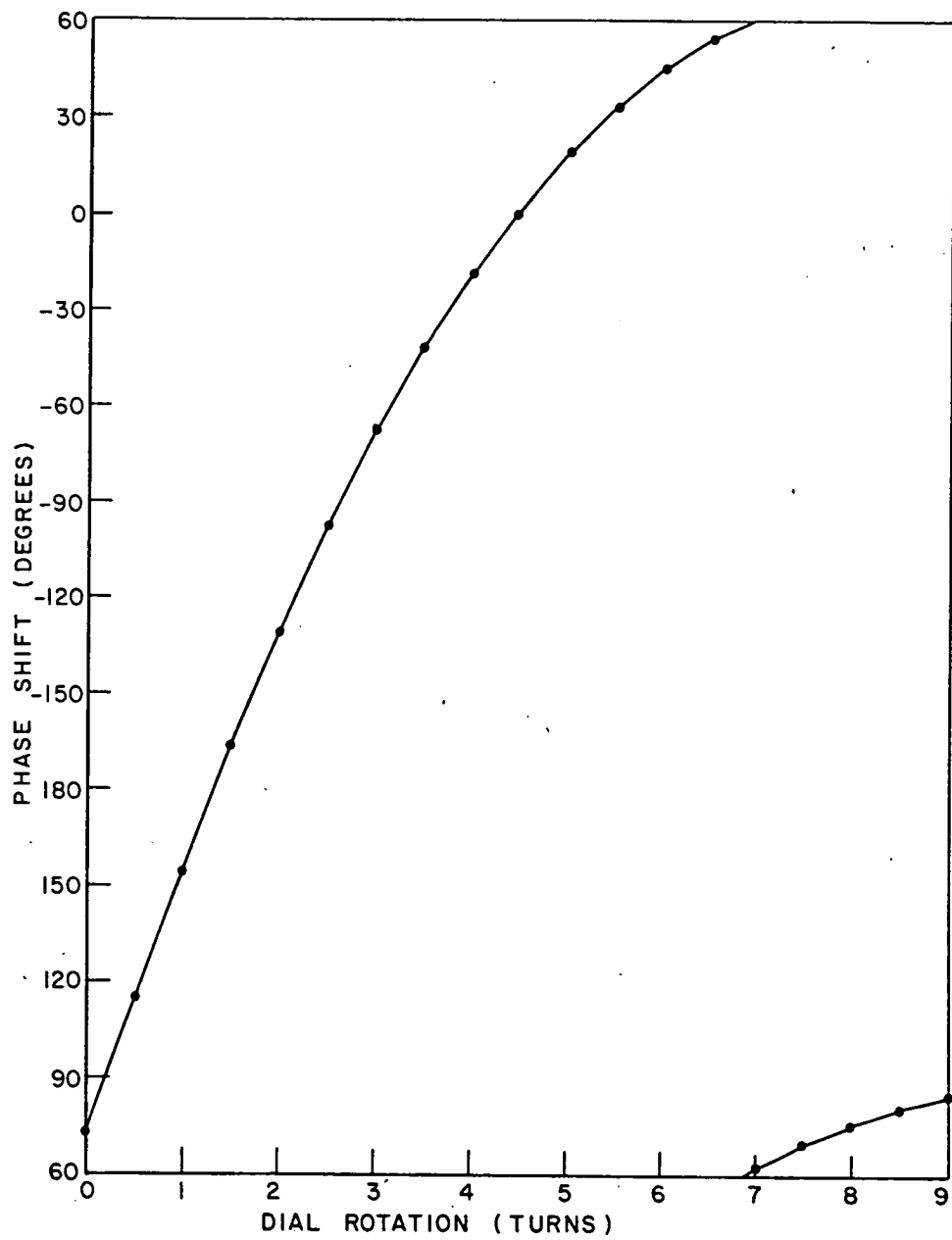


Figure 13. Phase shifter control characteristic.



digital computer enables us to compensate for any differential phase shift that may exist. Finally, to relate a particular phase shifter setting to the interelement phase shift induced, the phase shifters must be calibrated. System calibration is described in a later section.

Noise sources are used in the array simulator to simulate the cumulative effect of sky noise and receiver/amplifier thermal noise in each of the five antenna elements. Four separate noise sources, are used, as shown in Figure 11. Note that the noise in the correlator branches is from a different noise source than the noise in the signal branches, and therefore uncorrelated with the noise in the signal branches. Thus the four auxiliary channels are the inputs to two modified adaptive array feedback loops with complete noise decorrelation. Since the correlator branches do not contribute to the array output (in array processor) the same noise source is used for both auxiliary element correlator channels, effecting a hardware savings equal to the cost of one noise source.

The schematic diagram of a noise source is shown in Figure 14. It consists of a broadband, reverse biased breakdown noise diode encapsulated with current limiting resistor and DC blocking capacitor in ND1, a fixed gain IF amplifier, and a voltage variable attenuator for control. Voltage, and hence noise level control is also achieved through a potentiometer adjustable from the array simulator front panel. The IF amplifier gain is 46 dB. This gives the noise source a maximum output power of -31 dBm over the channel noise bandwidth of 8.4 MHz. The variable attenuator provides control over a noise power range of >40 dB from -75 dBm to -31 dBm. With the front panel control dials calibrated

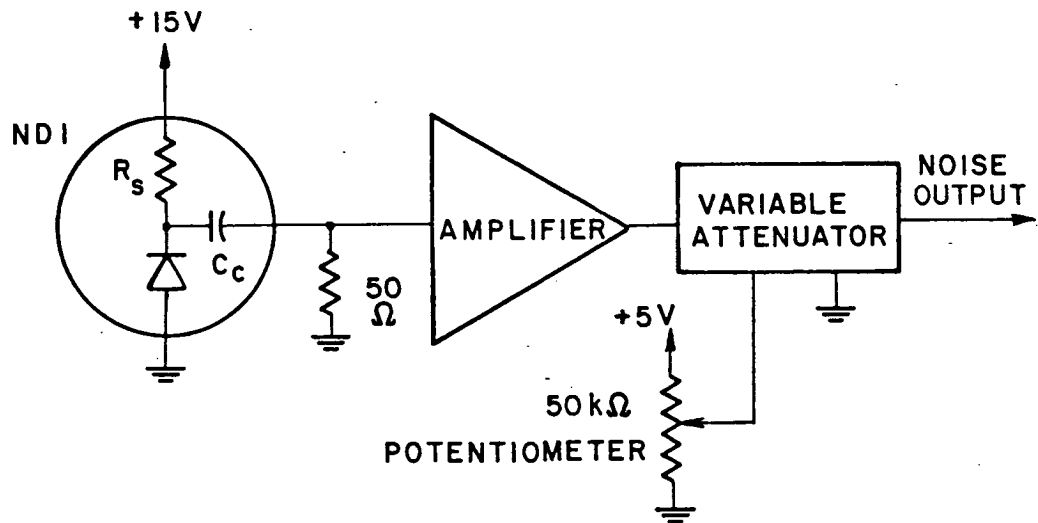


Figure 14. Schematic of a noise source.

in hundredths of turns, the noise level in any channel can be set to within 0.2 dB of the desired value. Figure 15 shows a calibrated noise source control characteristic. Details of noise source calibration are given in a later section.

### 3.6 Array Processor

Together with the system computer, the array processor forms the two modified feedback loops of the sidelobe canceler, through which the weight control algorithms are implemented. A simplified block diagram of the array processor is shown in Figure 16. The auxiliary channel correlator branch signals are down converted to baseband and quadrature detected, as is the array output. These baseband voltages are simultaneously sampled, A/D converted and read by the system computer

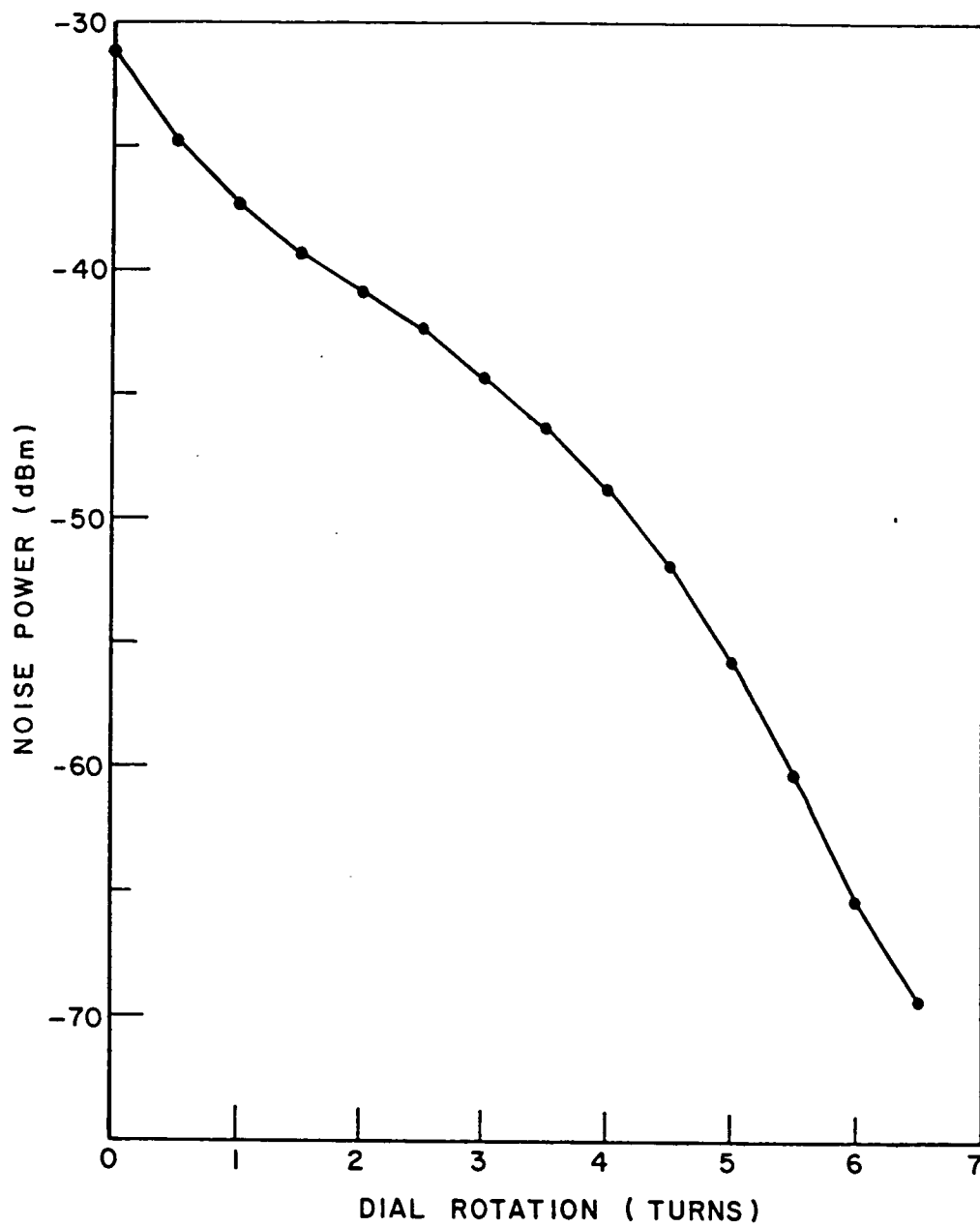


Figure 15. Noise source control characteristic.

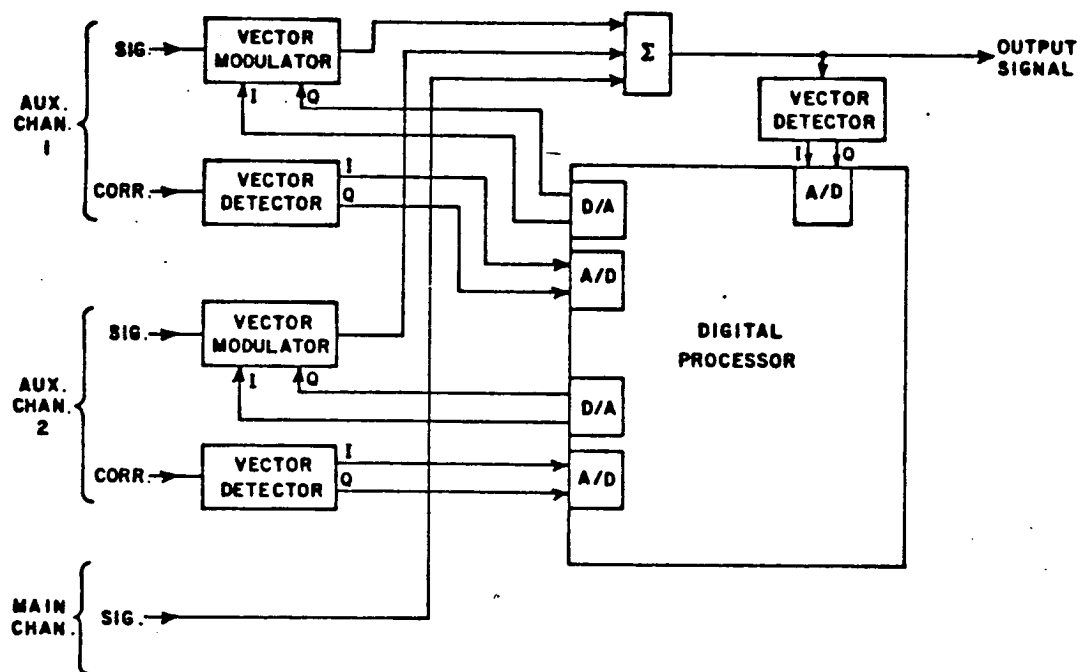


Figure 16. Simplified block diagram of the array processor.

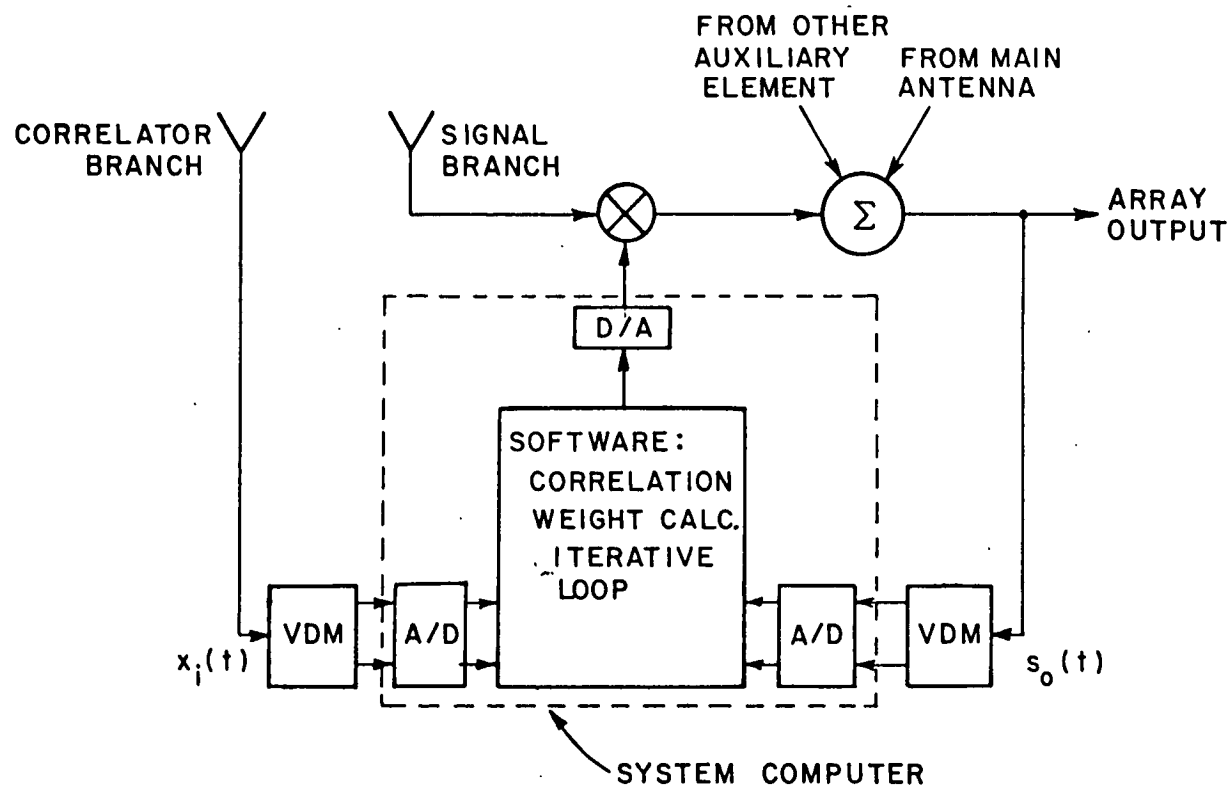


Figure 17. System implementation of a modified feedback loop.

which implements the weight control equation and calculates the array weights. The new weights are then D/A converted and applied to the auxiliary signal branches as I and Q control voltages of the two vector modulators. The weighted auxiliary elements are then summed with the main channel signal to form the array output.

The system is hybrid because analog weights are applied to analog signals, but the weights are calculated from discrete time samples of the element signals and the array output. The system implementation of a modified feedback loop is shown in Figure 17. The correlation between the auxiliary channels and the array output is done on the sampled data in software, which then updates the array weights. By implementing the weight control equation in software, many problems often encountered with analog feedback loops, especially at low signal levels, are avoided. These include effects of DC offset voltages, stray coupling and feedthrough associated with the correlator multiplier, and leakage and DC offset voltages in analog integrators. Also, the utilization of a digital computer in the experimental system provides great flexibility, not only in algorithm implementation, but also in system calibration and quantitative performance evaluation. Figure 18 is a detailed block diagram of the array processor. Bandpass filters limit the channel bandwidth to 6 MHz, that of a conventional broadcast television signal. 70 MHz IF components are used throughout the array processor. Power dividers  $\Delta 1$ - $\Delta 5$  provide test ports to the array processor front panel for convenient monitoring of the input signals. A variable attenuator,  $\alpha 1$ , controls the level of the main channel signal in the array output.  $\Sigma 1$  is the sum junction which forms the array output signal.

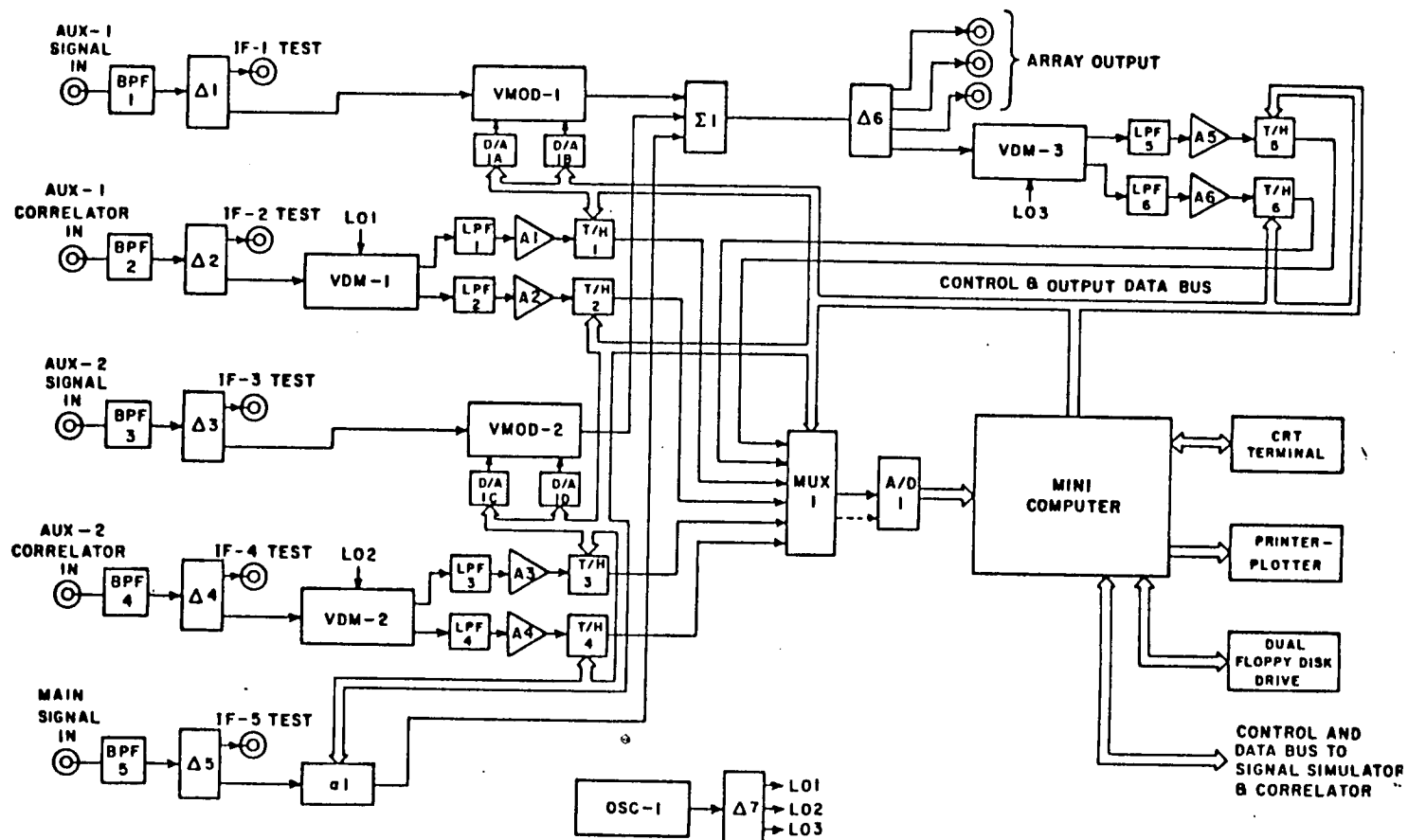


Figure 18. Detailed block diagram of the array processor.

Each auxiliary element correlator branch signal is down converted to I and Q video with vector detectors, or vector demodulators (VDMs). A schematic of one of these devices is given in Figure 19. The reference signal is local oscillator at the center frequency of 69 MHz. It is derived either from a separate oscillator or from the desired signal oscillator of the signal simulator. The multipliers in the figure are actually double balanced mixers, and the VDM is linear with respect to the signal when the reference signal (LO) is +10 dBm or larger and strong relative to the signal. Individual testing of these devices have shown their linearity down to signal levels of -60 dBm (CW into 50 ohms), and their accuracy as phase detectors to within  $\pm 5^\circ$ . A signal level of -60 dBm is the minimum detectable signal, or the sensitivity limit of the system.

The I and Q outputs of each vector demodulator are processed prior to being sampled and fed into the A/D converters of the system computer. A low-pass filter first removes the second harmonic, leaving baseband video. Then the baseband voltages are amplified to utilize the full dynamic range of the A/D converter. Track-and-Hold amplifiers (THAs) allow the multiplexing of all six VDM outputs to a single A/D converter. Triggering all the THAs simultaneously enables the A/D converter to sequentially digitize six channels, while maintaining the effective sampling of all six channels at the same real time. This is necessary to preserve the signal and noise correlation between samples of different channels. The THAs also allow the digitization of signals of higher bandwidths than the A/D converter can digitize alone. Detailed circuit diagrams of the VDM output circuitry is given in Appendix A.



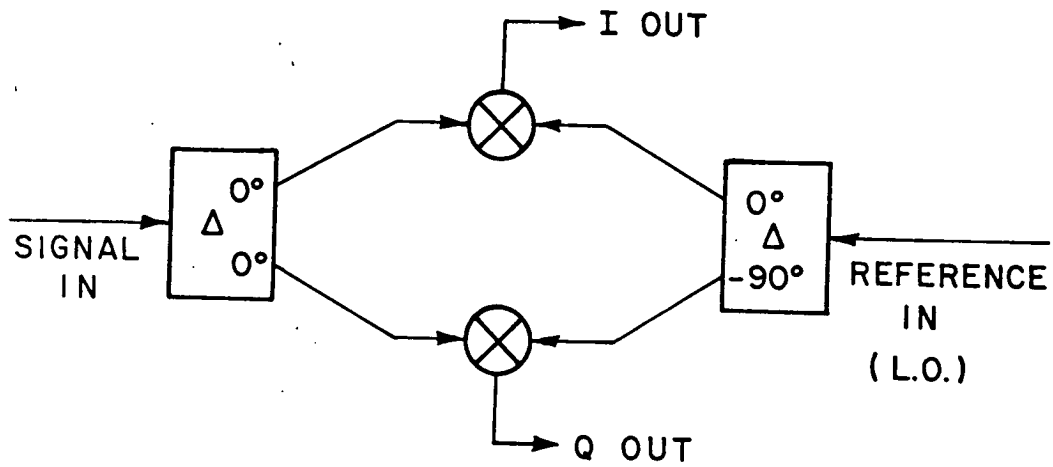


Figure 19. Schematic of vector demodulator.

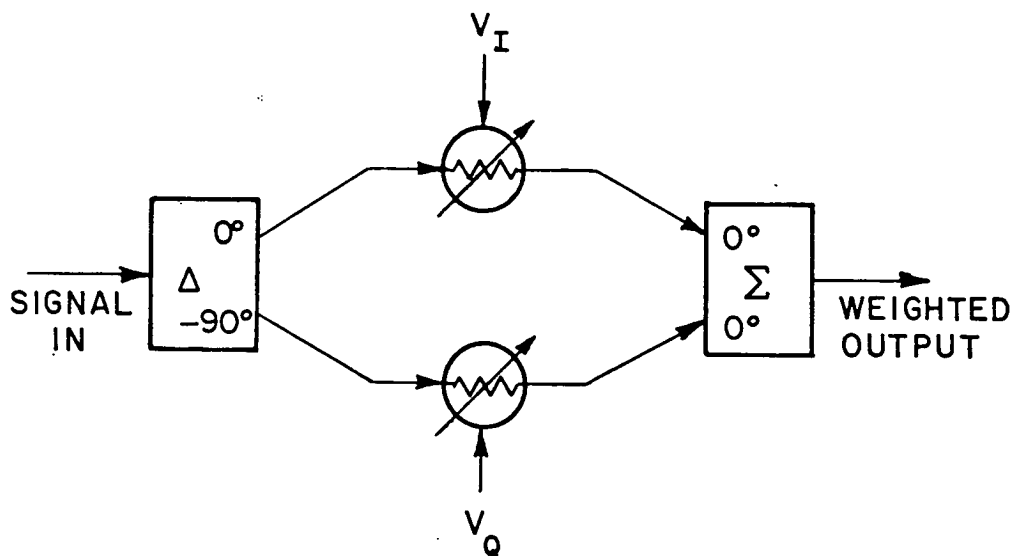


Figure 20. Schematic of vector modulator.

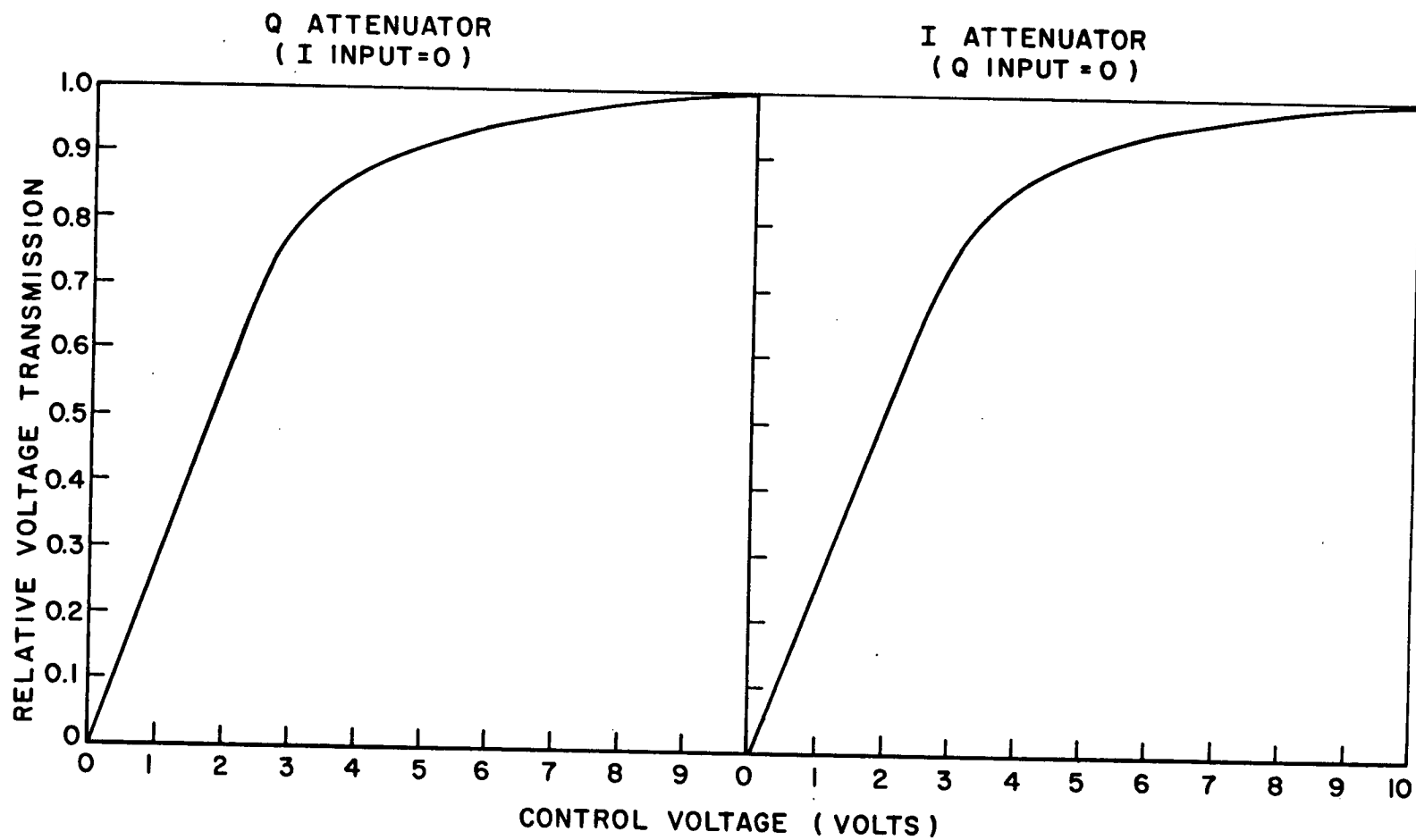


Figure 21. Vector modulator control characteristics.

After the computer samples the VDM outputs, the weights are calculated and applied to the processor via D/A converters to the vector modulators. As shown in Figure 20, a vector modulator consists of a quadrature hybrid which divides the input signal into orthogonal components, independently voltage controlled I and Q linear attenuators, and an in-phase power combiner forming the weighted output. The measured characteristics of one of these devices is shown in Figure 21. Increasing the I or Q voltage,  $V_I$  or  $V_Q$ , increases the voltage transmission in either the I or Q branch, corresponding to increasing the I or Q weight. When operation is constrained to the linear portion of the control curves:

$$w_{iI} = kV_{iI} , w_{iQ} = k V_{iQ} \quad (16)$$

or in complex form:

$$w_i = w_{iI} - jw_{iQ} = |w|e^{-j\theta} ;$$

$$|w| = k \sqrt{V_I^2 + V_Q^2} ;$$

$$\theta = \tan^{-1} \left( \frac{V_Q}{V_I} \right) \quad (17)$$

where  $k$  is the slope of the control curve in the linear region. The capabilities of this device are best illustrated by looking at the complex plane of Figure 22. The outer square is the complete range of weight values, with corners defined with both I and Q control voltages at maximum;  $V_I = \pm 10$  V,  $V_Q = \pm 10$  V. The insertion loss at these points is 6 dB. The inscribed circle is defined as the unit circle  $|w_i| = 1.0$ . Thus the unit circle is at 9 dB relative loss between vector modulator

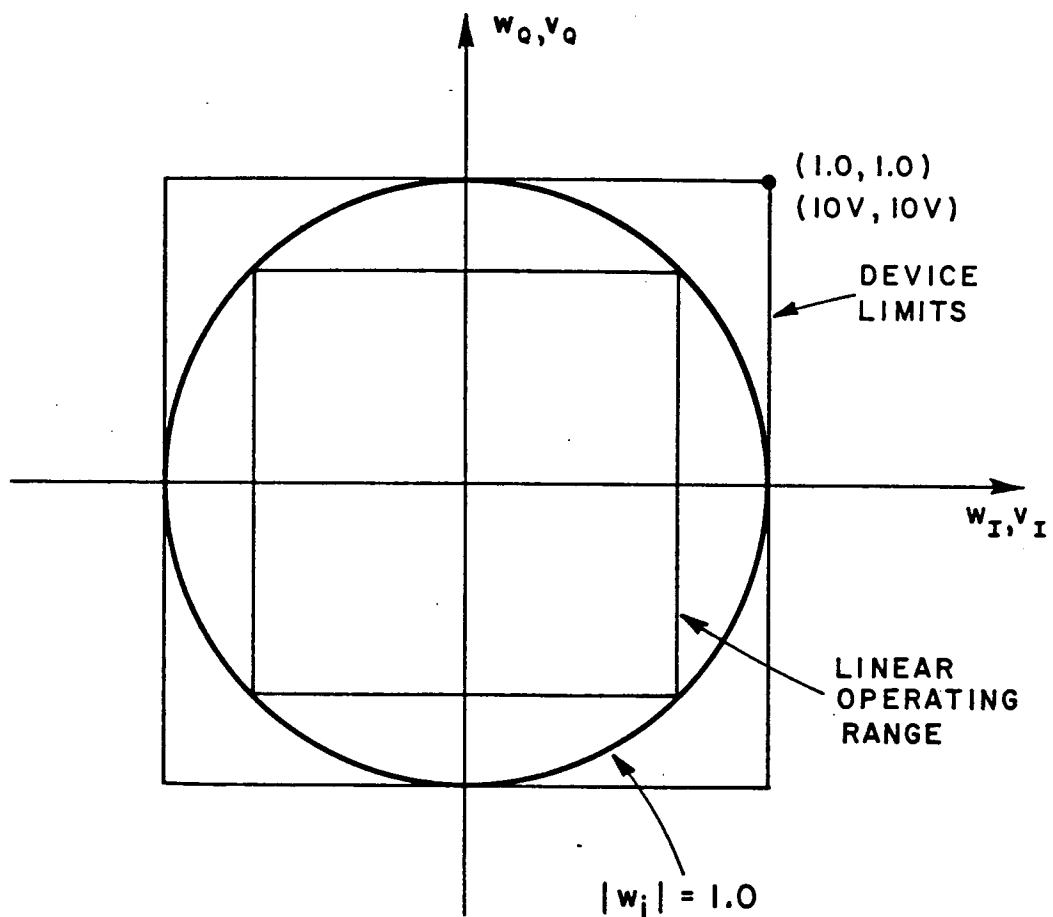


Figure 22. Vector modulator weighting capabilities.

input and output. The inner square of Figure 22 is the range of weight values achievable by restricting operation to the linear portion of the control characteristics, as seen from Figure 21 to be approximately

$$|w_{iQ}| < 0.707 \quad (18)$$

This restriction translates to a 3 dB loss in programmable weight magnitude. To utilize the full capabilities of the vector modulators, the data points of the control curves are digitized and stored in a look-up table in the system computer. The system software calculates the control voltages necessary to apply a desired weight vector by linearly interpolating between control curve data points, where the number of data points is sufficient to ensure an accurate representation of the control curve.

Because the VMODs are passive, the weighted auxiliary element signals will always be of smaller power than the auxiliary element signals themselves. This means that the adaptive array will be unable to null an interfering signal whose amplitude is larger in the main antenna than in the auxiliary elements. For all cases of interest here, the interfering signal is assumed to enter the MAIN channel through the main antenna sidelobes. Because the auxiliary elements are of at least moderate directivity and pointed in the interfering signal directions, the interfering signal levels in the auxiliary elements will be larger than their levels in the main antenna. For this reason, even the 6 dB inherent loss through the vector modulators does not hamper the ability of the system to suppress the interference. The inherent loss through the VMODs does affect adaptive array behavior in another way. Since

there is no corresponding loss in the main channel, the noise power at the array output will be predominantly due to the noise in the main channel. This is because even at maximum weight magnitudes, the noise power added by each auxiliary element is at least 6 dB below the noise level in the main channel. Actually, this is beneficial in that the output SNR will not be degraded as much by noise contributions from the weighted auxiliary elements.

For the experiments to be described here, the inputs to the processor are the signals from the array simulator. However, in future applications, this same array processor may be used in conjunction with signals from an actual antenna array, after down conversion to the processor IF of 69 MHz.

### 3.7 System Calibration

Before any experiments can be conducted with the experimental system, the system must be calibrated. Several procedures have been followed, some of which are repeated each time the system is used, which can be classified as calibration procedures.

First is the calibration of the continuously variable components of the array simulator, namely the phase shifters and the noise sources. These procedures were conducted once, when the system construction was completed. To be able to accurately simulate interfering signal angles of arrival, the phase shifter manual controls were calibrated with respect to the interelement phase shifts which they induce. A vector voltmeter was used in the phase measurement set-up shown in Figure 23 for this purpose. One of the resulting calibration curves is shown in

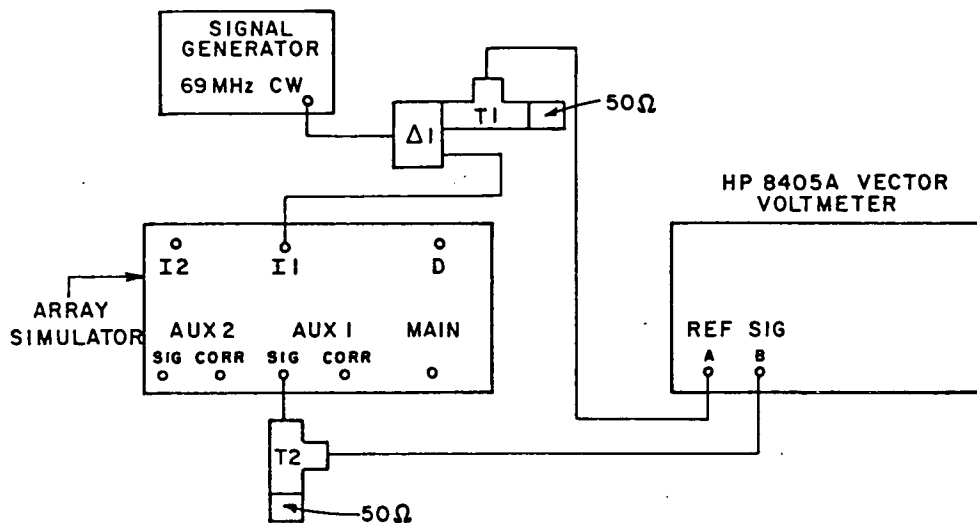


Figure 23. Phase measurement set-up.

Figure 13. To be able to fix given noise levels in each channel, the noise source controls were also calibrated. Noise power measurements were made at the array simulator outputs with a calibrated spectrum analyzer, and then normalized to the noise bandwidth of a channel in the experimental system. A plot of a noise source calibration curve was shown in Figure 15. Other variable devices, such as the step attenuators used in the array simulator, are factory calibrated and their performances were individually verified before being placed in the system.

Another calibration procedure, which is followed every time the system is powered up is the checking and zeroing of DC offset voltages in the detector amplifiers of the array processor. Potentiometers have been provided on each amplifier specifically for this purpose. For the most part, adjustments are not necessary, except when the system has

been idle for an extended period of time. Still, it is an important procedure because the presence of DC offsets can seriously degrade performance.

Finally, two other procedures which could be considered calibration, involve the use of sampled data, and are conducted with each experiment. One is the compensation for differential phase shifts which exist in each adaptive array feedback loop. The other is the use of sampled data to provide a continuing estimate of DC offset voltages at the detector amplifiers, and a correction to the received data. Mostly, this is done as an extra precaution against any offset drift during the course of an experiment. No such problems have been observed, but the precaution is left as a permanent part of the system software. More will be said about phase compensation as it arises in the context of algorithm implementation in Chapter IV.

### 3.8 System Computer

The computer for the experimental system is a Digital Equipment Corporation PDP-11/23. The system software is written in FORTRAN IV. It implements the weight control equation, controls data acquisition, and controls the other system blocks, through peripherals including A/D and D/A converter modules, a parallel line TTL output module, and a programmable clock module. Although the system software is a very important part of the experimental system, its description is essentially contained in the descriptions of the various functions it performs. The FORTRAN code for the programs and subroutines written for the experimental system are contained in Appendix B.



### 3.9 Data Acquisition

The most basic function of the system software is to obtain data by sampling the auxiliary channel and array output detector outputs. These samples are used both to compute and update the array weights and to evaluate adaptive array performance. However, the conversion time of the system A/D converter is much too large to allow real time sampling of the six output signals at a rate close to the Nyquist rate. Therefore, a sampling scheme is used which takes advantage of both the periodicity of the element signals and their pulsed nature to achieve an effective sampling rate much higher than is possible in real time.

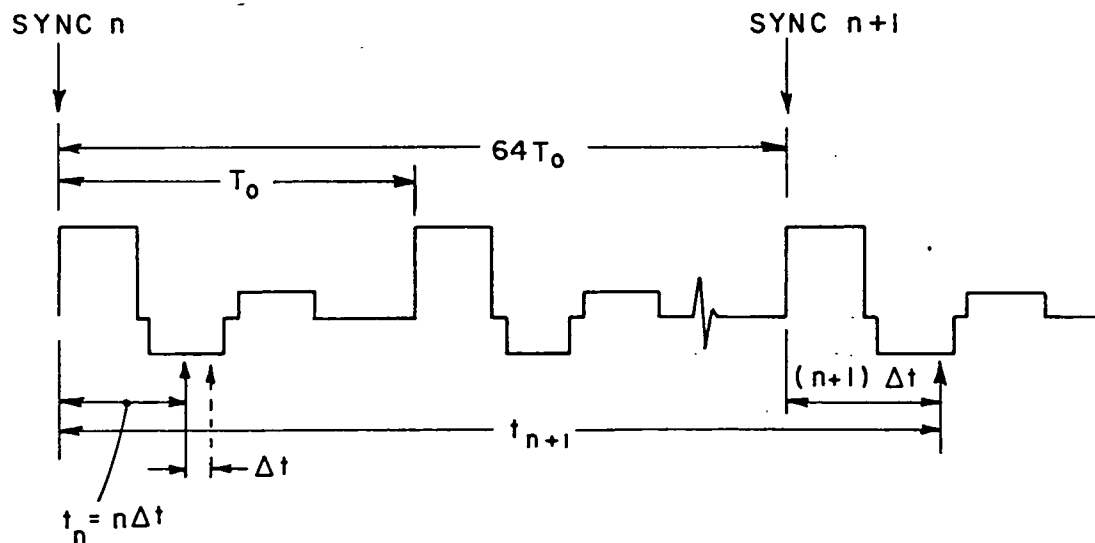


Figure 24. Diagram of sampling procedure.

A diagram showing this sampling procedure is shown in Figure 24. It depends on a trigger from the signal simulator which indicates to the computer the start of a pulse repetition period. This trigger, or sync signal, is a 246 Hz square wave originating from the pulse generator circuit of the signal simulator. The leading edge of this trigger signal is synchronized with the leading edge of the desired signal pulse modulation. The frequency of the trigger signal is slow enough to allow all A/D conversions plus software control to occur prior to the next triggering edge. Also, the time between triggering edges is long enough (4.06 msec) so that successive samples of the noise process are essentially uncorrelated. The sync signal starts a counter which counts a preset number, then generates an overflow pulse and stops. The array processor receives this overflow pulse which simultaneously puts the six track and hold amplifiers of the detector outputs into the 'hold' mode. The processor outputs are then sequentially A/D converted. After the sample values are read into the system computer, the software resets the THAs back to 'track' mode, and increments the clock count to prepare for the next set of samples. In other words, the delay from the sync signal to the sampling instant is varied so that successive samples are taken at different points in the waveform period. Successive samples are separated in real time by about  $64T_0$ , where  $T_0$  is the period of the desired signal pulse modulation. Because the signals are periodic, samples  $X_n$  and  $X_{n+1}$  taken at times  $t_n = n\Delta t$  and  $t_{n+1} = (n+1)\Delta t + 64T_0$  are equal to samples taken at times  $t_n = n\Delta t$  and  $t_{n+1} = (n+1)\Delta t$ . Thus the effective sampling interval is the delay increment  $\Delta t$ . As this process is repeated,  $t_n$  is varied (by changing the clock count) and the complete

modulation period is sampled through. The programmed clock rate is 1 MHz, so one count corresponds to a time interval of 1  $\mu$ sec. Since the waveform period is 63.49  $\mu$ sec; one scan of the pulse repetition period consists of 63 samples which are acquired at an effective sampling rate of 1 MHz. Large numbers of samples are obtained by repeating the complete waveform scan a programmed number of times. For the staggered pulse modulation of the signal simulator, the detector outputs have a baseband (first null) bandwidth of  $1/\tau=84$  kHz, where  $\tau$  is the pulse width of the modulation. Since the effective sampling rate is 1 MHz, which is several times the Nyquist rate for these output signals, there will be no aliasing effects in the sampled data.

In this chapter, the experimental system has been described. First the particular signal scenario being simulated was defined. The hardware details and functions of the individual system blocks were discussed. Finally, system calibration and the sampling procedure implemented were also discussed. The subject of the next chapter is the use of this sampled data for feedback control of the array weights and for performance evaluation.

## CHAPTER IV

### EXPERIMENTAL PROCEDURES

#### 4.1 Introduction

After the vector demodulator outputs are sampled, the system computer contains in memory a discrete time (discrete amplitude also, due to 12 bit A/D quantization) representation of the element signals and of the array output. This data is used for two purposes: First to implement the adaptive array algorithm and control the array weights, and second, to evaluate system performance. In this chapter, these procedures are described. In both cases, the use of sampled data and a digital computer to perform these functions allows system software to compensate for hardware constraints.

#### 4.2 Algorithm Implementation

##### 4.2.1 Weight Control

Once the demodulated element signals and array output are sampled, the system software performs the correlation necessary to update the array weights, according to the weight control equation given in Equation (1):

$$\frac{dw_i}{dt} = k \left( u_{si} - \tilde{x}_i^*(t) \tilde{s}_o(t) \right) \quad (19)$$

(19) is in complex form, and is equivalent to the real form [7]

$$\frac{d}{dt} w_{iP} = k \left( u_{siP} - x_{iP}(t) s_o(t) \right) \quad (20)$$

where  $P=I$  or  $Q$ .  $w_{iI}$  and  $w_{iQ}$  are the I and Q weights applied to the  $i^{\text{th}}$  auxiliary element.  $x_{iI}(t)$  and  $x_{iQ}(t)$  are the orthogonal signals output from quadrature hybrids at the  $i^{\text{th}}$  auxiliary element. In the experimental system,  $x_{iI}(t)$  and  $x_{iQ}(t)$  are formed internal to the vector modulators used in each feedback loop.

To implement the weight control equation with discrete time signals, Equation (20) is converted to a difference equation using a forward difference approximation to the derivative:

$$\frac{d}{dt} w_{iP} \sim \frac{w_{iP}(n+1) - w_{iP}(n)}{\Delta t} \quad (21)$$

Then (20) becomes

$$w_{iP}(n+1) = w_{iP}(n) + \gamma \left( u_{siP} - x_{iP}(n) s_o(n) \right) \quad (22)$$

where  $w_{iP}(n), x_{iP}(n), s_o(n)$  denote the values of  $w_{iP}(t), x_{iP}(t)$ , and  $s_o(t)$  at the sample time  $t=n\Delta t$ .  $\gamma=k\Delta t$  is the loop gain for the discrete case.

Because of A/D conversion speed limitations in the sampling hardware of the experimental system (and to avoid the expense of very high speed digital processing hardware) the sampling is done at baseband on the demodulated I and Q outputs of each vector detector. To implement Equation (22), the products  $x_{iP}(n)s_o(n)$  must be expressed in terms of the received data. Referring to Figure 25, let  $y_{iI}(n)$  and  $y_{iQ}(n)$  be the received samples from the  $i^{\text{th}}$  auxiliary channel vector demodulator. The auxiliary element signal into the VDM,  $x_i(t)$  is

$$x_i(t) = \sqrt{2} a(t) \cos(\omega_o t + b(t)) \quad (23)$$

where  $a(t)$  and  $b(t)$  are narrowband amplitude and phase modulation present, and  $\omega_o = 2\pi f_o$  is the carrier frequency. The local oscillator is a CW signal at the carrier frequency, and assumed to be coherent with

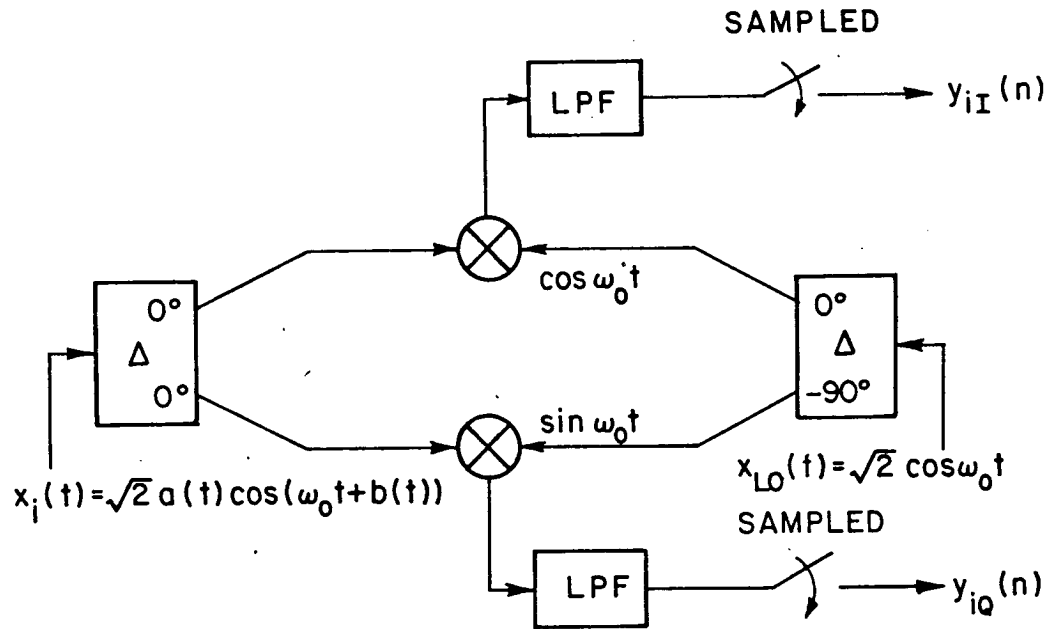


Figure 25. Signal processing in VDM.

the carrier component of  $x_i(t)$ . Then from Figure 25,

$$y_{iI}(t) = \frac{1}{2} a(t) \cos b(t) \quad (24)$$

$$y_{iQ}(t) = -\frac{1}{2} a(t) \sin b(t) . \quad (25)$$

Define

$$y_i(t) = y_{iI}(t) + jy_{iQ}(t) . \quad (26)$$

In terms of  $y_i(t)$ ,

$$x_i(t) = 2\sqrt{2} \operatorname{Re} \left\{ y_i^*(t) e^{j\omega_0 t} \right\} . \quad (27)$$

Splitting the element signal into I and Q components yields

$$x_{iI}(t) = 2 \operatorname{Re} \left\{ y_i^*(t) e^{j\omega_0 t} \right\} \quad (28)$$

$$x_{iQ}(t) = 2 \operatorname{Re} \left\{ -j y_i^*(t) e^{j\omega_o t} \right\} \quad (29)$$

Furthermore let the received signals at the array output VDM be denoted by  $z_I(t)$  and  $z_Q(t)$ . Then

$$s_o(t) = \operatorname{Re} \left\{ z^*(t) e^{j\omega_o t} \right\} \quad (30)$$

where  $s_o(t)$  is the array output and  $z(t) = 2\sqrt{2} \left( z_I(t) + jz_Q(t) \right)$ . The constant  $2\sqrt{2}$  is lumped with  $z(t)$  for mathematical convenience. In terms of I and Q received data, (28), (29), and (30) become

$$x_{iI}(t) = y_{iI}(t) \cos\omega_o t + y_{iQ}(t) \sin\omega_o t \quad (31)$$

$$x_{iQ}(t) = -y_{iQ}(t) \cos\omega_o t + y_{iI}(t) \sin\omega_o t \quad (32)$$

$$s_o(t) = z_I(t) \cos\omega_o t + z_Q(t) \sin\omega_o t \quad (33)$$

The correlation products of the weight control equation can now be expressed in terms of the received signals:

$$x_{iI}(t)s_o(t) = y_{iI}(t)z_I(t) \left( 1 + \cos 2\omega_o t \right) + y_{iQ}(t)z_Q(t) \left( 1 - \cos 2\omega_o t \right) + \left( y_{iI}(t)z_Q(t) + y_{iQ}(t)z_I(t) \right) \sin 2\omega_o t \quad (34)$$

$$x_{iQ}(t)s_o(t) = y_{iI}(t)z_Q(t) \left( 1 - \cos 2\omega_o t \right) - y_{iQ}(t)z_I(t) \left( 1 + \cos 2\omega_o t \right) + \left( y_{iI}(t)z_I(t) - y_{iQ}(t)z_Q(t) \right) \sin 2\omega_o t \quad (35)$$

The double frequency terms are integrated out, leaving

$$x_{iI}(t)s_o(t) = \operatorname{Re} \left\{ y_i^*(t) z(t) \right\} = \operatorname{Re} \left\{ y_i(t) z^*(t) \right\} \quad (36)$$

$$x_{iQ}(t)s_o(t) = -\operatorname{Im} \left\{ y_i(t) z^*(t) \right\} = \operatorname{Im} \left\{ y_i^*(t) z(t) \right\} \quad (37)$$

Converting back to discrete form yields the weight control equations involving the sampled data  $y_i(n), z(n)$ :

$$w_{iI}(n+1) = w_{iI}(n) + \gamma \left[ u_{siI} - \operatorname{Re} \left\{ y_i(n) z^*(n) \right\} \right] \quad (38)$$

$$w_{iQ}(n+1) = w_{iQ}(n) + \gamma \left[ u_{siQ} + \text{Im} \left( y_i(n) z^*(n) \right) \right] \quad (39)$$

In the experimental system, a pulse modulation scheme where only one signal (desired or interfering) is present at a time was implemented to facilitate quantitative study. For a realistic investigation, all signals must appear to be simultaneously present as far as the adaptive array is concerned. To do this, the correlation estimates used for each weight update are based on an average over several pulse repetition periods, rather than on the single product  $y_i(n)z(n)$ . This average, denoted  $C_i$ , is calculated as

$$C_i = \frac{1}{N} \sum_{j=1}^N y_i(j) z^*(j) \quad (40)$$

where  $N$  is the total number of samples taken for each weight iteration.

The weight control equations become:

$$w_{iI}(n+1) = w_{iI}(n) + \gamma \left[ u_{siI} - \text{Re} \{ C_i \} \right] \quad (41)$$

$$w_{iQ}(n+1) = w_{iQ}(n) + \gamma \left[ u_{siQ} + \text{Im} \{ C_i \} \right] \quad (42)$$

where  $n$  denotes the  $n^{\text{th}}$  weight update. Since  $C_i$  depends on samples from all incident signals, as well as thermal noise, each weight update is a response to the complete signal and interference environment.

There are several other reasons for averaging prior to each weight update. First, because the interfering signals are weak, a major component of each sample product  $y_i(n)z^*(n)$  is due to thermal noise. If the weights are updated with each sample, the weights will follow instantaneous noise fluctuations. However, because the noise components of the two feedback loops have been decorrelated, the average values of these weight fluctuations will equal the weight values determined solely by the interference. Thus the array weights will reach a steady state



in response to the interference and not the noise. Therefore, the weights will still reach a steady state in response to the interference and not the noise. Still, because the noise is always present, the weight variance about the steady state values will be large. On the other hand, performing a correlation over several pulse repetition periods effectively averages out the noise prior to each weight update. This reduces weight fluctuation due to noise and the weight variance about the steady state values is small. Secondly, in a typical earth station receive environment, the signal scenario is stationary, or very slowly varying. The desired and interfering signal locations are known, and change very little. The adaptive array weights will reach their steady state values and remain there, until either the interference ceases, or other interfering signals become incident on the array. Thus rapid weight updates are not necessary.

#### 4.2.2 Steering Vector Generation

To prevent any cancellation of the desired signal while suppressing the interference, and thus maximizing output SINR, the steering vector should be chosen equal to the desired signal correlation vector. In terms of individual I and Q components,

$$u_{siI} = E \left\{ \tilde{x}_{diI}^*(t) \tilde{x}_{do}(t) \right\} \sim \frac{1}{T} \int_0^T \tilde{x}_{diI}(t) \tilde{x}_{do}(t) dt \quad (43)$$

where  $\tilde{x}_{diI}(t)$  is the desired signal component of the  $i^{th}$  auxiliary element I or Q signal, and  $\tilde{x}_{do}(t)$  is the desired signal component of the

main antenna signal. The steering vector components are calculated from

knowledge of the desired signal angle of arrival, and the gain of the main and auxiliary antennas in this direction. In the experimental system, the interfering signals can be removed, leaving only the desired signal present in each channel. Thus the desired signal in the auxiliary antennas can be obtained from the samples of the auxiliary channel vector demodulator outputs. By fixing the array weights at zero the desired signal in the main channel can be sampled through the array output detector. Because the optimal steering vector is a correlation, it is computed (in software) from these samples in the same manner as the correlation  $C_i$  used in the weight control equation. Thus

$$u_{si_I} = \frac{1}{2} \operatorname{Re} \left\{ \frac{1}{N} \sum_n y_{di}(n) z_d^*(n) \right\} \quad (44)$$

$$u_{si_Q} = -\frac{1}{2} \operatorname{Im} \left\{ \frac{1}{N} \sum_n y_{di}(n) z_d^*(n) \right\} \quad (45)$$

where the d subscript indicates that only the desired signal is present.  $z_d$  is obtained with the array weights equal to zero. Equations (41) and (42) now simplify to

$$w_{iI}(n+1) = w_{iI}(n) - \gamma \operatorname{Re} \{ C_i - u_{si} \} \quad (46)$$

$$w_{iQ}(n+1) = w_{iQ}(n) + \gamma \operatorname{Im} \{ C_i - u_{si} \} \quad (47)$$

where

$$u_{si} = \frac{1}{N} \sum_n y_{di}(n) z_d^*(n) . \quad (48)$$

#### 4.2.3 Phase Compensation

For the array feedback loops to operate as desired, it is required that corresponding signal components in the two branches of each

feedback loop are highly correlated at the inputs to the loop correlator. In the hardware implementation of the array feedback loops (array processor), shown in Figure 26, a signal in the signal branch of the feedback loop undergoes a delay  $T_s$  in reaching the array output VDM, while the corresponding signal in the correlator branch is delayed by  $T_c$  in reaching the correlator channel VDM. The delay  $T_s$  consists of delays due to cabling, delay through the quadrature hybrids of the vector modulator, delay in the output sum hybrid, and delays through other hybrids not shown which provide test ports on the array processor. The delay  $T_c$  is due solely to a fixed cable length. Therefore  $T_s > T_c$ , and a differential time delay  $T_o = T_s - T_c$  exists between signals at the loop correlator inputs. This causes corresponding signal components to be partially decorrelated at the inputs to the loop correlator. This differential time delay appears as a differential phase shift between a signal component detected at one correlator input and the corresponding component of the signal detected at the other correlator input.

This differential time delay has two effects on array performance [5]. First, it causes the I channel to correlate with the Q channel, such that a change in  $w_I$  results in a change in  $w_Q$ , and vice versa. As a result, the weights oscillate during transients. For time delays such that the differential phase shift  $\phi_o$

$$\phi_o = \omega_o T_o \quad (49)$$

is in the range  $-\pi/2 < \phi_o < \pi/2 \pmod{2\pi}$ , the weight transients die out and the system reaches steady state. For differential phase shifts outside

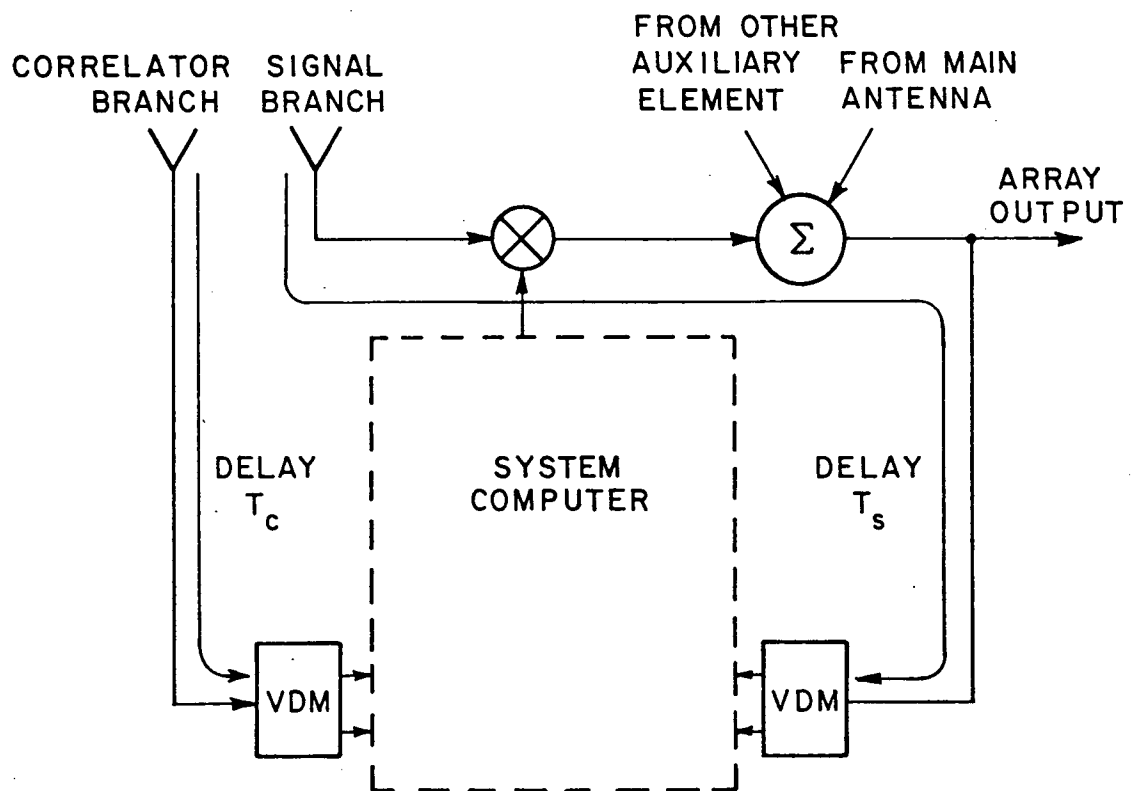


Figure 26. Time delays in feedback loops.

this range, the feedback loop becomes unstable. In fact, the observation of weight instability in the experimental system brought attention to this problem. In analog feedback loops, weight oscillation and weight instability can be avoided by inserting a delay line or a phase shifter in one of the feedback loop branches such that

$$\phi=0 \pmod{2\pi} \quad (50)$$

In the hybrid feedback loops of the experimental system, differential phase shift is compensated for by measuring the differential phase shift in each feedback loop, storing the values in the system computer, and using them as a software correction to the received data. To measure the differential phase in the  $i^{\text{th}}$  feedback loop,  $w_{iI}$  is set to a non-zero value, and  $w_{iQ}$  is set to zero, so that the weight itself does not induce a phase shift. The contributions to the array output from the other feedback loop and from the main channel are eliminated by appropriate array simulator settings. Then the detector outputs are sampled and the correlation  $C_i$  calculated

$$C_i = \frac{1}{N} \sum_n y_i(n) z^*(n) = M_i e^{j\theta_{ci}} \quad (51)$$

$\theta_{ci}$  is the differential phase shift. All subsequent data received at the correlator branch VDMs are phase adjusted by an amount  $\theta_{ci}$ , prior to performing the correlation with the array output samples. The phase compensated data,  $y'_i(n)$ , are obtained by a rotation in the complex plane of  $\theta_{ci}$ , which brings the received signals at the correlator branch input in phase with the corresponding signals at the SIGNAL branch input to the loop correlator:

$$y'_i(n) = y_i(n) e^{j\theta_{ci}} \quad (52)$$

The procedure of measuring the differential phase shifts present in each feedback loop is incorporated into the system software, and is repeated with each experiment, to keep track of any drift that may occur over time.

The second effect of differential time delays in the adaptive array feedback loops is to decorrelate the signals of the two branches, whenever the signals have non-zero bandwidth. This will occur whenever  $T_0$  is not exactly zero. This decorrelation is in addition to the decorrelation resulting from interelement propagation delays for non-zero bandwidth signals. The performance of an adaptive array with quadrature hybrid processing degrades as the interference bandwidth increases, even when the differential time delays are zero. The presence of differential time delays in the array feedback loops causes a further degradation in the nulling capability of the array, and this degradation also increases as the interference bandwidth increases.

#### 4.2.4 Loop Gain and Integration Time

The weight control equations implemented in software are, from (46) and (47)

$$w_{iI}(n+1) = w_{iI}(n) - \gamma \operatorname{Re} \left[ \frac{1}{N} \sum_{n=1}^N y'_i(n) z^*(n) - u_{si} \right] \quad (53)$$

$$w_{iQ}(n+1) = w_{iQ}(n) + \gamma \operatorname{Im} \left[ \frac{1}{N} \sum_{i=1}^N y'_i(n) z^*(n) - u_{si} \right] \quad (54)$$

where the  $y'_i$  are the phase compensated received samples from the auxiliary channel vector demodulators. The parameters left to discuss are the loop gain  $\gamma$ , and the number of samples  $N$  taken with each weight

iteration. To ensure the stability of the weights, the loop gain must satisfy the bound [7]

$$0 < \gamma < 1/P_t \quad (55)$$

where  $P_t$  is the total power received by the array. For each test with the experimental system, both  $\gamma$  and  $N$  are directly input to the software by the user. Optimum values for both are determined empirically through the observation of performance. The values settled upon are a compromise between weight variance and convergence time (number of iterations until the array weights reach steady state). A small value of loop gain tends to keep the weight variance small about the steady state weight values, but the number of iterations required to reach the steady state may be large. The convergence time is also highly dependent on the interference power incident on the array. For a fixed loop gain, the time required for the array weights to reach steady state decreases as the interference power incident on the array increases. Thus if the loop gain is fixed to maintain an acceptable weight jitter, the convergence time of the adaptive array will decrease as the gain of the auxiliary antennas in the directions of the interfering signals is increased. A similar trade-off exists with the number of samples taken for each iteration. Since the noise components of the two branches of each feedback loop are uncorrelated, with a perfect correlation estimate (infinite number of samples) noise will have no effect on the array weights and there will be no random weight jitter. For a correlation estimate based on a finite number of samples, the estimate improves as the number of samples is increased. Thus, increasing  $N$  reduces the effect of thermal noise on the array weights. However, acquiring a

larger number of samples for each iteration requires more time and the convergence time of the array is increased.

Typical values of  $\gamma$  used in the experiments range from 0.1 to 0.5, and  $N=640$  is typical of the number of samples used to compute each correlation  $C_1$ . Since the sampling interval is 1  $\mu\text{sec}$  and the pulse repetition period is 63.5  $\mu\text{sec}$  the correlations computed for each weight update are averages over about 10 pulse repetition periods. Using the sampling scheme described in Chapter III, slightly less than 3 seconds are required to complete the sampling for each iteration.

#### 4.3 Performance Evaluation

In addition to implementing the weight control algorithm in discrete form, the sampled data is used by the system software to compute performance. This function is made possible by the staggered pulse modulation scheme used in the signal simulator, which enables the separate calculation of the desired signal, interfering signal and noise powers present in each received signal and in the adapted array output. From this information, steady state adaptive array performance (interference suppression, output SINR) can be computed.

Figure 27 shows the I and Q outputs from one vector demodulator. The D pulses are the desired signal, and I1 and I2 are the interfering signals. Taking advantage of the modulation, the desired signal amplitudes are calculated from the sampled data over time interval  $\tau_1$ , and the interfering signal amplitudes are calculated from the samples over  $\tau_2$  and  $\tau_3$ . Samples from interval  $\tau_4$  are used to compute the noise



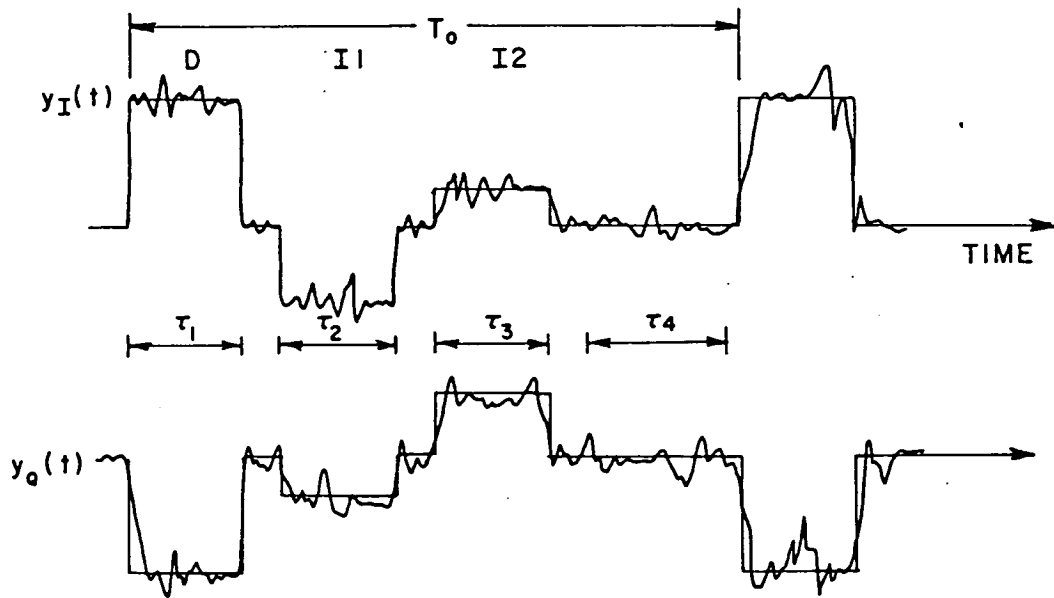


Figure 27. I and Q VDM outputs.

power in the I and Q outputs of each detector. The additive noise components consist of both thermal noise from the detector amplifiers and system thermal noise from the noise sources of the array simulator. The detector amplifier thermal noise is small relative to the levels of the noise source outputs used in the tests. The samples over  $\tau_4$  are also used to calculate and correct for any DC offset voltages due to the detector amplifiers. Even though these offset voltages have been nulled by adjustments at the amplifiers themselves, this correction is also done in software as a precaution against any drift that may occur during the course of an experiment. Left uncorrected, such offset voltages would cause errors in the correlation between element signals and degrade adaptive array performance.

The signal and noise power calculations are based on finite numbers of samples and thus are estimates of the actual levels present. Denoting the received signals for a particular detector as  $y_I(n)$  and  $y_Q(n)$ , these estimates are calculated as

$$\hat{o}_{I,Q} = \frac{1}{N} \sum_{n=1}^N y_{I,Q}(n) \text{ on } \tau_4 \quad (56)$$

$$\hat{d}_{I,Q} = \frac{1}{N} \sum_{n=1}^N y_{I,Q}(n) - \hat{o}_{I,Q} \text{ on } \tau_1 \quad (57)$$

$$\hat{j}_{1I,Q} = \frac{1}{N} \sum_{n=1}^N y_{I,Q}(n) - \hat{o}_{I,Q} \text{ on } \tau_2 \quad (58)$$

$$\hat{j}_{2I,Q} = \frac{1}{N} \sum_{n=1}^N y_{I,Q}(n) - \hat{o}_{I,Q} \text{ on } \tau_3 \quad (59)$$

$$\hat{\sigma}_{I,Q}^2 = \frac{1}{N} \sum_{n=1}^N (y_{I,Q}(n) - \hat{o}_{I,Q})^2 \text{ on } \tau_4 \quad (60)$$

for each of the three vector demodulators.  $\hat{o}_I, \hat{o}_Q$  are the DC offset estimates,  $\hat{d}_I$  and  $\hat{d}_Q$  are the desired signal I and Q pulse amplitudes,  $\hat{j}_{1I}, \hat{j}_{1Q}, \hat{j}_{2I}$ , and  $\hat{j}_{2Q}$  are the interfering signal I and Q pulse amplitudes, and  $\hat{\sigma}_I^2$  and  $\hat{\sigma}_Q^2$  are the I and Q channel noise power estimates.

The pulse amplitude calculations for each signal (desired and interfering) are obtained by signal averaging over the particular portion of the pulse repetition period corresponding to the signal under

measurement. The variances of these estimates\* depend on both the average power, or variance of the noise present, and the number of samples  $N$ . In the tests to be conducted, the element signals will have certain signal components at or below system thermal noise level. After adaptation, assuming the interference is suppressed, the interfering signal components of the array output will be as much as 35 dB below the noise level. Because the noise power is large compared to the interfering signal level at the array output, a very large number of samples will be required to obtain an accurate estimate. Thus to increase the accuracy of the signal power estimates, the system noise from the noise sources of the array simulator is removed prior to taking samples that are used for signal level calculations. Of course, the system noise is restored to obtain noise power estimates, and when adaptation is occurring.

From the I and Q output measurements, the average power of the desired and interfering signal components,  $P_D$ ,  $P_{I1}$ ,  $P_{I2}$ , and the noise power,  $P_N$  are calculated, and then the SNR, INR, and SIR at each element and at the array output are computed:

$$P_D = (\hat{d}_I^2 + \hat{d}_Q^2) \delta \quad (61)$$

$$P_{I1} = (\hat{j}_{1I}^2 + \hat{j}_{2Q}^2) \delta \quad (62)$$

---

\* When a coherent LO is used in the VDMs, estimating the pulse amplitude in the presence of noise is equivalent to estimating the mean of a Gaussian random process. The averages (56)-(60) are efficient maximum likelihood estimates of the pulse amplitudes with variance (Cramer-Rao bound)  $\sigma^2/N$ , where  $\sigma^2$  is the noise power and  $N$  is the number of observations [9].

$$P_{I2} = (\hat{j}_{2I}^2 + \hat{j}_{2Q}^2) \delta \quad (63)$$

$$P_N = \hat{\sigma}_I^2 + \hat{\sigma}_Q^2 \quad (64)$$

$$SNR = P_D / P_N \quad (65)$$

$$INR_1 = P_{I1} / P_N \quad (66)$$

$$INR_2 = P_{I2} / P_N \quad (67)$$

$$SIR = P_D / (P_{I1} + P_{I2}) \quad (68)$$

$\delta$  is the duty cycle of the pulse modulation,  $INR_1$  is the INR due to interfering signal I1 alone and  $INR_2$  is the INR due solely to I2. Because the I and Q components of narrowband noise are uncorrelated [10], the total noise power in a particular channel is the sum of the noise powers at the I and Q outputs of that detector.

During an experiment, these calculations are made prior to adaptation and stored in the system computer, providing measurements of the signal scenario set up by the array simulator settings. Main channel data is obtained by setting the array weights to zero and sampling the array output signals. After adaptation, or at any intermediate point, the same calculations are again performed on samples from the array output, with the array weights frozen at the values arrived at from the last iteration. The desired signal suppression  $\eta_D$ , and the interference suppression,  $\eta_I$ , defined as

$$\eta_D = \frac{P_D |_{\text{at output}}}{P_D |_{\text{main}}} \quad (69)$$

$$\eta_I = \frac{(P_{I1} + P_{I2}) |_{\text{at output}}}{(P_{I1} + P_{I2}) |_{\text{in main}}} \quad (70)$$

are then calculated.  $\eta_D$  and  $\eta_I$ , and the SNR and SIR at the adapted array output are the performance measures used to evaluate steady state adaptive array behavior.

Measuring interference suppression is essentially measuring the depth of the nulls which the adaptive array steers in the directions of the interfering signal sources. There exists an inherent difficulty in trying to quantify a 'null' because of the finite resolution and sensitivity of practical devices. In the experimental system, there are several factors which limit the interference suppression which can be measured from the sampled data. Since the interference suppression measurement is a power ratio (as are SIR and SNR), its accuracy is dependent on the linearity of the vector detectors over a wide range of signal levels. However, the detectors used are indeed very linear and not a major source of error. The measurement accuracy is also limited by two sources of noise: the quantization noise of the A/D converter (12 bits with a LSB of 2.5mV), and the detector amplifier thermal noise. Of these, detector thermal noise is dominant. Once the interfering signals are suppressed to a level below that of this thermal noise, signal averaging no longer produces an accurate estimate. The minimum detectable signal input to the vector demodulators was found to be -60 dBm. This is a lower bound on the interfering signal level which can be detected at the array output, and thus limits the amount of interference

suppression which can be accurately computed, given an initial interference level in the main antenna.

In this chapter both the implementation of the weight control equation and the method of performance evaluation were described. The use of a hybrid system with digital processing provided several advantages. It allowed the differential phase shifts in the array feedback loops to be compensated for in software. Along with the signal control provided through the array simulator, the processing of sampled data is used to compute the perfect steering vector for each experiment. In performance evaluation and in weight control, the sampled data is used to make DC offset voltage corrections to the received data. Using these methods, tests are conducted and results are obtained on adaptive array performance, and they are the subjects of the next chapter.

## CHAPTER V

### EXPERIMENTS AND RESULTS

#### 5.1 Introduction

The purposes of this chapter are to describe the experiments conducted and present the results obtained with the experimental system. First a description of the procedures followed with each experiment, including a hardware check and software calibration, is given. The tests conducted are then described. Adaptive array performance is characterized by the interference suppression, output SIR, and output SNR obtained after adaptation. The experiments show the dependence of performance on INR in the main channel, INR in the auxiliary elements, and the interelement phase shifts varied through the array simulator. These tests use the signal simulator for the array inputs.

#### 5.2 Experimental Procedure

The sequence of events undertaken with each experiment is given in Table 1. The complete procedure is dictated by the system software.

#### 5.3 Tests and Results

Figures 28 and 29 show the performance of the adaptive array as the INR in the main channel.  $\text{INR}(\text{main})$  is varied by changing the interference level in the main channel. This corresponds to varying the sidelobe level of the main antenna in the directions of the interference. The  $\text{SNR}(\text{main})$  is fixed at 13.6 dB. As the  $\text{INR}(\text{main})$  is varied from -10 dB to 0 dB, the  $\text{SIR}(\text{main})$  varies from 23.6 dB to 13.6

Table 1

Experimental Procedure

(1) Set-up and Software Calibration

- a. Power up system
- b. Manual check (oscilloscope) of detector amplifier offset voltages
- c. Software calibration of DC offsets and differential phase shifts
  - i. Reduce desired signal and leakage to zero (one interfering signal in each auxiliary channel)
  - ii. Reduce system noise to zero
  - iii. Set weights to  $1.0 + j0.0$  (so weights do not induce phase shifts)
  - iv. Measure DC offset voltages
  - v. Measure feedback loop differential phase shifts
- d. Set up array simulator for desired conditions
- e. Set initial weight vector
- f. Sample and measure initial signal scenario
- g. Set desired noise level in all channels
- h. Sample and measure initial noise levels

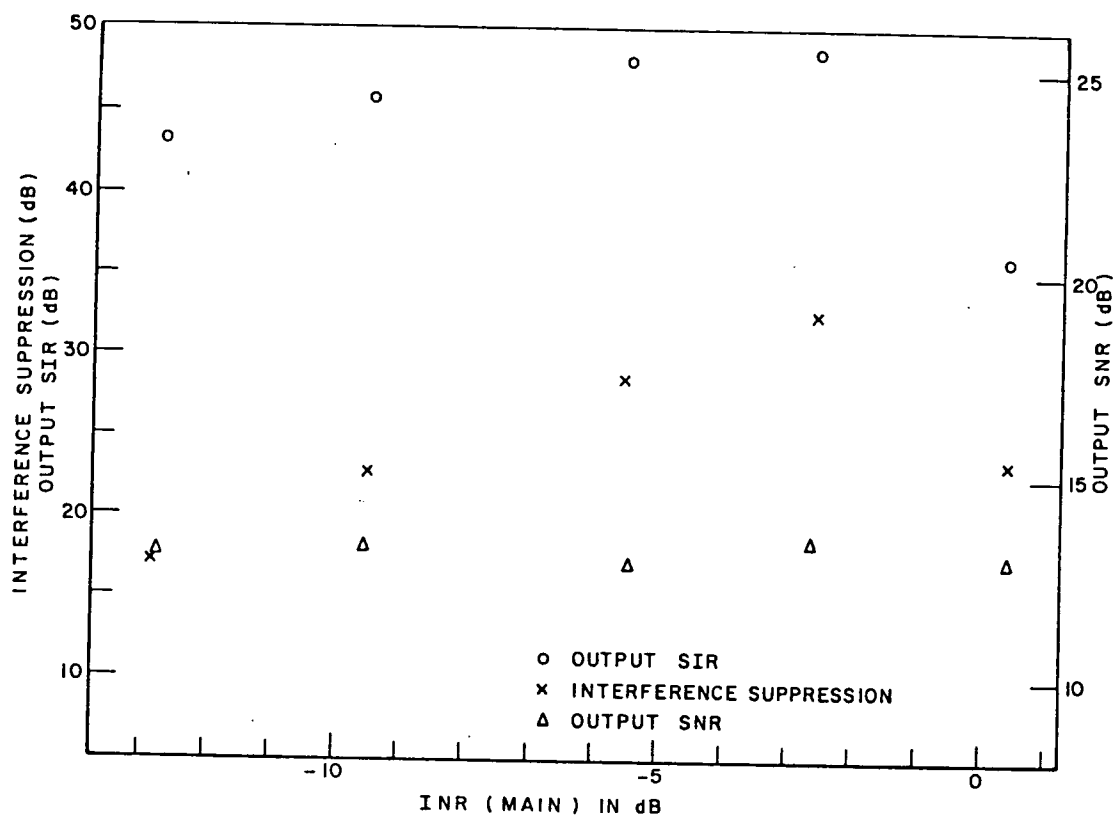
(2) Algorithm execution

- a. Calculate steering vector if desired
  - i. Remove interference and noise
  - ii. Set array weights to zero (so only main channel is at output)
  - iii. Compute  $u_{si} = E\{\tilde{x}_{di}^*(t)\tilde{x}_{do}(t)\}$
  - iv. Restore initial weights, interference and noise levels
- b. Set loop gain and number of samples (integration time)
- c. Start adaptation--updating array weights
- d. Continue (c.) until user intervenes (steady state reached)

(3) Performance evaluation

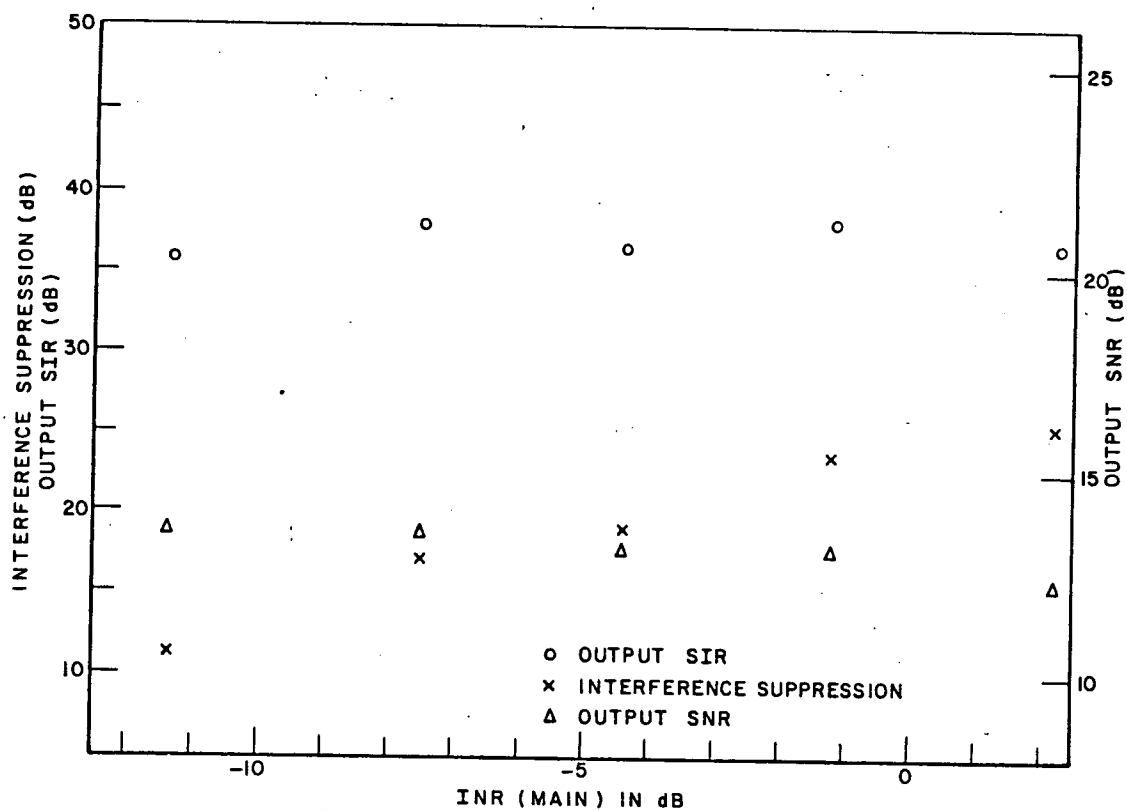
- a. Freeze array weights
- b. Remove system noise
- c. Sample and measure signal levels at array output
- d. Restore noise
- e. Sample and measure noise level at array output
- f. Compute interference suppression, output SIR, and output SNR
- g. Output results
- h. Continue adaptation (return to (2c.)) or exit





One interfering signal  
 $\text{INR}(\text{aux-1}) = 8.8 \text{ dB}$   
 $\text{SNR}(\text{main}) = 13.6 \text{ dB}$   
 $\theta_1 = 4^\circ$   
 No desired signal present in  
 auxiliary elements

Figure 28. Performance vs.  $\text{INR}(\text{main})$ .



Two interfering signals  
 $INR_1(aux-1)=INR_2(aux-2)=8.8$  dB  
 $SNR(main) = 13.6$  dB  
 $\theta_1 = 4^\circ, \theta_2 = -4^\circ$   
 No desired signal present in  
 auxiliary elements

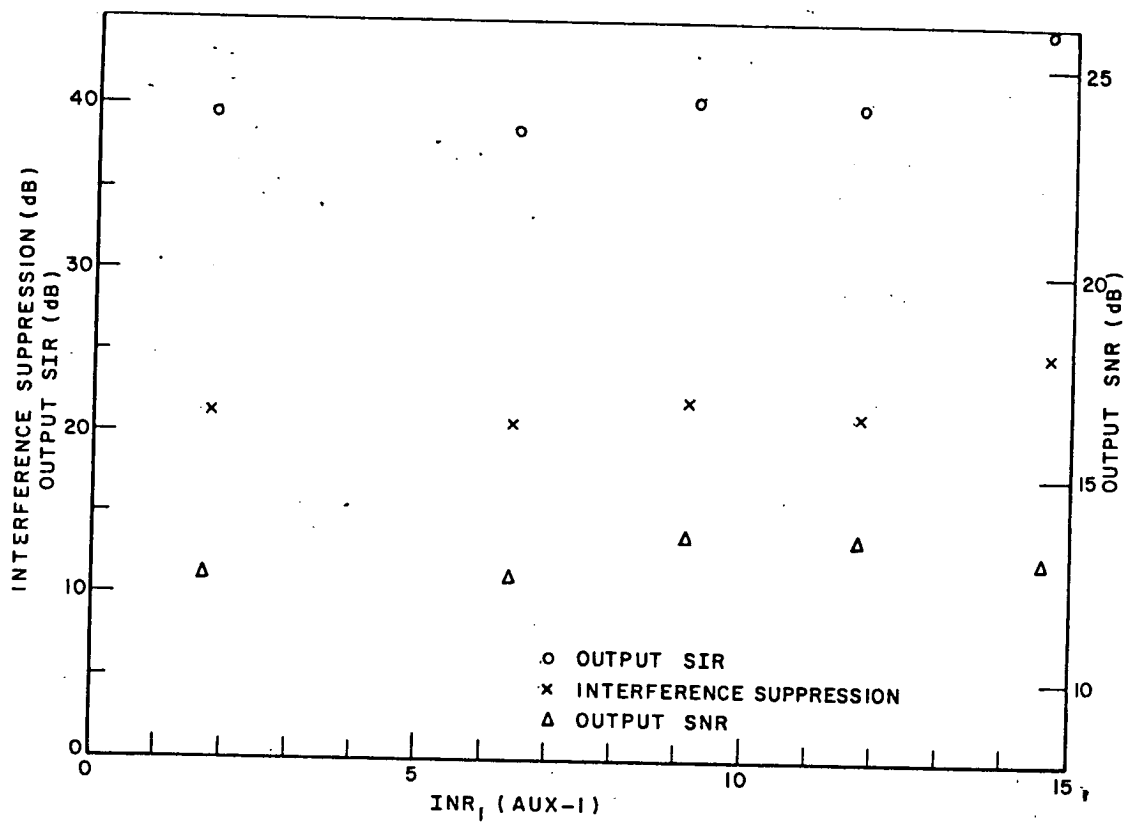
Figure 29. Performance vs. INR(main).

dB. In these plots there is no desired signal present in the auxiliary elements. Thus the steering vector is not used ( $u_{si}=0.0$ ) and there is no possibility of desired signal cancellation by the weighted auxiliaries.

In Figure 28 only one interfering signal is incident on the array. The  $INR(aux-1)$  is fixed at 8.8 dB. The noise level in the main channel is equal to the noise level in the auxiliary elements. Thus the auxiliary-1 channels represent moderately directive antennas (but less directive than the main antenna where  $SNR=13.6$  dB) which are pointed in the direction of the interfering signal. The phase shifter settings correspond to an interfering signal angle of arrival of  $4^\circ$  off broadside. The figure shows that for  $INR(main) > -10$  dB, the interfering signal is suppressed by more than 20 dB. Furthermore the interference suppression increases as  $INR(main)$  increases. However, the output SIR is maintained fairly constant at 47 dB to 48 dB. This indicates that the interference is suppressed to the measurable limit each time. The output SNR curve shows little change. This is because of several factors. As  $INR(main)$  increases, the magnitude of the array weights necessary to suppress the interfering signal also increases. Thus the weighted auxiliaries add more noise to the output and the SNR should decrease. However, it was discussed in Chapter III that due to losses in the auxiliary channels of the array processor, the noise power added by an auxiliary element is, at maximum weight magnitude, still 6 dB below the noise in the main channel. Thus any decrease in output SNR due to the auxiliary channels will be small, and in fact may be hidden by the noise power measurement error which is on the order of  $\pm 0.5$  dB.

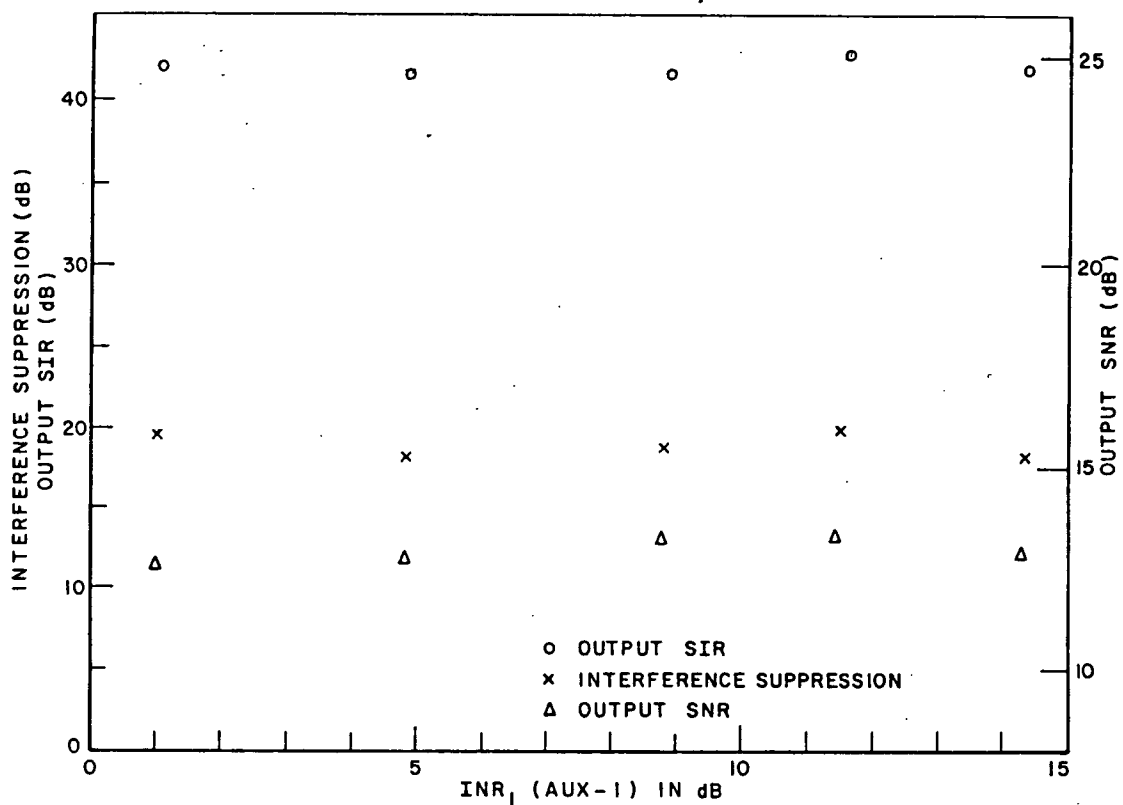
Figure 29 shows the case where two interfering signals are incident on the array. Both the INR of interfering signal I1 in the main channel ( $\text{INR}_1(\text{main})$ ) and the INR of I2 in the main channel ( $\text{INR}_2(\text{main})$ ) are varied such that  $\text{INR}_1(\text{main}) = \text{INR}_2(\text{main})$ . Performance is plotted versus the total INR in the main channel. Also  $\text{INR}_2(\text{aux-2}) = \text{INR}_1(\text{aux-1})$ . Thus the auxiliary elements are of the same gain, with auxiliary element 1(AUX-1) pointed in the direction of I1, and the AUX-2 antennas pointed towards interfering signal I2. The phase shifters are set for an I1 angle of arrival of  $4^\circ$  off broadside and an I2 angle of arrival of  $-4^\circ$  off broadside. Interfering signal I1 is also present in AUX-2, and I2 in AUX-1. As  $\text{INR}_1(\text{main})$  and  $\text{INR}_2(\text{main})$  are varied,  $\text{INR}_1(\text{aux-2})$  and  $\text{INR}_2(\text{aux-1})$  also change such that  $\text{INR}_1(\text{aux-2}) = \text{INR}_1(\text{main}) - 3 \text{ dB}$  and  $\text{INR}_2(\text{aux-1}) = \text{INR}_2(\text{main}) - 3 \text{ dB}$ . The 3 dB difference is a constraint imposed by the design of the array simulator. Referring to the figure, the interference suppression again increases as the interference level in the main channel is increased, while the output SIR is maintained relatively constant between 36 dB to 38 dB. Thus, irrespective of the interference level in the main channel, the output SIR is maintained quite high. Interfering signals 14 dB below thermal noise level are still being suppressed by 12 dB to 13 dB. For this case, both auxiliary elements are active, since both degrees of freedom are needed to null the two interfering signals. Thus the weighted auxiliaries are contributing more noise to the array output than in the one interfering signal only case. The resultant output SNR degradation, is still very small, as is evident in Figure 29.

Figures 30 through 32 show the performance of the adaptive array as a function of  $\text{INR}_1(\text{aux-1})$ . Varying  $\text{INR}_1(\text{aux-1})$  is analogous to changing the gain of the aux-1 antennas in the direction of interfering signal I1. In Figure 30,  $\text{INR}_1(\text{main})$  is fixed at -5.0 dB, and the  $\text{SNR}(\text{main})$  is 13.6 dB. Thus the SIR in the main channel is 18.6 dB. The I1 phase shifters are fixed at values which correspond to an I1 angle of arrival of  $4^\circ$  from broadside. Both the interference suppression and output SIR curves are approximately constant. Even for low gain auxiliary elements ( $\text{INR}_1(\text{aux-1}) = 1.5$  dB), the interference is being suppressed by 21 dB, yielding an SIR at the output of 40 dB. Thus, it appears that the performance in terms of interference suppression is essentially independent of the auxiliary antenna gain, as long as the gain is large enough to keep the weights from becoming too large for the system to accommodate. This behavior is due to the fact that the noise components of the signals in the two feedback loop branches have been completely decorrelated. The array weights are solely dependent on the interfering signal levels in the auxiliary elements and in the main channel. If the noise components of these signals are partially correlated, the gain of the auxiliary antennas (in the interfering signal directions) required to achieve a given interference suppression increases as this correlation increases [1]. The output SNR curve in Figure 30 shows a very slight dependence on  $\text{INR}_1(\text{aux-1})$ . The output SNR is smaller for low  $\text{INR}_1(\text{aux-1})$ . Since the interfering signal level in the main channel is fixed, as  $\text{INR}_1(\text{aux-1})$  is decreased the weight magnitude necessary to cancel the interfering signal increases. This results in a small increase in the noise power at the output (less than 1 dB) and a decrease in output SNR.



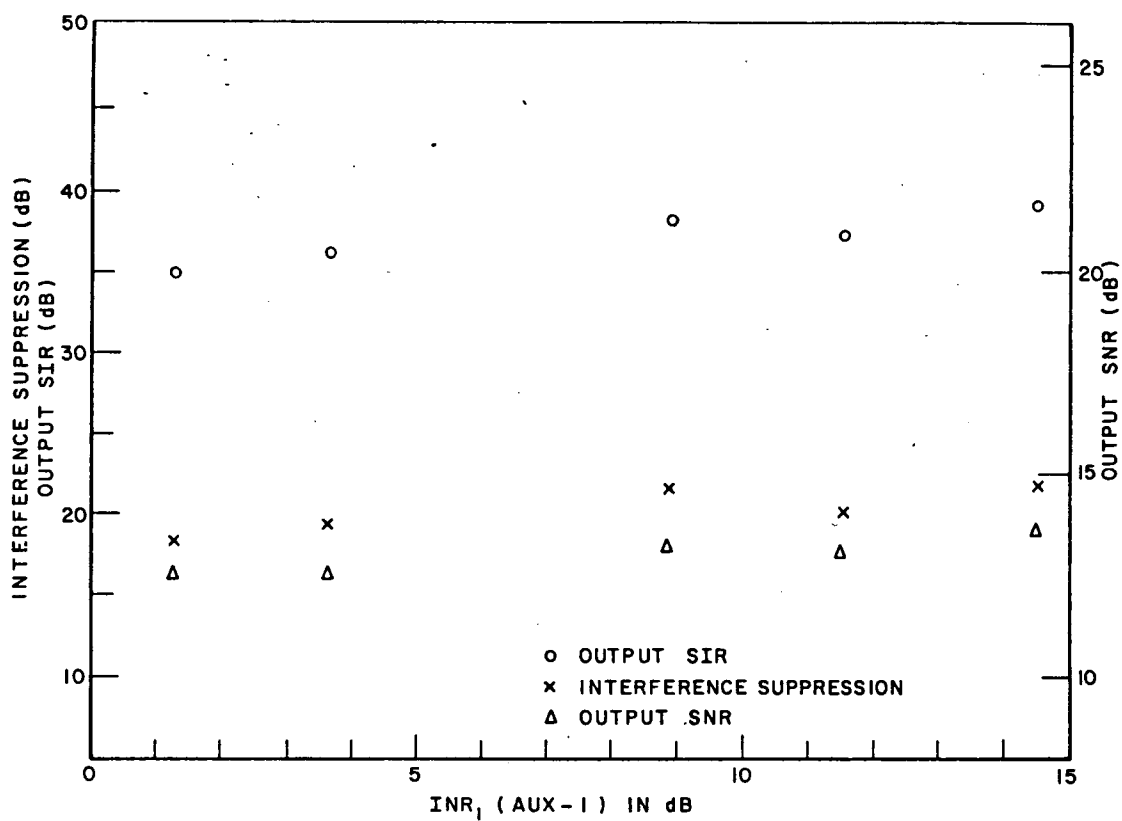
One interfering signal  
 $INR_1(\text{main}) = -5.0 \text{ dB}$   
 $SNR(\text{main}) = 13.6 \text{ dB}$   
 $\theta_1 = 4^\circ$   
 No desired signal present in  
 auxiliary elements

Figure 30. Performance vs.  $INR_1(\text{aux-1})$ .



One interfering signal  
 $\text{INR}_1(\text{main}) = -9.5 \text{ dB}$   
 $\text{SNR}(\text{main}) = 13.5 \text{ dB}$   
 $\theta_1 = 4^\circ$   
 No desired signal present in  
 auxiliary elements

Figure 31. Performance vs.  $\text{INR}_1(\text{aux-1})$ .



Two interfering signals  
 $INR_1(\text{aux-1}) = INR_2(\text{aux-2})$   
 $INR_1(\text{main}) = INR_2(\text{main}) = -6.5$  dB  
 $SNR(\text{main}) = 13.6$  dB  
 $\theta_1 = 4^\circ$ ,  $\theta_2 = -4^\circ$   
 No desired signal present in  
 auxiliary elements

Figure 32. Performance vs.  $INR_1(\text{aux-1})$ .



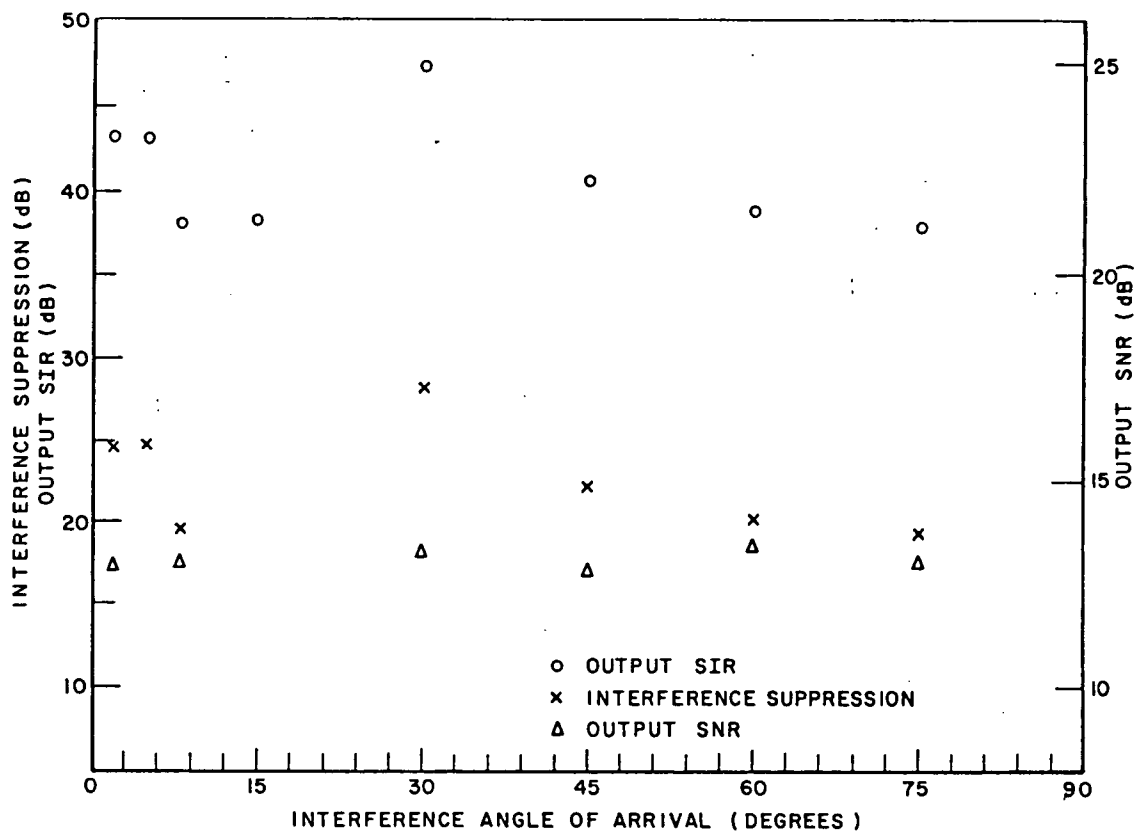
In Figure 31, all parameters are the same as in the test of Figure 30, except that the  $INR_1(\text{main})$  is now fixed at  $-9.5$  dB. The performance of the array is nearly identical with that shown in Figure 30. Here both the interference suppression and the output SIR are nearly constant and thus independent of the auxiliary element gain. The interfering signal is suppressed 18 dB to 20 dB to yield an output SIR of 41 dB to 43 dB. The same remarks made above concerning output SNR also apply to Figure 31.

Figure 32 shows the two interfering signal case. Both  $INR_1(\text{aux-1})$  and  $INR_2(\text{aux-2})$  are varied such that they are approximately equal. Thus the aux-1 antennas and the aux-2 antennas are elements of the same directivity, but pointed in different directions. The aux-1 antennas are pointed towards interfering signal I1 and the aux-2 antennas towards I2 (see Fig. 7). The  $INR_1$  and  $INR_2$  in the main channel are fixed at  $-6.5$  dB, and the  $SNR(\text{main})$  is 13.6 dB. The performance measures plotted involve the total interference power at the output. In this case, the results do indicate a slight dependence on  $INR_1(\text{aux-1})$  and  $INR_2(\text{aux-2})$ . As  $INR_1(\text{aux-1})$  is varied from 1.2 dB to 14.5 dB, the interference suppression increases from 18 dB to 21 dB. Because the desired signal is unsuppressed, the output SIR data follows the suppression curve and increases from 35 to 39 dB. Although performance is still good, it is slightly degraded from that of the one interfering signal case. This degradation is most likely because both degrees of freedom are used to cancel the interference. Thus any correlation errors will result in performance degradation. The output SNR behavior of Figure 32 shows the

same slight increase with auxiliary element gain as was observed and explained in relation to Figures 30 and 31.

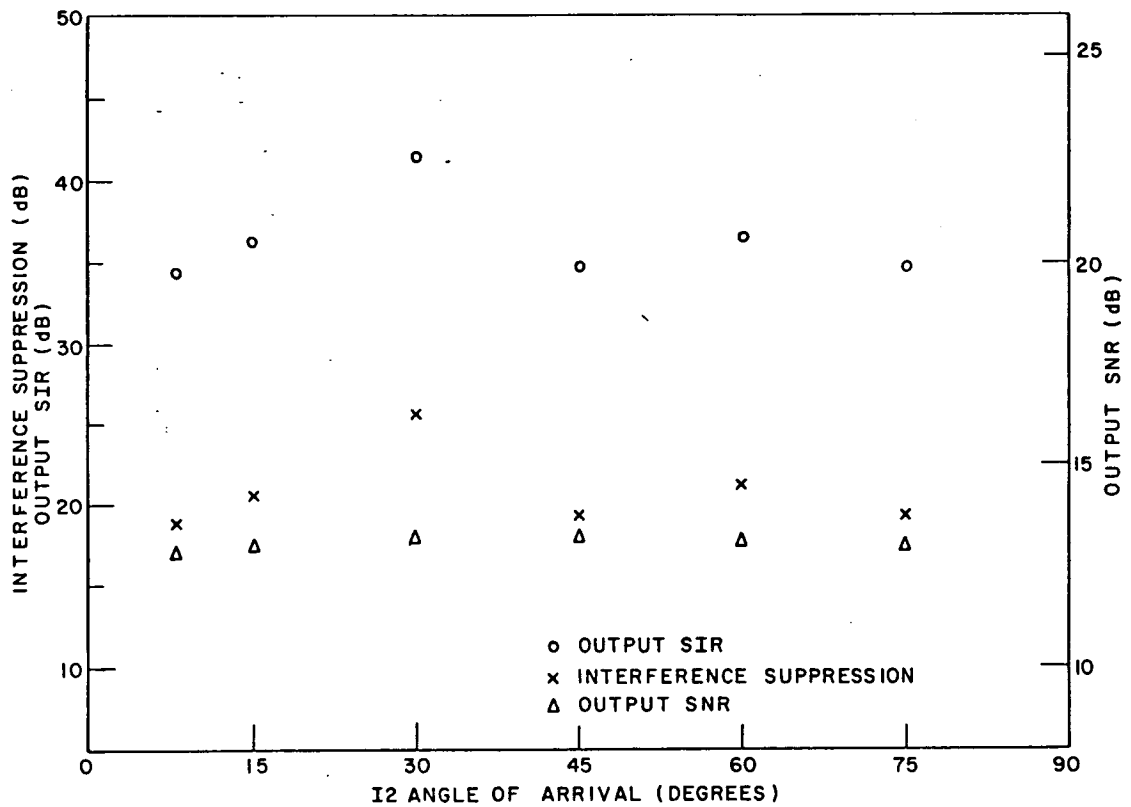
The performance of the adaptive array as a function of the interelement phase shifts between interfering signal components of the element signals is shown in Figures 33 and 34. These phase shifts are varied to simulate different interfering signal angles of arrival. An interelement spacing of one-half wavelength is assumed. In Figure 33, the signal and interference levels are fixed such that  $SNR_{(main)}=13.6$  dB,  $INR_1(main)=-5.0$  dB,  $INR_1(aux-1)=8.8$  dB, and  $INR_1(aux-2)=-8.0$  dB. The results plotted indicate a wide variation in interference suppression as the interference angle of arrival is varied. Across the complete range, the suppression varies between 19 dB and 29 dB. Because the desired signal is not suppressed (still no desired signal present in the auxiliary channels) the output SIR also varies by 10 dB, from 38 dB to 48 dB, tracking the variation in interference suppression. Figure 34 shows the two interfering signal case.  $INR_1(main)=INR_2(main)$ ,  $INR_1(aux-2)=INR_1(aux-1)$ , and  $INR_2(aux-1)=INR_1(aux-2)$ . The I2 angle of arrival is varied, with the angle of arrival of I1 fixed at  $4^\circ$ . These results also show the same type of erratic behavior evident in the one interfering signal case.

The problem causing the performance variations in Figures 33 and 34 also pervades the other plots. This can be seen by observing the jitter around some constant value in Figures 30-32, and in the interference suppression curves of Figures 28-29 which are not strictly monotonic as expected. This jitter is too much to attribute to measurement error. The problem is weight variance caused by the strong



One interfering signal  
 $INR_1(\text{aux-1}) = 8.8 \text{ dB}$   
 $INR_1(\text{main}) = -5.0 \text{ dB}$   
 $SNR(\text{main}) = 13.6 \text{ dB}$   
 No desired signal present in  
 auxiliary elements

Figure 33. Performance vs. interfering signal I1 angle of arrival.



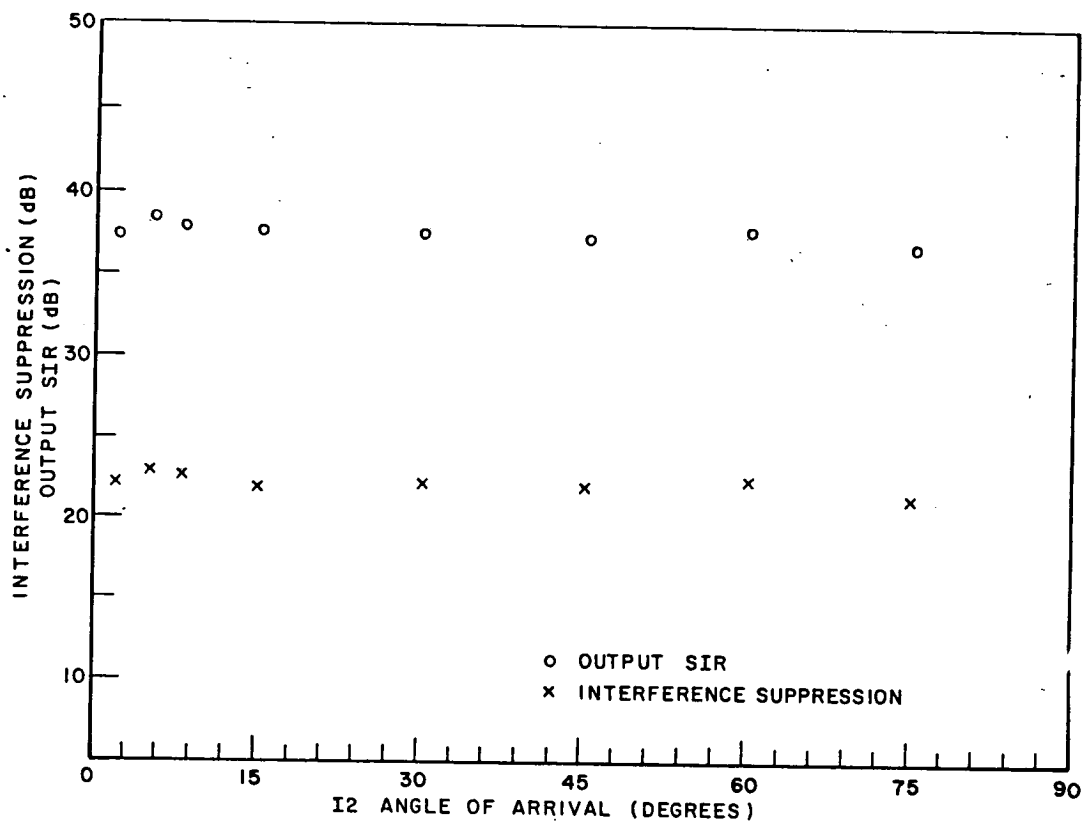
Two interfering signals  
 $INR_1(\text{aux-1}) = INR_2(\text{aux-2}) = 8.8 \text{ dB}$   
 $INR_1(\text{main}) = INR_2(\text{main}) = -5.0 \text{ dB}$   
 $SNR(\text{main}) = 13.6 \text{ dB}$   
 $\theta_1 = 4^\circ$   
 No desired signal present in  
 auxiliary elements

Figure 34. Performance vs. I2 angle of arrival.

desired signal component of the main channel present at the array output, and partly attributable to the pulsed nature of the signals. Over a large number of iterations, the weights vary enough about their 'steady state' values to cause the interference suppression and output SIR to fluctuate 7-10 dB. Furthermore, other tests have shown that these random weight fluctuations are not due to thermal noise alone, but also because of desired signal presence. Figures 35 and 36 are results of experiments conducted under the same conditions as Figure 34, except that in Figure 35 the system noise is removed, and in Figure 36 the desired signal is attenuated 20 dB and the noise is restored. In both cases the wide variation in performance observed in Figures 33 and 34 is absent. More importantly, in Figure 36, not only is the random fluctuation absent but the level of performance is 8-9 dB better than that of Figure 35, where the desired signal is unattenuated.

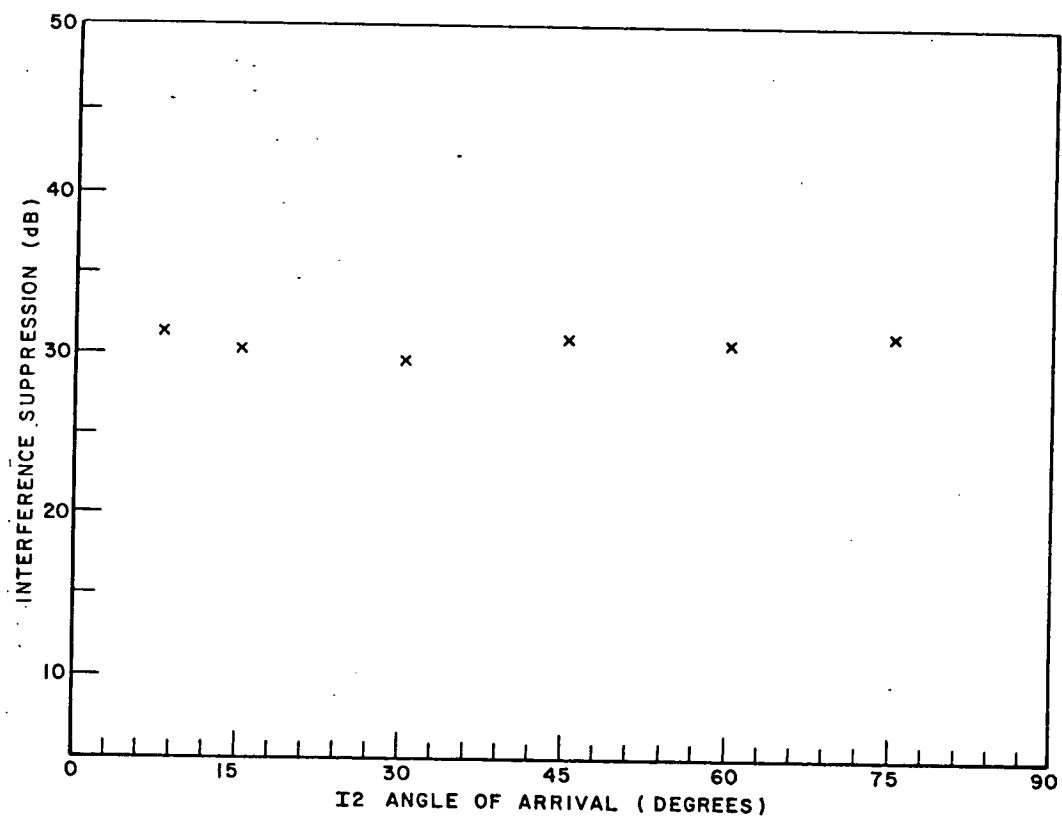
This change in performance depending on whether or not the desired signal is present can be explained as follows. Assume for the moment that there is no desired signal in the auxiliary elements. Because of the modulation of the signal simulator, the correlation between auxiliary element signals and array output can be split into the sum of two parts: one being the correlation over the desired signal portion of the pulse repetition period and the other being the correlation over the rest of the period. Since there is no desired signal component in the auxiliary elements, the correlation over the desired signal portion of the period,  $c_{di}$ , is

$$c_{di} = \frac{1}{N} \sum_j (A+n_o(j))(n_i(j)) = \frac{A}{N} \sum_j n_i(j) + \frac{1}{N} \sum_j n_o(j)n_i(j) \quad (71)$$



Two interfering signals  
 $SIR_1(\text{main}) = SIR_2(\text{main}) = 18.5 \text{ dB}$   
 $\theta_1 = 4^\circ$   
 No desired signal present in  
 auxiliary elements

Figure 35. Performance vs. I2 angle of arrival -- no injected system noise.



Two interfering signals  
 $\text{INR}_1(\text{aux-1}) = \text{INR}_2(\text{aux-2}) = 8.8 \text{ dB}$   
 $\text{INR}_1(\text{main}) = \text{INR}_2(\text{main}) = -5.0 \text{ dB}$   
 $\theta_1 = 4^\circ$   
 No desired signal present in  
 auxiliary elements

Figure 36. Performance vs. I2 angle of arrival -- desired signal attenuated, 20 dB.

where  $A$  is the strong desired signal pulse amplitude in the array output from the main channel,  $n_0(j)$  are samples of the noise in the array output, and  $n_i(j)$  are samples of the noise in the  $i^{\text{th}}$  auxiliary element. Ideally (infinite number of samples)  $c_{di}$  will equal zero because the noise components are uncorrelated with each other and have zero mean. Because the correlation estimate is based on a finite number of samples, neither term of Equation (70) is exactly zero.  $A^2$  is on the order of 20 dB higher than the noise power (desired signal portion of period) and thus the  $\frac{A}{N} \sum n_i(j)$  term of  $c_{di}$  is dominant. Once the interfering signals are suppressed to a point where the correlation over the interference portion of the period is on the order of the error term  $c_{di}$ , this error term will affect the array weights. This prevents any further suppression of the interference. The randomness of  $c_{di}$  causes weight variance over a large number of iterations. The problem is less severe when only one interfering signal is incident on the array, because the leftover degree of freedom can be used to correct for this random portion of the correlation. When two interfering signals are incident, both degrees of freedom are used to cancel interfering signals. The error term  $c_{di}$  appears to the array as additional interference which cannot be nulled. The array tries to minimize the total correlation, including the error term, and overall performance degrades. This accounts for the difference in performance levels achieved between one and two interfering cases of previous experiments. The presence of this error term also accounts for the dependence of performance on  $\text{INR}_1(\text{aux}-1)$  in Figure 32. The performance limit is reached when the interference correlation is of the order of the correlation error term.



As the INR in the auxiliaries is decreased, the interference level in the array output required for the interference correlation to reach this lower limit is increased. Thus, as the auxiliary antenna gains in the interfering signal directions are decreased, the interference suppression achievable before the correlation error  $c_{di}$  limits performance also decreases.

#### 5.4 Results Using the Steering Vector

Up to this point, there has been no desired signal present in the auxiliary elements in the experiments conducted, and thus a steering vector of zero was used. The more realistic case is where there is a desired signal component of the auxiliary antenna signals. In the satellite communications scenario of interest it is likely that the desired signal will enter the auxiliary element signals through the auxiliary antenna sidelobes. Thus the SIR in the auxiliaries will be of the order of the auxiliary antenna sidelobe level. In this case, the steering vector is calculated by the system as described in Chapter IV according to Equation (11):

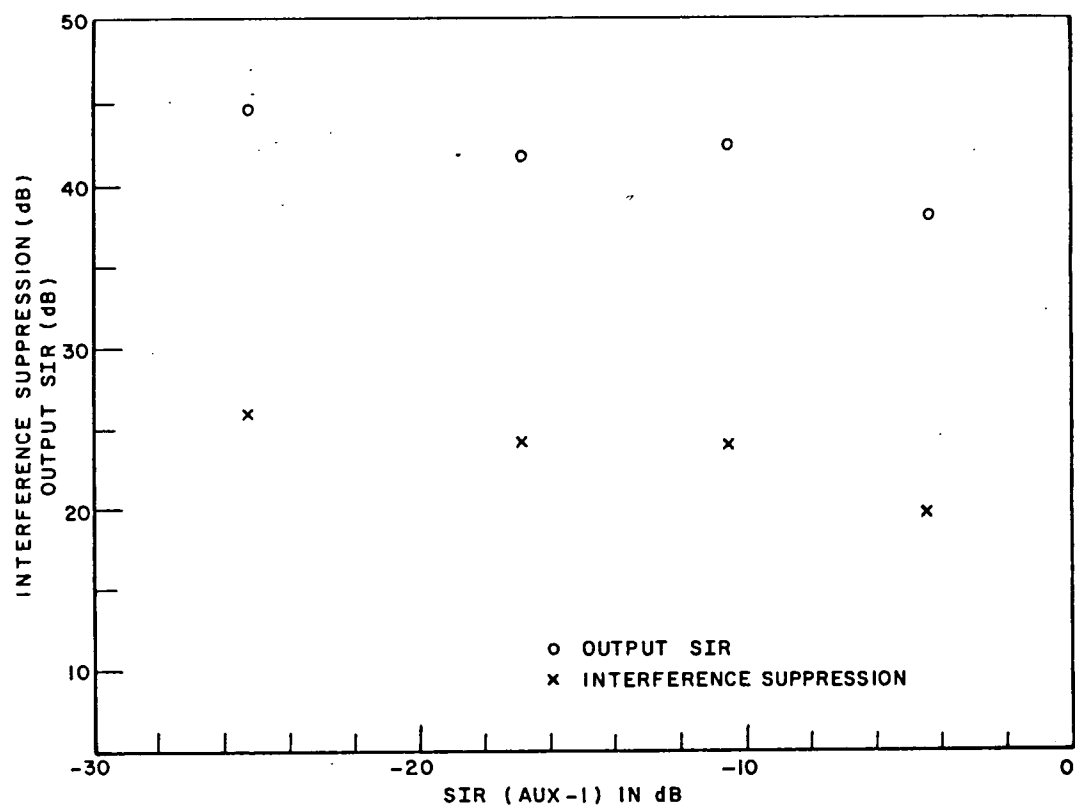
$$U_s = U_d = E\left\{X_d^* \tilde{x}_{do}(t)\right\} \quad (72)$$

Its purpose is to remove the component of the correlation present in each feedback loop that is due to the desired signal, thus preventing the array weights from nulling the desired signal. With a perfect steering vector the performance level attained should equal that obtained when no desired signal was present in the auxiliary elements.

Figure 37 shows the results of an experiment with one interfering signal and the desired signal incident on the array. The steering

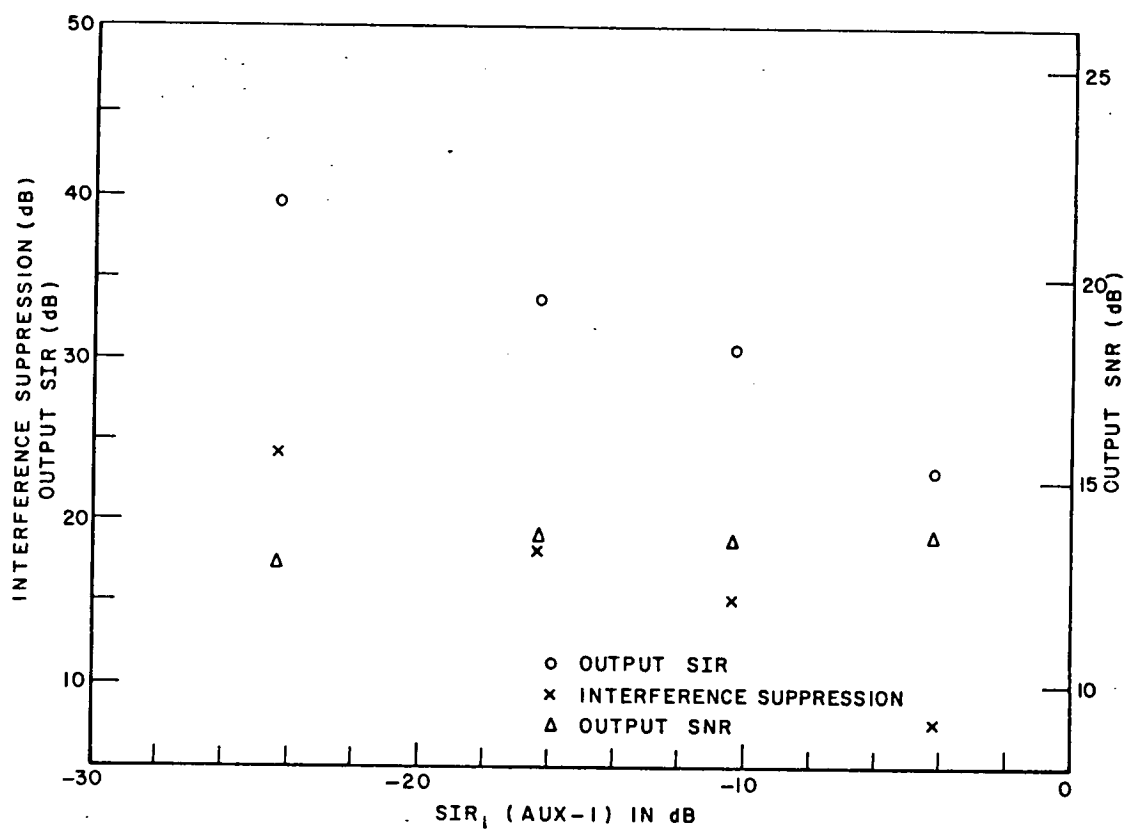
vector is used to prevent the weights from moving to suppress the desired signal. Performance is plotted as a function of the  $SIR_1$  in auxiliary element 1 ( $SIR_1(\text{aux-1})$ ), which is varied by changing the desired signal level in the aux-1 channels and keeping the I1 level fixed. The  $INR_1(\text{main}) = -5.0$  dB,  $SNR(\text{main}) = 13.6$  dB,  $INR_1(\text{aux-1}) = 8.8$  dB and are fixed. The phase shifters are set corresponding to an I1 angle of arrival of  $4^\circ$  off broadside. The interference suppression is 20 dB or greater for  $SIR_1(\text{aux-1}) < -5.0$  dB, but a slight degradation as  $SIR_1(\text{aux-1})$  is increased is clearly evident. The fact that the output SIR data tracks the interference suppression data indicates that this degradation is not due to desired signal cancellation, but rather to a degradation in interference suppression.

Figure 38 shows the results of the two interfering signal case. All parameters are the same as in Figure 37, except now  $INR_2(\text{main}) = INR_1(\text{main})$ ,  $INR_2(\text{aux-2}) = INR_1(\text{aux-1})$ ,  $INR_2(\text{aux-1}) = INR_1(\text{aux-2})$ , and  $SIR_1(\text{aux1}) = SIR_2(\text{aux-2})$ . These results show a very severe degradation in both interference suppression and in output SIR, as the desired signal level in the auxiliaries is increased. The SIR degradation is again due solely to a lack of interference suppression, because, as the output SNR data indicates, the desired signal level at the output is maintained. This degradation is much worse than that observed when only I1 is incident on the array. The reasons for this performance follow. The array output contains desired signal components from both the main channel signal and the weighted auxiliary element signals. The steering vector removes the desired signal component of the correlation between array output and auxiliary element signal which is due to the main



One interfering signal  
 $INR_1(\text{aux-1}) = 8.8 \text{ dB}$   
 $INR_1(\text{main}) = -5.0 \text{ dB}$   
 $SNR_1(\text{main}) = 13.6 \text{ dB}$   
 $\theta_1 = 4^\circ$

Figure 37. Performance vs.  $SIR_1(\text{aux-1})$  -- using steering vector.



Two interfering signals  
 $SIR_2(\text{aux-2}) = SIR_1(\text{aux-1})$   
 $INR_2(\text{aux-1}) = INR_1(\text{aux-2}) = 8.8 \text{ dB}$   
 $INR_1(\text{main}) = INR_2(\text{main}) = -5.0 \text{ dB}$   
 $SNR(\text{main}) = 13.6 \text{ dB}$   
 $\theta_1 = 4^\circ, \theta_2 = -4^\circ$

Figure 38. Performance vs.  $SIR_1(\text{aux-1})$  -- using steering vector.

channel signal. Because the weighted auxiliaries also contain the desired signal, the correlations between auxiliary channels and the array output still have a component due to the desired signal. This component is not removed by the steering vector and therefore does affect the array weights. Its magnitude varies as the array weights change. As a result, the array weights will move to cancel the desired signal in the output due to the weighted auxiliary elements. In the case where the number of degrees of freedom is equal to the number of interfering signals, this can only be done by reducing the magnitudes of the array weights. Thus the interference suppression is degraded. The reason for the much larger degradation in the two interfering signal case is again because of the two degrees of freedom limitation of the experimental adaptive array.

A steering vector which would remove all desired signal components of the correlation is necessary to avoid this degradation. The form of such a steering vector component,  $u'_{si}$  is

$$\begin{aligned} u'_{si} &= E\left\{\tilde{x}_{di}^*(t) \left(\tilde{x}_{do}(t) + \sum_j w_j \tilde{x}_{dj}(t)\right)\right\} \\ &= u_{si} + \sum_j w_j E\left\{\tilde{x}_{di}^*(t) \tilde{x}_{dj}(t)\right\} \end{aligned} \quad (73)$$

where  $u_{si}$  is the steering vector component as calculated in Equation (72).  $\tilde{x}_{di}(t)$  and  $\tilde{x}_{dj}(t)$  are the desired signal components of the  $i^{\text{th}}$  and  $j^{\text{th}}$  auxiliary elements. Expanding into vector form yields

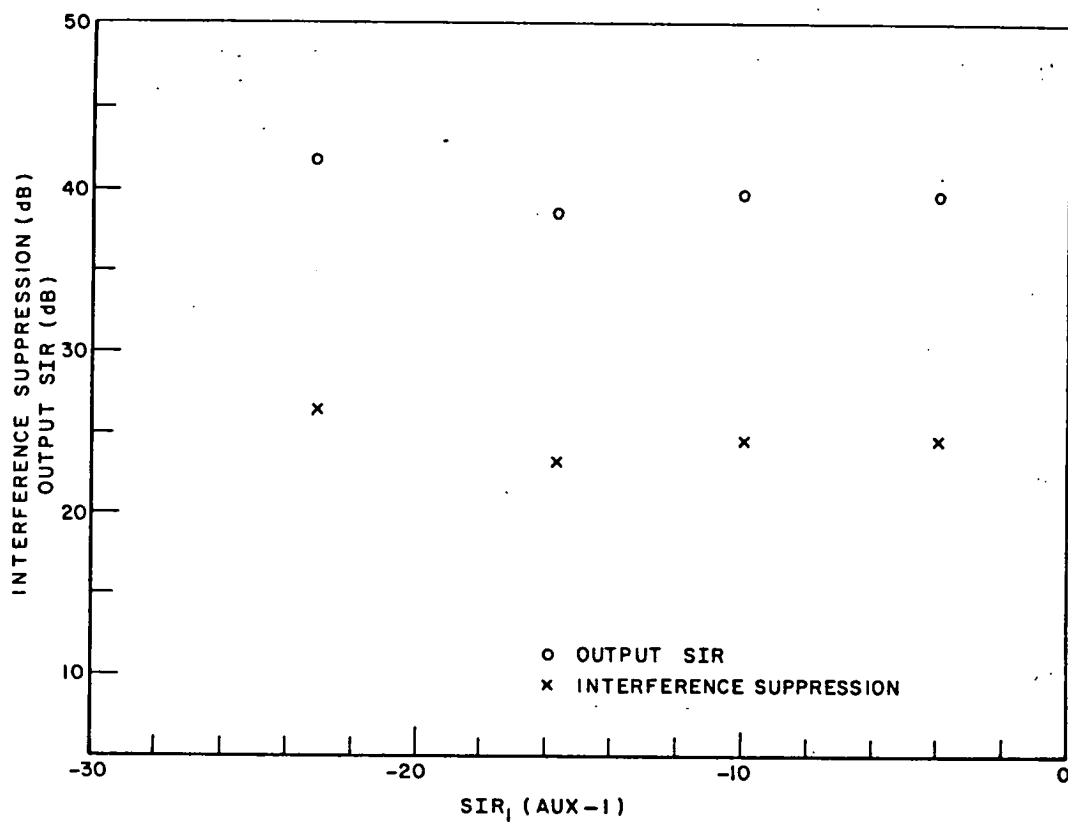
$$U'_s = U_s + \Phi_d W \quad (74)$$

$U'_s$  will be called the modified steering vector,  $U_s$  is the steering vector of (72) due only to the main channel, and  $\Phi_d$  is the covariance matrix of the desired signal components of the auxiliary element signals. Note that the modified steering vector depends on the weight

vector  $W$ . The hybrid nature of the experimental system lends itself to the implementation of Equation (74) with only a few software changes. The weights are kept in memory at each iteration and can be used to update the modified steering vector. The products  $E\{\tilde{x}_{di}^*(t)\tilde{x}_{dj}(t)\}$  of  $\Phi_d$  can be calculated in the same manner as the steering vector was previously computed. Only an additional step of removing the main channel from the array output for these calculations is necessary.

Figure 39 shows the performance of the adaptive array using the modified steering vector. All parameters are the same as in Figure 38. The degradation in performance with increasing SIR(aux) is absent. Interference suppression is 23 dB to 26 dB independent of the desired signal level. The corresponding output SIR is also maintained quite high at 38 dB to 41 dB. Thus the modified steering vector is successful in removing all desired signal components from the correlation computed in each feedback loop, allowing the array to use both degrees of freedom to null the interfering signals. The problem of random correlation errors which cause weight variance and performance fluctuation, is however still present. In fact, the problem may be more severe now that the steering vector itself depends on the array weights.

The necessity of a modified steering vector is due to several factors related to the particular application of a ground station receive antenna for satellite communications. In some applications, such as pulsed radar systems, the desired signal is present such a small fraction of the time that the steering vector is unnecessary. The steering vector is necessary in a satellite communications system because the desired signal is always present. The results show that the



Two interfering signals  
 $SIR_2(\text{aux-2}) = SIR_1(\text{aux-1})$   
 $INR_1(\text{aux-1}) = INR_2(\text{aux-2}) = 8.8 \text{ dB}$   
 $INR_1(\text{main}) = INR_2(\text{main}) = -5.0 \text{ dB}$   
 $SNR(\text{main}) = 13.6 \text{ dB}$   
 $\theta_1 = 4^\circ, \theta_2 = -4^\circ$

Figure 39. Performance vs.  $SIR_1(\text{aux-1})$  -- using modified steering vector.

modified steering vector is necessary when the desired signal is very strong in the auxiliaries and the degrees of freedom of the array are limited. The desired signal is strong in the auxiliary elements when, for example the desired and interfering signal sources are spatially close enough together so that they are of approximately the same level in the auxiliary element. Thus both signals are in the main beam of a moderately directive auxiliary element. (It is assumed that the interfering signal is still in the sidelobes of the main antenna, or the array would not be able to distinguish between desired and undesired signals.) The degrees of freedom are limited when experiments were conducted with two interfering signals, since there are only two auxiliary elements in the experimental system. The use of the modified steering vector in this case is also made necessary since a sidelobe canceler adaptive array is used. For a fully adaptive array, the conventional steering vector will provide the necessary interference suppression.

## 5.5 Summary

In this chapter the results obtained from tests with the experimental system have been presented. It was shown that the system suppresses weak interfering signals (0 dB to 10 dB below noise level in the main channel) by 15 dB to 30 dB. The interference suppression increases as the input INR in the main channel increases, tending to maintain a constant output SIR. Because of the complete decorrelation between noise components of different feedback loop branches, interference suppression is essentially independent of auxiliary antenna



gain. Performance was also independent of interfering signal angle of arrival. This will be the case as long as the auxiliary elements are pointed in the general directions of the interference and the interfering signals are not so spatially close to the desired signal that they also reside in the main beam of the main antenna. However, two problems remain. One is the random correlation error due to the desired signal, and is the major factor limiting performance. It results from the strong desired signal pulse in the main channel and small DC offsets from both errors in the DC offset estimate and the non-zero average of the thermal noise (finite number of samples). In addition to limiting the performance, this correlation error also causes performance fluctuation due to random weight jitter about the steady state weights. These problems would be less severe if the desired signal were a continuous, zero mean process rather than a pulse with a large average value. Degrees of freedom limitations cause these sources of performance degradation to be more serious when two interfering signals are incident on the array. The other problem is the need for a modified steering vector in some cases. This is discussed along with other conclusions reached from this investigation in the next chapter.

## CHAPTER VI

### SUMMARY AND CONCLUSIONS

In this study, an experimental adaptive antenna array used to suppress weak interfering signals was described. It is a sidelobe canceler with two auxiliary elements. Thus, up to two interfering signals can be suppressed by the array. Modified feedback loops are used to control the array weights. Two spatially separate antennas form the inputs to each modified feedback loop. Therefore, the total number of antenna elements is five. The experimental adaptive array was implemented and the hardware details of this implementation were described.

Various tests were then conducted with the experimental system to study the performance of the adaptive array in the presence of weak interfering signals. The performance was evaluated quantitatively as well as qualitatively. The results of the quantitative performance evaluations were presented. It was shown that interfering signals 0 dB to 10 dB below the thermal noise level in the main channel were suppressed by 20 dB to 30 dB. The interference suppression increased as the interference level in the main channel was increased, tending to maintain a constant output signal to interference ratio (SIR). In all cases, the output SIR was greater than 35 dB, with little degradation ( $< 1$  dB) in output signal to noise ratio (SNR). Furthermore, performance was shown to be essentially independent of the auxiliary antenna gain. This is due to the complete decorrelation between the noise components in the different branches of each feedback loop. When the noise

components of the signals in the feedback loop branches are partially correlated, the interference suppression will increase as the gains of the auxiliary antennas in the directions of the interfering signals are increased. The performance was also independent of interfering signal angle of arrival. This will be the case as long as the auxiliary antennas are pointed in the general directions of the interfering signals, and the interfering signals are not in the main beam of the main antenna. For the quantitative tests, the pulse modulated signals of the signal simulator were used. The performance of the experimental system was also evaluated qualitatively. In these tests, the desired signal was a television channel 4 video signal. Both pulse modulated signals and other channel 4 video signals were input as interfering signals. The experimental system was also successful in suppressing these interfering signals. Performance was observed through the improvement in television picture quality as the array adapted. Therefore, it has been shown experimentally that, with modifications to the adaptive array feedback loops and the use of directive auxiliary antennas, an adaptive array is capable of suppressing weak interfering signals. Thus, adaptive arrays can be used to provide interference protection to earth stations receiving satellite communications.

For cases where the desired signal component of the auxiliary element signals is strong, and the number of degrees of freedom is limited, it was shown that the amount of interference suppression decreases. This problem is characteristic to sidelobe canceler adaptive arrays. A modified steering vector was proposed which prevents both the desired signal component of the main channel and the desired signal

components of the weighted auxiliaries from affecting the array weights. In a test conducted using this modified steering vector, the performance attained was equal to that obtained when no desired signal was present in the auxiliary elements (Figure 39). Furthermore, there was no degradation in performance as the desired signal level in the auxiliary elements was increased. A more detailed study of the use of this modified steering vector, and its effects on sidelobe canceler adaptive array behavior, should be performed.

In the experimental system, instead of actual antennas, the signals received by the array elements were synthesized in the array simulator. In the future, for operational use, the signal simulator and the array simulator may be replaced by an actual antenna array, whose signals would be down converted to the system IF of 70 MHz, and fed into the array processor. In this case, the locations of the auxiliary element antennas will have to be carefully selected to maintain the desired and interfering signal correlations between branches of each feedback loop, while at the same time providing noise decorrelation.

## REFERENCES

- [1] I.J. Gupta, "Adaptive Arrays for Weak Interfering Signals," Technical Report 716111-2, Grant NAG3-536, for National Aeronautic and Space Administration, Lewis Research Center, Cleveland, Ohio, January 1985.
- [2] I.J. Gupta and A.A. Ksienski, "Adaptive Arrays for Satellite Communications," Technical Report 716111-1, Grant NAG3-536, for National Aeronautic and Space Administration, Lewis Research Center, Cleveland, Ohio, June 1984.
- [3] B. Widrow, P.E. Mantey, L.J. Griffiths and B.B. Goode, "Adaptive Antenna Systems," Proceedings of IEEE, Vol. 55, No. 12, pp. 2143-2159, December 1967.
- [4] S.P. Applebaum, "Adaptive Arrays," IEEE Trans. on Antennas and Propagation, Vol. AP-24, No. 5, pp. 585-598, September 1976.
- [5] R.T. Compton, Jr., "The Effect of Differential Time Delays in the LMS Feedback Loop," IEEE Trans. on Aerospace and Electronic Systems, Vol. AES-17, No. 2, pp. 222-228, March 1981.
- [6] R.T. Compton, Jr., "Multiplier Offset Voltages in Adaptive Arrays," IEEE Trans. on Aerospace and Electronic Systems, Vol. AES-12, No. 15, pp. 616-627, September 1976.
- [7] R.T. Compton, Jr., Adaptive Antennas - Concepts and Performance, Prentice Hall, Inc., Englewood Cliffs, NJ, in press.
- [8] I.J. Gupta, W.G. Swarner and E.K. Walton, "Adaptive Antenna Arrays for Satellite Communications - Design and Testing," Technical Report 716111-3, Grant NAG3-536, for National Aeronautic and Space Administration, Lewis Research Center, Cleveland, Ohio, September, 1985.
- [9] H.L. Van Trees, Detection, Estimation and Modulation Theory, Part 1, Wiley, New York, 1968.
- [10] R.E. Ziemer and W.H. Tranter, Principles of Communications, 2nd Ed., Houghton Mifflin Co., Boston, 1985.

**Page intentionally left blank**

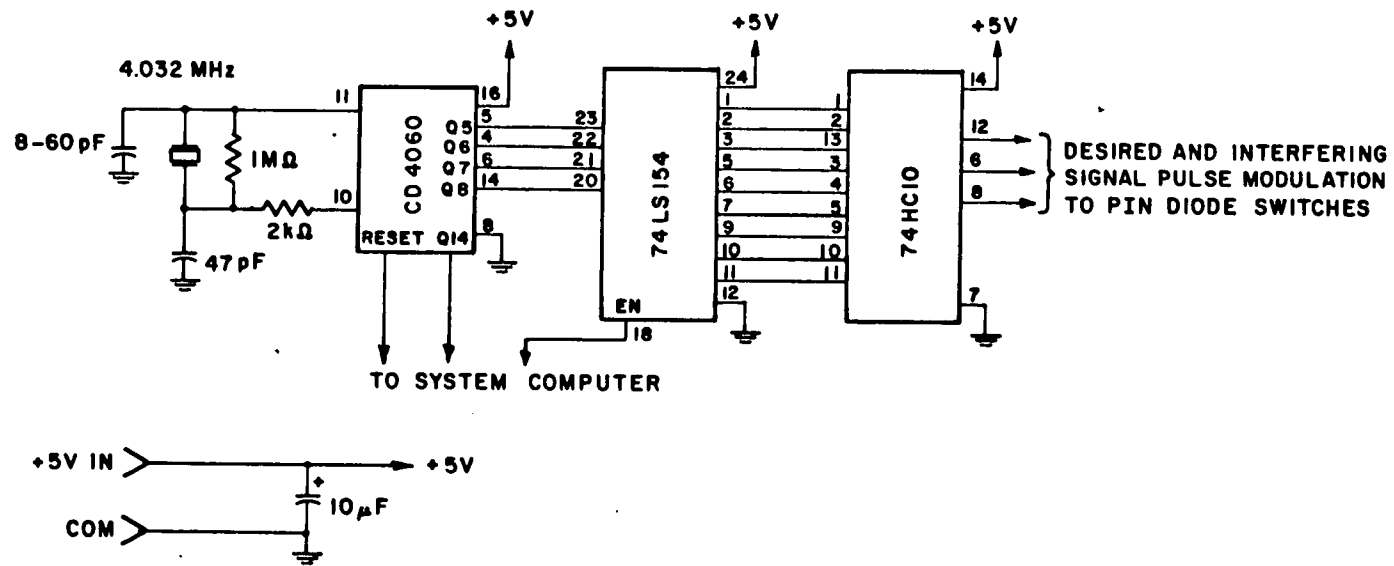


Figure 40. Pulse generator circuit of signal simulator.

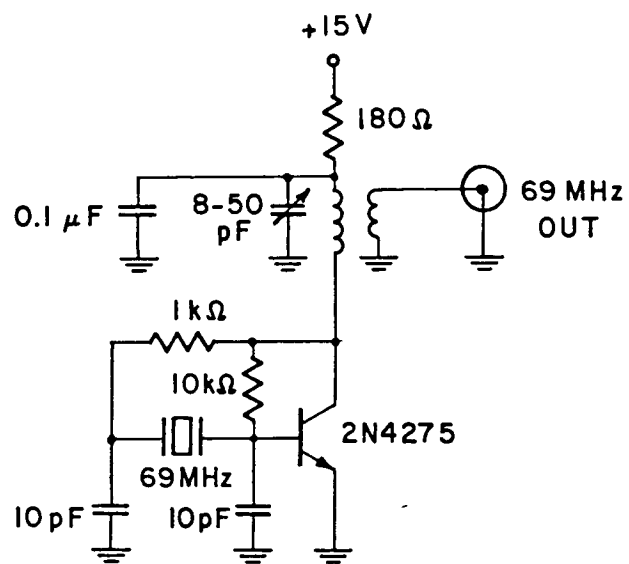


Figure 41. 69 MHz oscillator circuit.



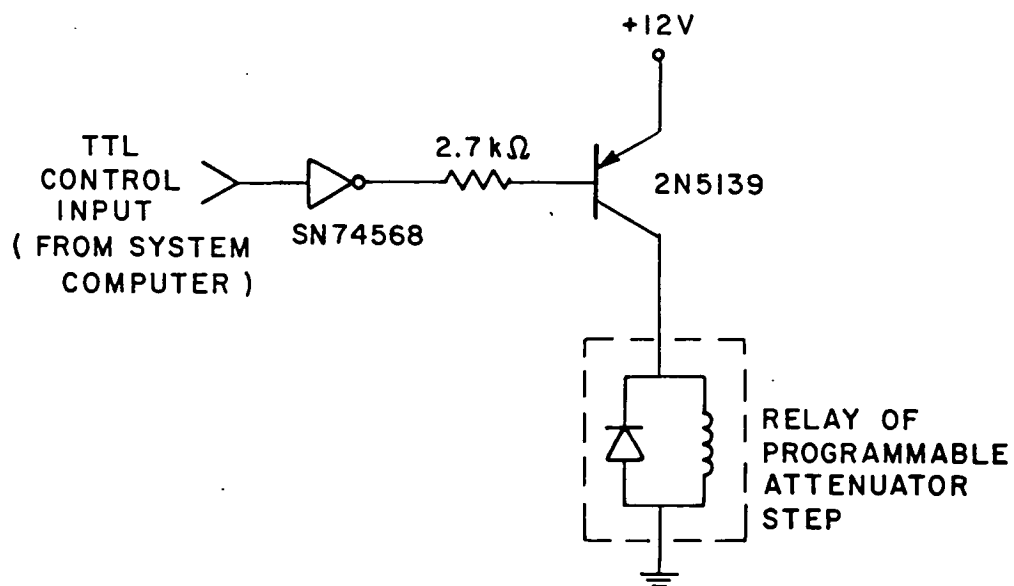


Figure 42. Level shifting circuit for programmable attenuator control.

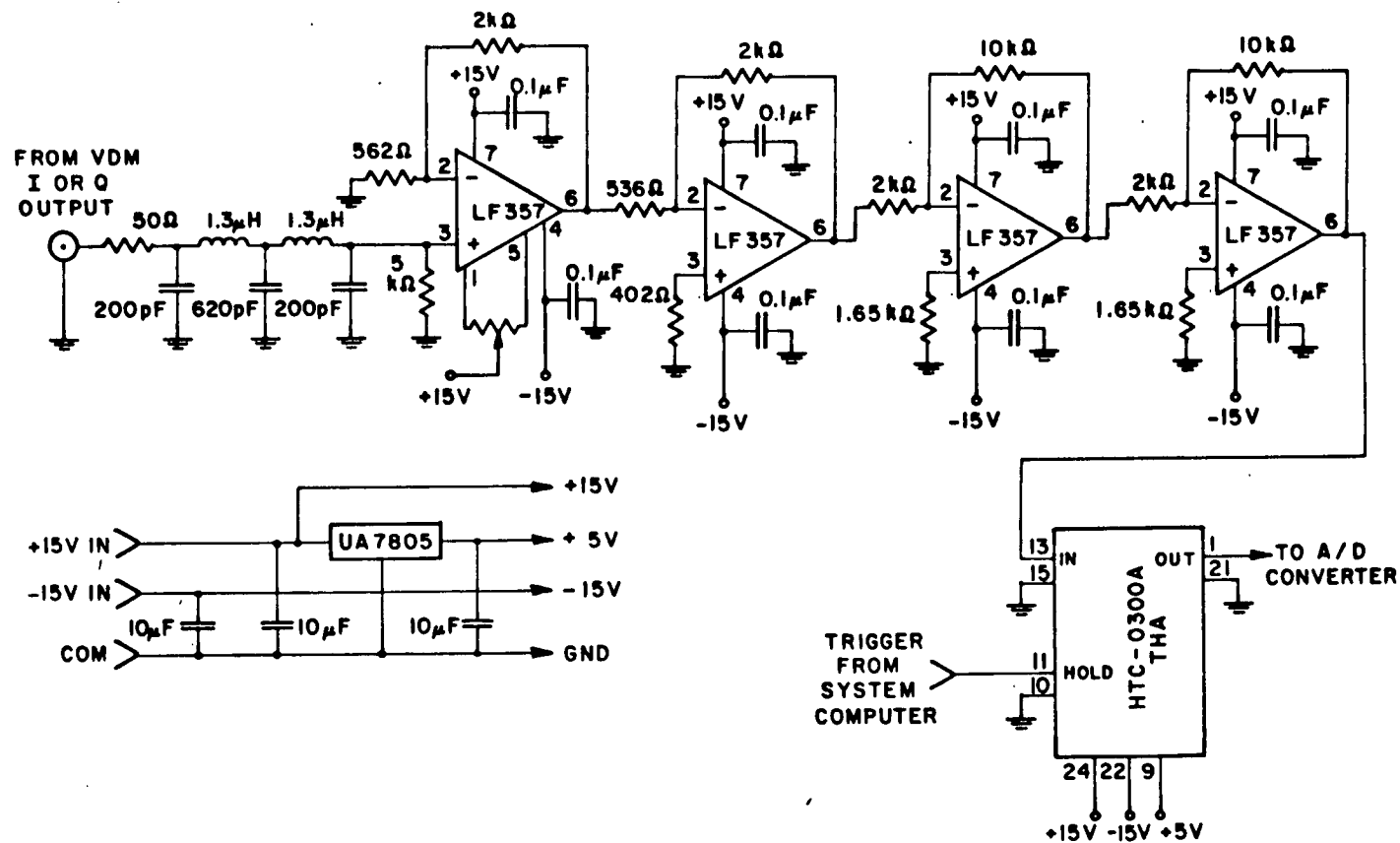


Figure 43. Array output VDM output circuitry.

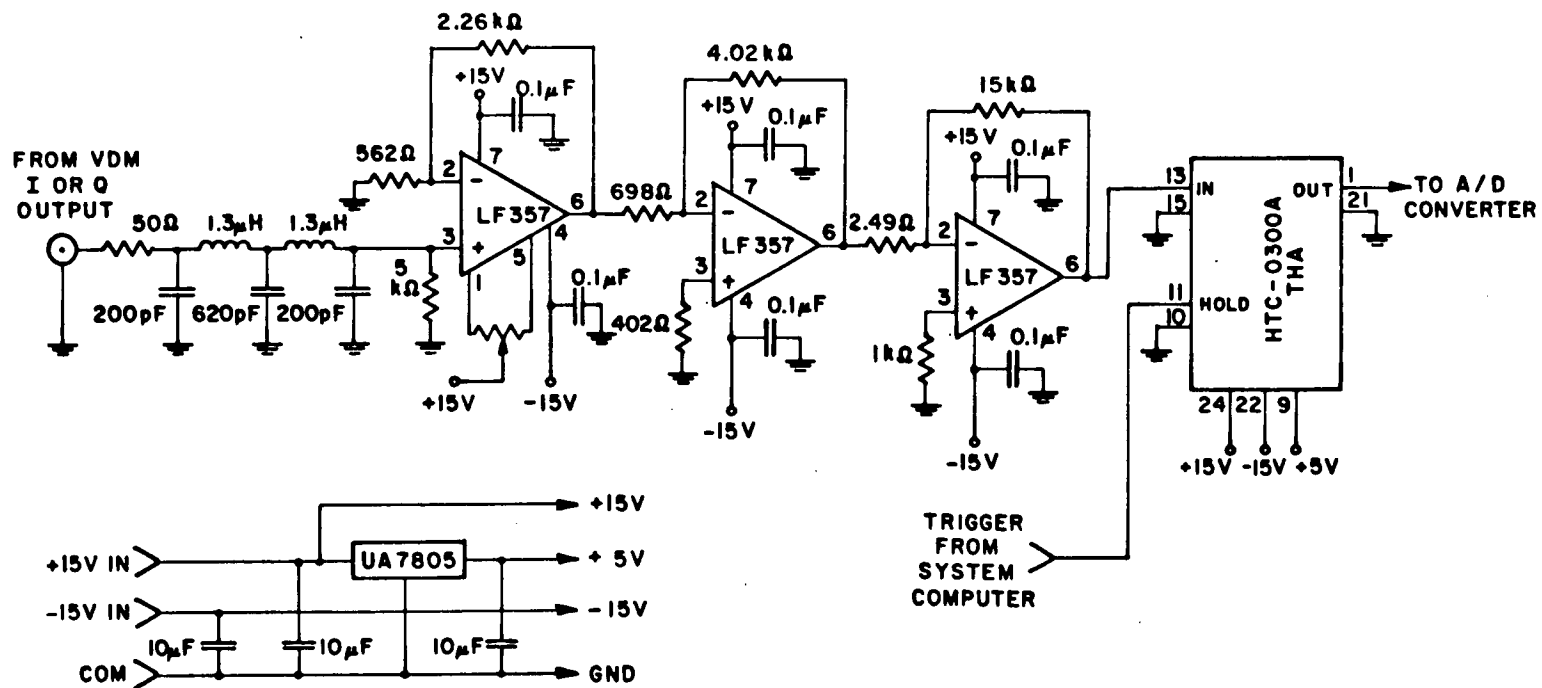


Figure 44. Auxiliary channel VDM output circuitry.

**APPENDIX B**

**SYSTEM SOFTWARE**

```

C      MASTER PROGRAM FOR RUNNING ADAPTIVE ARRAY SYSTEM
COMMON/OUTDTA/X,AVE,AVCOR,OFF,
X LMAG,HMAG,LPH,HPH,NSC,CPhi
COMMON/CTST/AVCD,AVIF,AVNSE
COMMON/SCNRO/LATT,LPHI,PN
COMMON/WTBLK/LDA0,WI,WQ,VMX,VMY,NW
COMMON/SPWRS/PWR,PNSE,ITER,IFL,OFLAG,NFLAG,AIS,AIST
COMPLEX X(3,64),AVCOR(2),OFF(3),US(2),AVCD(2),AVIF(2),AVNSE(2)
REAL VMX(40,4),VMY(40,4)
REAL PWR(3,3),PNSE(3),PB(3),PA(3),AIS(3),AIST,CPhi(2)
REAL AVE(6,3),LMAG(2),HMAG(2),LPH(2),HPH(2),PI,P(2)
REAL LPHI(2,2),PN(4),WI(2),WQ(2),TEMP1(2),TEMPQ(2),WI0(2),WQ0(2)
INTEGER IDAC0,LATT(3),LDA0,OFLAG,NW(4)
LOGICAL*1 FLNME(6),FTYPE(4),FLSPEC(15),NME(9,4)
DATA FTYPE/' ','D','A','T'/CPhi/2*0.0/
DATA IDAC0/"170440/OFF/3*(0.0,0.0)/
DATA WI/2*0.7071/WQ/2*0.0/NSC/10/
DATA PI/3.1415927/NFLAG/0/
C      Reading data for VMOD control
CALL SCOPY('VM1I.DAT',NME(1,1))
CALL SCOPY('VM1Q.DAT',NME(1,2))
CALL SCOPY('VM2I.DAT',NME(1,3))
CALL SCOPY('VM2Q.DAT',NME(1,4))
DO 15 I=1,4
  OPEN(UNIT=10,NAME=NME(1,I),TYPE='OLD',FORM='UNFORMATTED')
  DO 10 J=1,40
10    READ(10,END=11) VMX(J,I),VMY(J,I)
11    NW(I)=J
    CLOSE(UNIT=10)
15  CONTINUE
C      Enable pulse generator and set THA's to TRACK mode
CALL IPOKE(IDAC0,"40000")
CALL JWWT
C      Phase calibration of feedback loops
TYPE 918
TYPE 919
PAUSE
CALL JWISC
CALL CORREL
DO 20 J=1,2
  CPhi(J)=-1.0*ATAN2(AIMAG(AVCOR(J)),REAL(AVCOR(J)))
20  CONTINUE
  C=180.0/PI
  TYPE 974
  TYPE 973,C*CPhi(1),C*CPhi(2)
C      Enter Array Simulator parameters
25  CALL JWINIT
C      Enter initial weight vector AND apply to processor
TYPE 930
DO 30 L=1,2
  US(L)=(0.0,0.0)
  TYPE 931,L
  ACCEPT 935,WI(L)
  TYPE 932,L
  ACCEPT 935,WQ(L)
30  CONTINUE
  CALL JWWT
  TYPE *,',',
  TYPE *,',', To constrain W1 to its initial value-----Enter 1'
  TYPE *,',', To constrain W2 to its initial value-----Enter 2'
  TYPE *,',', To constrain neither W1 nor W2-----Enter 0'
  TYPE 975
  ACCEPT 921,ICF
40  TYPE 919
  PAUSE
  TYPE 879

```

```

CALL JWISC
DO 60 L=1,3
60   PB(L)=PWR(L,3)
      PINT=PWR(1,3)+PWR(2,3)
      TYPE 929
      PAUSE
      NFLAG=1
      TYPE 879
      CALL JWISC
      IFL=1
      CALL JWOTPT
      TYPE 928
      ACCEPT 921,IRC
      IF (IRC .EQ. 1) GOTO 40
65   TYPE 937
      ACCEPT 921,ISV
      IF (ISV .EQ. 1) GOTO 75
      IF (ISV .NE. 0) GOTO 65
      GOTO 115
75   TYPE 933
      TYPE 934
      PAUSE
      TYPE 976
      NSC=20
      DO 95 L=1,2
        WI0(L)=WI(L)
        WQ0(L)=WQ(L)
        WI(L)=0.0
        WQ(L)=0.0
95   CONTINUE
      CALL JWWT
      CALL CORREL
      US(1)=AVCOR(1)
      US(2)=AVCOR(2)
      TYPE *,(US(I),I=1,2)
      DO 110 L=1,2
        WI(L)=WI0(L)
        WQ(L)=WQ0(L)
      TYPE 928
      ACCEPT 921,IRC
      IF (IRC .EQ. 1) GOTO 75
110  CONTINUE
      CALL JWWT
      TYPE 936
      PAUSE
115  TYPE 927
      TYPE *, ' for later examination----Enter 1:'
      TYPE *, ' If not-----Enter 0:'
      TYPE 920
      ACCEPT 921,IRSP
      IF (IRSP .EQ. 0) GOTO 340
      IF (IRSP .NE. 1) GOTO 115
      TYPE 925
      ACCEPT 926,NCH,(FLNME(I),I=1,NCH)
      CALL CONCAT(FLNME,FTYPE,FLSPEC,NCH+4)
      OPEN (UNIT=10,NAME=FLSPEC,FORM='UNFORMATTED')
      WRITE (10) (WI(I),WQ(I),I=1,2),((0.0,0.0),I=1,8),0
340  TYPE 964
      ACCEPT 971,GAMMA
      TYPE 965
      ACCEPT 970,NSC
C    Start adaptation loop
      TYPE 968
      TYPE 969
      TYPE 966
      ITER=1

```

```

375     IF (ICODE .NE. 1) GOTO 490
        TYPE 967
        ICODE=0
490     CALL CORREL
C      Weight vector calculation and application:
        DO 600 K=1,2
            TEMPI(K)=WI(K)
            TEMPQ(K)=WQ(K)
            IF (ICF .EQ. K) GOTO 580
            WI(K)=WI(K)-GAMMA*REAL(AVCOR(K)-US(K))
            WQ(K)=WQ(K)+GAMMA*AIMAG(AVCOR(K)-US(K))
            IF (ABS(WI(K)).LE.1.0 .AND. ABS(WQ(K)).LE.1.0) GOTO 580
            TYPE 972,K,K
            WI(K)=TEMPI(K)
            WQ(K)=TEMPQ(K)
580     IF (MOD(ITER,5) .NE. 0) GOTO 600
        IF (K .EQ. 1) TYPE 884,ITER
        TYPE 885,K,K
        TYPE 887,TEMPI(K),TEMPQ(K),WI(K),WQ(K)
        TYPE *,''
600     CONTINUE
        CALL JWWT
        IF (IRSP .EQ. 0) GOTO 640
        IF (ITER .LE. 250) WRITE(10) (WI(I),WQ(I),I=1,2),
X      (AVCOR(I),I=1,2),(AVCD(I),I=1,2),(AVIF(I),I=1,2),(AVNSE(I),I=1,2)
X,ITER
640     IMCH=ITTINR()
        ICRLF=ITTINR()
        ICRLF=ITTINR()
        IF (IMCH .LT. 0) GOTO 800
        IF (IMCH .EQ. 83) GOTO 650
        TYPE 878
        GOTO 800
650     IF(MOD(ITER,5) .EQ. 0) GOTO 670
        TYPE 884,ITER
        DO 660 K=1,2
            TYPE 885,K,K
            TYPE 887,TEMPI(K),TEMPQ(K),WI(K),WQ(K)
            TYPE *,''
660     CONTINUE
670     TYPE 888
        TYPE *,'      Continue adaptation-----Enter 1'
        TYPE *,'      Exit adaptation loop-----Enter 2'
        TYPE *,'      Calculate jammer suppression--Enter 3'
        TYPE *,'      Output intermediate results---Enter 4'
        TYPE 880
        ACCEPT 881,ICODE
        IF (ICODE .EQ. 1) GOTO 800
        IF (ICODE-3) 850,710,720
710     TYPE 919
        PAUSE
        TYPE 879
        CALL JWISC
        DO 715 I=1,3
715     AIS(I)=10.0*ALOG10(PB(I)/PWR(I,3))
        AIST=10.0*ALOG10(PINT/(PWR(1,3)+PWR(2,3)))
        TYPE 929
        PAUSE
        NFLAG=1
        TYPE 879
        CALL JWISC
        TYPE 890,AIST
        TYPE 889,(AIS(I),I=1,3)
        GOTO 670
720     CALL JWOTPT
        GOTO 670

```

```

800     ITER=ITER+1
      GOTO 375
850     IF (IRSP .EQ.1) CLOSE(UNIT=10)
      TYPE 877
      TYPE *,'      End program execution-----Enter 2'
      TYPE 880
      ACCEPT 881,IECD
      IF (IECD .EQ. 2) GOTO 990
      IF (IECD .NE. 1) GOTO 850
      GOTO 25
877     FORMAT(// ' Conduct another test-----Enter 1')
878     FORMAT(// ' INADVERTANT CHARACTER ENTERED'/)
879     FORMAT(// ' Power levels being computed . . .')
880     FORMAT(' Enter code for desired option: ', $)
881     FORMAT(I1)
884     FORMAT(//10X,'Iteration number ',I3)
885     FORMAT(//13X,'LAST W(',I1,')',17X,'CURRENT W(',I1,')')
887     FORMAT(5X,2(E10.3,2X),4X,2(E10.3,2X))
888     FORMAT(// ' OPTIONS:')
889     FORMAT(// ' Jammer-1: ',F8.4,' Jammer-2: ',F8.4,' Desired
X Sig: ',F8.4/)
890     FORMAT(// ' INTERFERENCE SUPPRESSION: ',F8.4/)
918     FORMAT(// ' For phase calibration, set all leakage attenu
Xators to 70dB.')
919     FORMAT(// ' Remove noise and hit [RETURN]:')
920     FORMAT(// ' Enter code for storing weight values: ', $)
921     FORMAT(I1)
925     FORMAT(// ' Enter filename(<=6 characters): ', $)
926     FORMAT(Q,8A1)
927     FORMAT(// ' To store(on floppy) weight vector and its
X progression')
928     FORMAT(// ' Enter 1 to recalculate else enter 0: ', $)
929     FORMAT(// ' Restore noise and hit [RETURN]:')
930     FORMAT(// ' Enter initial weight values:')
931     FORMAT('      W',I1,'I= ', $)
932     FORMAT('      W',I1,'Q= ', $)
933     FORMAT(// ' Remove interference and noise for steering vector')
934     FORMAT(' calculation and hit [RETURN]:')
935     FORMAT(F7.4)
936     FORMAT(// ' Restore interference and noise and hit [RETURN]')
937     FORMAT(// ' Enter 1 to compute and use steering vector
X else enter 0: ', $)
964     FORMAT(// ' Enter loop gain: ', $)
965     FORMAT(// ' Enter number of scans to average over: ', $)
966     FORMAT(// ' Beginning Adaptation...'/)
967     FORMAT(// ' Continuing Adaptation...'/)
968     FORMAT(// ' Type 'S' and hit [RETURN] to suspend iteration')
969     FORMAT(' at any point and go to OPTION menu')
970     FORMAT(I3)
971     FORMAT(F10.6)
972     FORMAT(// ' WEIGHT #',I1,' TOO LARGE FOR VMOD-',I1,' TO HANDLE'/)
973     FORMAT('      AUX-1= ',F7.2,3X,' AUX-2= ',F7.2/)
974     FORMAT(// ' Feedback loop differential phase shifts:')
975     FORMAT(' Enter weight constraint code: ', $)
976     FORMAT(// ' Steering vector being computed...'/)
990     TYPE *,' THE END'
999     STOP
      END
      SUBROUTINE CORREL
      COMMON/OUTDTA/X,AVE,AVCOR,OFF,LMAG,HMAG,LPH,HPH,NSC,CPhi
      COMMON/CTST/AVCD,AVIF,AVNSE
      COMPLEX AVCD(2),CD(2),AVDIF(2),CDIF(2),AVNSE(2),AVIF(2)
      COMPLEX X(3,64),AVCOR(2),CORR(2),OFF(3),XC
      REAL AVE(6,3),LMAG(2),HMAG(2),LPH(2),HPH(2),CPhi(2)
90     DO 95 K=1,2
      CORR(K)=(0.0,0.0)

```



```

        AVCOR(K)=(0.0,0.0)
        CD(K)=(0.0,0.0)
        AVCD(K)=(0.0,0.0)
        CDIF(K)=(0.0,0.0)
        AVDIF(K)=(0.0,0.0)
95      CONTINUE
        DO 500 M=1,NSC
          CALL JWSCAN
C      Correlating auxiliary outputs with total array output
          DO 150 K=1,2
            CI=COS(CPHI(K))
            CQ=SIN(CPHI(K))
            DO 100 J=1,64
              XC=(X(K,J)-OFF(K))*CMPLX(CI,CQ)
              CORR(K)=CORR(K)+XC*CONJG(X(3,J)-OFF(3))
              IF(J.EQ. 15) CD(K)=CORR(K)
              IF(J.EQ. 45) CDIF(K)=CORR(K)
100          CONTINUE
              CD(K)=CD(K)/64.0
              CDIF(K)=CDIF(K)/64.0
              CORR(K)=CORR(K)/64.0
              AVCOR(K)=AVCOR(K)+CORR(K)
              AVCD(K)=AVCD(K)+CD(K)
              AVDIF(K)=AVDIF(K)+CDIF(K)
150          CONTINUE
C          IF (M.NE. 1) GOTO 300
C          T1=CABS(CORR(1))
C          T2=CABS(CORR(2))
C          P1=C*ATAN2(AIMAG(CORR(1)),REAL(CORR(1)))
C          P2=C*ATAN2(AIMAG(CORR(2)),REAL(CORR(2)))
C          LPH(1)=P1
C          HPH(1)=P1
C          LPH(2)=P2
C          HPH(2)=P2
C          LMAG(1)=T1
C          HMAG(1)=T1
C          LMAG(2)=T2
C          HMAG(2)=T2
C300         DO 400 J=1,2
C             CM=CABS(CORR(J))
C             CP=C*ATAN2(AIMAG(CORR(J)),REAL(CORR(J)))
C             IF (CP.LT. LPH(J)) LPH(J)=CP
C             IF (CP.GT. HPH(J)) HPH(J)=CP
C             IF (CM.LT. LMAG(J)) LMAG(J)=CM
C             IF (CM.GT. HMAG(J)) HMAG(J)=CM
C400         CONTINUE
500         CONTINUE
          DO 600 I=1,2
            AVCOR(I)=AVCOR(I)/NSC
            AVCD(I)=AVCD(I)/NSC
            AVDIF(I)=AVDIF(I)/NSC
            AVIF(I)=AVDIF(I)-AVCD(I)
            AVNSE(I)=AVCOR(I)-AVDIF(I)
600         CONTINUE
          RETURN
        END

```

```

C Subprogram JWINIT--set array simulator parameters
C Program to test control of programmable attenuators of array
C simulator using parallel output port(DRV11)
      SUBROUTINE JWINIT
      COMMON/SCNRO/LATT,LPHI,PN
      INTEGER DRBUF,IVAL,LATT(3),IM(3),IP(3)
      REAL LPHI(2,2),PN(4)
      DATA DRBUF/"167772/IBNO/15*0/
      DATA IM,IP/3*0,3*0/K2/-1/
      IVAL=0
C Desired signal parameters: array index 1
C Jammer 1 signal parameters: array index 2
C Jammer 2 signal parameters: array index 3
20      FORMAT(// ' Enter Main signal leakage attenuation(dB): ', $)
21      FORMAT(' Enter Jammer-',I1,' leakage attenuation(dB): ', $)
25      FORMAT(I3)
30      FORMAT(' Set Main signal leakage rotary attenuator to ',I2,'dB')
31      FORMAT(' Set Jammer-',I1,' leakage rotary attenuator to ',I2,'dB')
32      FORMAT(' and hit [RETURN]')
40      FORMAT(' Enter phase shift from Jammer-',I1,
X      ' to MAIN(degrees): ', $)
41      FORMAT(' Enter phase shift from Jammer-',I1,' to AUX-',I1,' : ', $)
45      FORMAT(F8.2)
50      FORMAT(' Enter Main channel noise power(dBm): ', $)
51      FORMAT(' Enter Correlator channel noise power(dBm): ', $)
52      FORMAT(' Enter AUX-',I1,' signal channel noise power(dBm): ', $)
55      FORMAT(F7.2)
      DO 500 J=1,3
      K=J-1
      IF (J .EQ. 1) TYPE 20
      IF (J .NE. 1) TYPE 21,K
      ACCEPT 25,LATT(J)
      IM(J)=INT(0.1*LATT(J)-2.15)*10
      IF( IM(J) .LT. 0) IM(J)=0
      IP(J)=LATT(J)-IM(J)
      IF (J .EQ. 1) TYPE 30,IM(J)
      IF (J .NE. 1) TYPE 31,K,IM(J)
      TYPE 32
      PAUSE
      IVAL=IVAL+IP(J)*2**(K*5)
500      CONTINUE
      CALL IPOKE(DRBUF,IVAL)
C Enter in leakage phase shifts, noise powers that are manually set:
      DO 600 J=1,2
      K2=-1.0*K2
      TYPE 40,J
      ACCEPT 45,LPHI(J,1)
      TYPE 41,J,K2
      ACCEPT 45,LPHI(J,2)
600      CONTINUE
      TYPE *, ' '
      DO 700 J=1,4
      IF (J .EQ. 1) TYPE 50
      IF (J .EQ. 4) TYPE 51
      IF (J .NE. 1 .AND. J .NE. 4) TYPE 52,J-1
      ACCEPT 55,PN(J)
700      CONTINUE
      RETURN
      END

```

```

C      SUBPROGRAM TO SCAN AND A/D CONVERT SAMPLES FROM A WAVEFORM
      SUBROUTINE JWSCAN
      COMMON/OUTDTA/X,AVE
      COMMON/WTBLK/LDA0
      COMPLEX X(3,64)
      REAL D(6,64),AVE(6,3)
      INTEGER ADCSR,CLCSR,ADDBR,CLBPR,KCSR,IAD(6,64),IDAC0,LDA0
      DATA ADCSR,ADDBR,CLCSR,CLBPR/"170400","170402","170420","170422"/
      DATA IDAC0/"170440"/
      DO 10 IFX=1,6
        DO 9 JFX=1,3
9        AVE(IFX,JFX)=0.0
10       CONTINUE
C      TYPE 10
C      ACCEPT 11,ICNT
C10      FORMAT (3X,'Enter initial count before clock overflow:',$)
11      FORMAT (I5)
C      Configure clock for external start(ST2) and single interval mode
      KCSR=8200
      IST0="40000+LDA0
      ICNT2=-63
      CALL IPOKE(CLBPR,ICNT2)
C      CHECK REGISTER CONTENTS
C      TYPE *,'ADCSR=',IPEEK(ADCSR)
C      TYPE *,'CLCSR=',IPEEK(CLCSR)
C      TYPE *,'CLBPR=',IPEEK(CLBPR)
C      GOTO 999
C      Using TTL bit from DAC0 holding register to start pulse generator(ACT.LOW)
C      and put THA's to track mode
      CALL IPOKE(IDAC0,IST0)
      CALL IPOKE(CLCSR,KCSR)
C      Loop to check A/D done bit and read converted values
      DO 100 J=1,64
50       IC=IPEEKB(CLCSR)
C      Check clock overflow bit, then flag overrun bit
      IF (IC .LT. 128) GOTO 50
      IF (IPEEKB("170421") .AND. "20) GOTO 900
      CALL IPOKE(CLCSR,KCSR)
      CALL IPOKE(CLBPR,ICNT2-J)
      DO 95 K=1,6
        IASR=K*256+1
        CALL IPOKE(ADCSR,IASR)
C      Check for A/D done bit before reading converted data
60       IF (IPEEKB(ADCSR) .LT. 128) GOTO 60
C      IF (IPEEKB("170401") .GE. 128) GOTO 910
        IAD(K,J)=IPEEK(ADDBR)
95      CONTINUE
C      Reset THA's back to TRACK
      CALL IPOKE(IDAC0,LDA0)
      CALL IPOKE(IDAC0,IST0)
100     CONTINUE
C      Disable clock starts, leaving pulse gen running
      CALL IPOKE(CLCSR,0)
      CALL IPOKE(IDAC0,LDA0)
C      Convert data from offset binary
      DO 200 J2=1,64
        DO 195 K2=1,6
          D(K2,J2)=(IAD(K2,J2)-"4000")*0.0025
C          TYPE *,K2,J2,D(K2,J2)
195     CONTINUE
          CINV=-1.0
          DO 199 J=1,3
            IF (J .EQ. 3) CINV=1.0
            X(J,J2)=CINV*CMPLX(D(2*J-1,J2),D(2*J,J2))
199     CONTINUE
200     CONTINUE

```

```

C   Averaging pulse levels for comparison
C   MAIN--from samples 2-13
      DO 450 I=1,6
      DO 300 J2=2,13
300   AVE(I,3)=AVE(I,3)+D(I,J2)
C   J1--from samples 17,28
      DO 350 J2=17,28
350   AVE(I,1)=AVE(I,1)+D(I,J2)
C   J2--from samples 33,44
      DO 400 J2=33,44
400   AVE(I,2)=AVE(I,2)+D(I,J2)
      AVE(I,1)=AVE(I,1)/12.
      AVE(I,2)=AVE(I,2)/12.
      AVE(I,3)=AVE(I,3)/12.
450   CONTINUE
      GOTO 999
900   TYPE *, ' FLAG OVERRUN BIT SET IN KWCSR', 'J=', J
C910  TYPE *, ' A/D ERROR BIT SET'
999   RETURN
      END

C   Program to calculate signal and noise power at array output,
C   from samples taken with JWSCAN, then calculate J/N ratios
C   and the interference suppression
      SUBROUTINE JWISC
      COMMON/OUTDTA/X, AVE, AVCOR, OFF
      COMMON/SPWRS/PWR, PNSE, ITER, IFL, OFLAG, NFLAG
      COMPLEX X(3,64), OFF(3), Y, AVCOR(2)
      REAL PWR(3,3), PNSE(3), AVE(6,3), S(3,3,2), OFFR(3), OFFI(3)
      INTEGER IFL, OFLAG, NFLAG
C   Enter number of samples
C20   FORMAT(/' Enter number of scans to average over ')
C21   FORMAT('      for power calculations: ', $)
25    FORMAT(I3)
C     TYPE 20
C     TYPE 21
C     ACCEPT 25, NUM
      NUM=10
      NSMP=NUM*12.0
      NSMP2=NUM*16.0
      IF (NFLAG .EQ. 1) GOTO 853
      DO 15 J=1,3
      DO 10 K=1,3
      PWR(J,K)=0.0
      S(J,K,1)=0.0
      S(J,K,2)=0.0
10    CONTINUE
      OFF(J)=(0.0,0.0)
15    CONTINUE
      DO 810 J=1, NUM
      CALL JWSCAN
      DO 800 KCH=1,3
      DO 90 K=47,62
90     OFF(KCH)=OFF(KCH)+X(KCH,K)
505    DO 650 IM=1,3
      DO 600 M=1,2
      L=2*KCH-2+M
      S(IM,KCH,M)=S(IM,KCH,M)+AVE(L,IM)
600    CONTINUE
650    CONTINUE
800    CONTINUE
810    CONTINUE
      DO 850 M=1,3
      OFF(M)=OFF(M)/NSMP2
      OFFR(M)=REAL(OFF(M))
      OFFI(M)=AIMAG(OFF(M))
      DO 840 N=1,3

```

```

      S(N,M,1)=S(N,M,1)/NUM
      S(N,M,2)=S(N,M,2)/NUM
      PWR(N,M)=(S(N,M,1)-OFFR(M))**2+(S(N,M,2)-OFFI(M))**2
840      CONTINUE
850      CONTINUE
      GOTO 900
C   Noise power calculations over portion of PRP when no signal present.
853      DO 854 M=1,3
854      PNSE(M)=0.0
855      DO 890 N=1,NUM
      CALL JWSCAN
      DO 888 M=1,3
      DO 870 K=47,62
      Y=X(M,K)-OFF(M)
      PNSE(M)=PNSE(M)+CABS(Y)**2
870      CONTINUE
888      CONTINUE
890      CONTINUE
891      DO 895 M=1,3
895      PNSE(M)=PNSE(M)/NSMP2
900      TYPE 910,(PWR(N,1),N=1,3)
      TYPE 911,(PWR(N,2),N=1,3)
      TYPE 912,(PWR(N,3),N=1,3)
      IF (NFLAG .EQ. 1) TYPE 913,(PNSE(N),N=1,3)
910      FORMAT(/5X,'AUX-1 POWERS:',3(2X,E12.5))
911      FORMAT(/5X,'AUX-2 POWERS:',3(2X,E12.5))
912      FORMAT(/5X,'ARRAY OUT POWERS:',3(2X,E12.5))
913      FORMAT(/5X,'NOISE POWERS:',3(2X,E12.5))
      NFLAG=0
9999      RETURN
      END

```

```

C Subroutine to print/type data from a particular experiment(JWMSTR)
  SUBROUTINE JWOTPT
    COMMON/OUTDTA/X,AVE,AVCOR,OFF
X ,LMAG,HMAG,LPH,HPH,NSC
    COMMON/SCNRO/LATT,LPHI,PN
    COMMON/SPWRS/PWR,PNSE,ITER,IFL,OFLAG,NFLAG,AIS,AIST
    COMPLEX X(3,64),AVCOR(2),OFF(2)
    REAL AVE(6,3),LMAG(2),HMAG(2),LPH(2),HPH(2),PI,AIS(3),AIST
    LOGICAL*1 OLATT(34,3),OLPHI(48,2,2),OPN(40,4)
    LOGICAL*1 OT(36,2),OT1(36,2),OT2(36,2),OT3(36,2)
    LOGICAL*1 OTCOR(48,2),CRLF(2),OTOFF(44,3),OTNS(52)
    LOGICAL*1 SPHG(37),SPDA(75),THDG(26)
    DATA CRLF/13,10/
    INTEGER LATT(3),OFLAG,NFLAG
    REAL LPHI(2,2),PN(4),PWR(3,3),PNSE(3)
    KD=-1
    ICR=13
    ILF=10
15  TYPE 111
    TYPE *, ' Select Output Media:'
    TYPE *, '   Monitor display-----Enter 1'
    TYPE *, '   Printer hard copy----Enter 0'
    TYPE 20
    ACCEPT 41,OFLAG
20  FORMAT(' Enter output media code: ', $)
25  TYPE *, ' '
    TYPE *, ' Select Output:'
    TYPE *, '   Signal Scenario-Simulator parameters--Enter 1'
    TYPE *, '   Signal/Jammer and Signal/Noise ratios'
    TYPE *, '   at each detector-----Enter 2'
    IF (IFL .EQ. 1) GOTO 34
    TYPE *, '   Sampled data from last scan-----Enter 3'
    TYPE *, '   DC Offsets,Correlation range for'
    TYPE *, '   last iteration(ave over NSC scans)---Enter 4'
    TYPE *, '   Interference suppression-----Enter 5'
34  TYPE *, '   Change output media-----Enter 6'
35  TYPE *, '   Done-Return to Main Program-----Enter 7'
40  FORMAT (' Enter code for desired output: ', $)
41  FORMAT (I1)
    TYPE 40
    ACCEPT 41,IPCODE
    IF (IPCODE .EQ. 7) GOTO 9999
    IF (IPCODE .EQ. 6) GOTO 15
    IF (IPCODE .EQ. 5) GOTO 700
    IF (IPCODE .EQ. 4) GOTO 500
    IF (IPCODE-2) 150,970,950
    TYPE 111
100  FORMAT(' Main leakage attenuation= ',I2,' dB',2A1)
101  FORMAT(' Jammer-',I1,' leakage atten.= ',I2,' dB ',2A1)
105  FORMAT(' J',I1,'/MAIN leakage phase shift=',F7.2,' degrees'
X ,2X,2A1)
106  FORMAT(' J',I1,'/Aux-',I1,' leakage phase shift=',F7.2,' degrees'
X,1X,2A1)
108  FORMAT(' Main channel noise power=',F6.2,' dBm',2X,2A1)
109  FORMAT(' Corr. channel noise power=',F6.2,' dBm',1X,2A1)
110  FORMAT(' Aux-',I1,' channel noise power= ',F6.2,' dBm',2A1)
111  FORMAT(/)
150  IF (OFLAG .NE. 1) GOTO 340
    TYPE 100,LATT(1)
    DO 190 J=2,3
190  TYPE 101,J-1,LATT(J)
    TYPE 111
    DO 220 J=1,2
    KD=(-1)**(J-1)
    TYPE 105,J,LPHI(J,1)
    TYPE 106,J,J+KD,LPHI(J,2)

```

```

220    CONTINUE
      TYPE 111
      TYPE 108,PN(1)
      TYPE 110,1,PN(2)
      TYPE 110,2,PN(3)
      TYPE 109,PN(4)
      GOTO 25
340    CALL IBSEND(CRLF,2,23)
      DO 350 J=1,3
        IF (J .EQ. 1) ENCODE (34,100,OLATT(1,J)) LATT(J),ICR,ILF
        IF (J .NE. 1) ENCODE (34,101,OLATT(1,J)) J-1,LATT(J),ICR,ILF
        CALL IBSEND(OLATT(1,J),34)
350    CONTINUE
      CALL IBSEND(CRLF,2)
      DO 380 J=1,2
        KD=-1*KD
        ENCODE (48,105,OLPHI(1,J,1)) J,LPHI(J,1),ICR,ILF
        ENCODE (48,106,OLPHI(1,J,2)) J,J+KD,LPHI(J,2),ICR,ILF
        CALL IBSEND(OLPHI(1,J,1),48)
        CALL IBSEND(OLPHI(1,J,2),48)
380    CONTINUE
      CALL IBSEND(CRLF,2)
      DO 400 J=1,4
        IF (J .EQ. 1) ENCODE (40,108,OPN(1,1)) PN(1),ICR,ILF
        IF (J .EQ. 4) ENCODE (40,109,OPN(1,4)) PN(4),ICR,ILF
        IF (J .GT. 1 .AND. J .LT. 4) ENCODE(40,110,OPN(1,J)) J-1,PN(J)
        X ,ICR,ILF
        CALL IBSEND(OPN(1,J),40)
400    CONTINUE
      CALL IBSEND(CRLF,2)
      GOTO 25
C   Program section to output dc offset, correlation range,etc.
500    IF(OFLAG .NE. 1) GOTO 810
      TYPE 111
      TYPE 910,NSC
      TYPE 111
      DO 550 J=1,2
550    TYPE 906,J,OFF(J)
      TYPE 911,OFF(3)
      DO 600 J=1,2
        TYPE 905,J,AVCOR(J)
        TYPE 901,J,LPH(J)
        TYPE 902,J,HPH(J)
        TYPE 903,J,LMAG(J)
        TYPE 904,J,HMAG(J)
        TYPE 111
600    CONTINUE
      GOTO 25
C   Output interference calculations
700    IF(OFLAG .NE. 1) GOTO 750
      TYPE 111
      TYPE 878
      TYPE 111
      TYPE 880,AIST
      TYPE 882,(AIS(J),J=1,3)
      TYPE 111
      GOTO 25
750    CALL IBSEND(CRLF,2,23)
      ENCODE(26,878,THDG) ITER,ICR,ILF
      ENCODE(37,880,SPHG) AIST,ICR,ILF
      ENCODE(75,882,SPDA) (AIS(J),J=1,3),ICR,ILF
      CALL IBSEND(THDG,26)
      CALL IBSEND(SPHG,37)
      CALL IBSEND(SPDA,75)
      GOTO 25
810    CALL IBSEND(CRLF,2,23)

```

```

      ENCODE(54,910,OTNS) NSC,ICR,ILF
      CALL IBSEND(OTNS,54)
      CALL IBSEND(CRLF,2)
      DO 815 JX=1,3
        IF(JX.EQ. 3) ENCODE(46,911,OTOFF(1,JX)) OFF(JX),ICR,ILF
        IF(JX.NE. 3) ENCODE(46,906,OTOFF(1,JX)) JX,OFF(JX),ICR,ILF
        CALL IBSEND(OTOFF(1,JX),46)
815    CONTINUE
      CALL IBSEND(CRLF,2)
      DO 820 J=1,2
        ENCODE(50,905,OTCOR(1,J)) J,AVCOR(J),ICR,ILF
        ENCODE(38,901,OT(1,J)) J,LPH(J),ICR,ILF
        ENCODE(38,902,OT1(1,J)) J,HPH(J),ICR,ILF
        ENCODE(38,903,OT2(1,J)) J,LMAG(J),ICR,ILF
        ENCODE(38,904,OT3(1,J)) J,HMAG(J),ICR,ILF
        CALL IBSEND(OTCOR(1,J),50)
        CALL IBSEND(OT(1,J),38)
        CALL IBSEND(OT1(1,J),38)
        CALL IBSEND(OT2(1,J),38)
        CALL IBSEND(OT3(1,J),38)
        CALL IBSEND(CRLF,2)
820    CONTINUE
      CALL IBSEND(CRLF,2)
      GOTO 25
878    FORMAT (' After ',I3,' iterations: ',2A1)
880    FORMAT (' INTERFERENCE SUPPRESSION: ',F8.4,2A1)
882    FORMAT (' Jammer-1: ',F8.4,' dB', ' Jammer-2: ',F8.4,' dB',
X ' Desired Sig.: ',F8.4,' dB',2A1)
901    FORMAT (' SMALLEST AUX-',I1,' CORR. PHASE=',F8.3,2A1)
902    FORMAT (' LARGEST AUX-',I1,' CORR. PHASE=',F8.3,2A1)
903    FORMAT (' SMALLEST AUX-',I1,' CORR. MAG.= ',E8.2,2A1)
904    FORMAT (' LARGEST AUX-',I1,' CORR. MAG.= ',E8.2,2A1)
905    FORMAT (' AVE. AUX-',I1,' CORRELATION=',2(1X,E11.4),2A1)
906    FORMAT (' AVE. AUX-',I1,' DC OFFSET=',2(1X,E10.3),2A1)
910    FORMAT (' # SCANS FOR OFFSET= 10; # SCANS FOR AVE. CORR.= ',I3
X ',2A1)
911    FORMAT (' ARRAY OUT DC OFFSET= ',2(1X,E10.3),2A1)
950    CALL JWPRNT
      GOTO 25
970    CALL JWPRAT
      IF (IFL.EQ. 1) GOTO 9999
      GOTO 25
9999   IFL=0
      RETURN
      END
C      SUBPROGRAM TO PRINT DATA FROM SUBROUTINE JWSCAN
      SUBROUTINE JWPRNT
      COMMON/OUTDTA/X
      COMPLEX X(3,64)
      REAL A(6,64),PI
      INTEGER ICR,ILF
      BYTE FF
      BYTE CRLF(2),OTPT(77),OTIS(24)
      DATA CRLF/13,10/FF/12/PI/3.1415927/
      ICR=13
      ILF=10
      TYPE *,' '
10     TYPE *,' Enter code for desired output form:'
      TYPE *,'      MAG,PHASE--Enter 1'
      TYPE *,'      I,Q-----Enter 2'
      ACCEPT 20,IPCODE
20     FORMAT(I2)
      IF (IPCODE.EQ. 1) GOTO 150
      IF (IPCODE.NE. 2) GOTO 10
      DO 50 J=1,64
      DO 50 K=1,3

```



```

      L=2*K-1
      A(L,J)=REAL(X(K,J))
      A(L+1,J)=AIMAG(X(K,J))
50      CONTINUE
      GOTO 250
150     C=180.0/3.1415927
      DO 230 J2=1,64
      DO 220 K2=1,3
          L=2*K2-1
          A(L,J2)=CABS(X(K2,J2))
          A(L+1,J2)=C*ATAN2(AIMAG(X(K2,J2)),REAL(X(K2,J2)))
220     CONTINUE
230     CONTINUE
250     CALL IBSEND(CRLF,2,23)
      CALL IBSEND(CRLF,2)
      DO 500 J3=1,64
          ENCODE (77,550,OTPT) J3,(A(K3,J3), K3=1,6),ICR,ILF
          CALL IBSEND(OTPT,77)
500     CONTINUE
      CALL IBSEND(FF,1)
550     FORMAT(1X,I2,6(1X,E11.4),2A1)
999     RETURN
      END

```

C Subroutine jwprat, to calculate and output the S/J,S/N ratios,  
C and simulated sidelobe levels associated with a given exper-  
C iment.

```

      SUBROUTINE JWPRAT
      COMMON/SPWRS/PWR,PNSE,ITER,IFL,OFLAG
      LOGICAL*1 SH0(47),OSLL(38),OSLM(31),H1(36),OD1(65)
      LOGICAL*1 H2(55),OD2(61),BHDG(22),CRLF(2),OD3(32)
      INTEGER IFL,OFLAG
      REAL PWR(3,3),PNSE(3),SLL(3),PRAT(3,2),SNR(3),SIR
      DATA CRLF/13,10/
      ICR=13
      ILF=10
      PRAT(1,1)=10.0*ALOG10(PWR(1,1)/PWR(2,1))
      PRAT(1,2)=10.0*ALOG10(PWR(1,1)/PWR(3,1))
      PRAT(2,1)=10.0*ALOG10(PWR(2,2)/PWR(1,2))
      PRAT(2,2)=10.0*ALOG10(PWR(2,2)/PWR(3,2))
      PRAT(3,1)=10.0*ALOG10(PWR(3,3)/PWR(1,3))
      PRAT(3,2)=10.0*ALOG10(PWR(3,3)/PWR(2,3))
      SIR=10.0*ALOG10(PWR(3,3)/(PWR(1,3)+PWR(2,3)))
      SLL(1)=AMIN1(PRAT(1,1),PRAT(1,2))
      SLL(2)=AMIN1(PRAT(2,1),PRAT(2,2))
      SLL(3)=AMIN1(PRAT(3,1),PRAT(3,2))
C The factor -7.27 is due to the average power of our pulsed
C sinusoids, Pave=(Ac**2)/2*(duty cycle). The quantity PWR(I,I)
C represents (Ac**2)/2. The duty cycle cancels when taking signal to
C signal ratios, but must be included for SNR computations.
      DO 18 I=1,3
18       SNR(I)=10.0*ALOG10(PWR(I,I)/PNSE(I))-7.27
          IF (OFLAG .NE. 1) GOTO 349
          TYPE 899
          IF (IFL .EQ. 1) TYPE 898
49       DO 100 J=1,2
          K=(-1)**J
          TYPE 900,J
          TYPE 901,J,J-K,PRAT(J,1),J,PRAT(J,2),J,SNR(J)
100      CONTINUE
          TYPE 902
          TYPE 903,PRAT(3,1),PRAT(3,2),SNR(3)
          TYPE 904,SIR
          GOTO 990
349     CALL IBSEND(CRLF,2,23)
          IF (IFL .NE. 1) GOTO 360
          ENCODE(22,898,BHDG) ICR,ILF

```

```

      CALL IBSEND(BHDG,22)
360 DO 400 J=1,2
      K=(-1)**J
      ENCODE(36,900,H1) J,ICR,ILF
      ENCODE(65,901,OD1) J,J-K,PRAT(J,1),J,PRAT(J,2),J,SNR(J),ICR,ILF
      CALL IBSEND(H1,36)
      CALL IBSEND(OD1,65)
400 CONTINUE
      ENCODE(55,902,H2) ICR,ILF
      ENCODE(61,903,OD2) PRAT(3,1),PRAT(3,2),SNR(3),ICR,ILF
      ENCODE(32,904,OD3) SIR,ICR,ILF
      CALL IBSEND(H2,55)
      CALL IBSEND(OD2,61)
      CALL IBSEND(OD3,32)
898 FORMAT(' Before Adaptation: ',2A1)
899 FORMAT(//)
900 FORMAT('  AUXILIARY ELEMENT ',I1,' PARAMETERS: ',2A1)
901 FORMAT('    J',I1,'/J',I1,'= ',F8.4,' dB',' J',I1,'/D= ',F8.4,
X ' dB',' J',I1,'/NOISE= ',F8.4,' dB',2A1)
902 FORMAT('  ARRAY OUTPUT(MAIN ANTENNA IF WEIGHTS=0) PARAMETERS:'
X ',2A1)
903 FORMAT('    D/J1= ',F8.4,' dB',' D/J2= ',F8.4,' dB',' D/N=',
X F8.4,' dB',2A1)
904 FORMAT('    D/I=D/(J1+J2)= ',F8.4,' dB',2A1)
990 RETURN
      END

```

```

C   SUBPROGRAM TO APPLY I,Q WEIGHTS USING DAC-11 D/A CONVERTERS
C   PROGRAMMING BOTH MAGNITUDE AND PHASE
      SUBROUTINE JWWT
      COMMON/WTBLK/LDA0,WI,WQ,VMX,VMY,NW
      REAL WI(2),WQ(2),VMX(40,4),VMY(40,4)
      REAL A(4),XLSB,MAG,PHI
      INTEGER ID(4),NW(4),J,IADDRI,IADDRQ,LDA0
      XLSB=20./4095
      DO 150 J=1,2
        K=2*J
        L=K-1
50      TI=WCV(VMX(1,L),VMY(1,L),NW(L),ABS(WI(J)))
        TQ=WCV(VMX(1,K),VMY(1,K),NW(K),ABS(WQ(J)))
        VI=SIGN(TI,WI(J))
        VQ=SIGN(TQ,WQ(J))
C      TYPE *,WI(J),VI,WQ(J),VQ
80      IDI=INT(VI/XLSB+"4000+0.5)
        IF(J.EQ.1) LDA0=IDI
        IDQ=INT(VQ/XLSB+"4000+0.5)
        IADDRI="170440+(J-1)*4
        IADDRQ=IADDRI+2
        CALL IPOKE(IADDRI,IDI)
        CALL IPOKE(IADDRQ,IDQ)
150     CONTINUE
999     RETURN
      END
      FUNCTION WCV(X,Y,N,Y1)
      REAL X(40),Y(40),Y1
      DO 100 J=1,N
        Q=Y(J)
        R=Y(J+1)
        IF (Q.LE.Y1 .AND. Y1.LE.R) GOTO 150
100     CONTINUE
150     SLPE=(R-Q)/(X(J+1)-X(J))
        WCV=(Y1-Q)/SLPE+X(J)
      RETURN
      END

```